



ALMA MATER STUDIORUM
UNIVERSITÀ DI BOLOGNA

DEPARTMENT OF INDUSTRIAL ENGINEERING

SECOND CYCLE DEGREE

LM-20 - Aerospace and Astronautic Engineering

**Human-Centred Design in Air Traffic Control
Systems: a study on Arrival Manager (AMAN)**

Supervisor:
Prof. Sara Bagassi

Presented by:
Matteo Rossi

Co-Supervisor:
Eng. Tommaso Fadda
Dr. Eng. Carlo Alfredo Persiani

Examiner:
Prof. Fabio Olivetti

Academic Year 2023-2024

Acknowledgements

I would like to express my thanks to Professor Sara Bagassi for having accepted the role of Supervisor and for providing support throughout the activities related to my internship and thesis. Her availability and effective guidance were deeply appreciated.

I also wish to thank Professor Fabio Olivetti for accepting the role of examiner and for granting me the opportunity to carry out my thesis and internship activities at ENAV Training Center.

A special thanks goes to Eng. Tommaso Fadda, Dr. Eng. Carlo Alfredo Persiani and to my internship supervisor Gianluigi Bo for their expert guidance and continuous support.

Additionally, I extend my gratitude to ENAV as a company for allowing me to conduct my thesis and internship within its operational facilities and offices, providing me with a valuable experience. I would like to sincerely thank the air traffic controllers who participated in the survey and generously shared their expertise, greatly contributing to my research.

I deeply thank my family for always supporting my academic choices and allowing me to pursue my passion. A particular thanks to my grandfather Alberto for the assistance throughout the development of this work.

I would like to thank my university mates, who have also become great friends. Having shared these years of study with them has allowed me to fully enjoy this journey.

Finally, I would like to express my gratitude to my friends, who have been a constant source of inspiration and energy. Their encouragement has always pushed me to think big and aim higher.

Abstract

This work focuses on Air Traffic Management (ATM) solutions for increasing efficiency, safety, environmental sustainability, service quality and face the increasing demand for air transport. Particular attention is paid to the Arrival Manager (AMAN) system, a relatively new technology developed by the Single European Sky ATM Research (SESAR) and implemented in congested hubs all over Europe. Due to its low acceptability by air traffic controllers, its use is limited. After observing the operative environment, the main causes of the issue seem to be related to the Human-Machine Interface (HMI). For this reason, a Human Factors analysis of the HMIs is conducted. First, a simulator replicating the current AMAN system and logic is built as a reference framework. Then, a new solution interface is proposed and studied in its Human Factors aspects such as data accessibility, workload and Situational Awareness. The simulator is stable in different scenarios and provides reasonable results. The Human Factors analysis on the proposed interface, carried out involving operative air traffic controllers, highlights the need of establishing a communication, currently absent, between the radar interface and the AMAN HMI. In particular, the study underlines the need to provide the AMAN delay advice output in the aircraft label presented on the radar interface and to use a color gradient to represent the magnitude of the delay assigned by the system.

Contents

Introduction	1
1 Air Traffic Demand Analysis	5
1.1 European Statistics and Demand	5
1.2 Italian Statistics and Demand	7
2 Air Traffic Management (ATM) - Frame of Reference	11
2.1 Fundamentals of ATM and Airspace Organization	11
2.1.1 International Civil Aviation Organization (ICAO)	11
2.1.2 Air Traffic Management (ATM)	12
2.1.3 Air Traffic Services	12
2.1.4 Airspace Volumes	13
2.1.5 Airspace Classification	20
2.1.6 Air Navigation Aids	20
2.1.7 Flight Phases and Procedures	21
2.1.8 Separation and Separation Minima	23
2.2 Single European Sky ATM Research	24
3 The Arrival Manager (AMAN): a Human Factors Perspective	30
3.1 State of Work	30
3.2 AMAN Structure and Logic	32
3.2.1 Inputs	33
3.2.2 Outputs	35
3.2.3 Processing	35
3.3 Human Factors Limitations in AMAN	43
3.3.1 Human Factors in Air Traffic Management	43
3.3.2 Workload	44
3.3.3 Situational Awareness	48
4 AMAN Simulator - Methodology and Simulation Model	50
4.1 Hypothesis	50
4.2 Inputs	51
4.3 Processing & Outputs	55
4.3.1 Trajectory Prediction	56
4.3.2 Sequencer	74

5	Human Factors Study on the Solution AMAN Interface	78
5.1	AMAN and Radar Interface	78
5.2	Baseline HMI	78
5.2.1	Radar Screen	79
5.2.2	AMAN Screen	81
5.3	Solution HMI	82
5.4	Human Factors Analysis	84
6	Results and Discussion	86
6.1	Simulation Results and Considerations	86
6.2	Human Factors Analysis Results	90
	Conclusions	95
A	Appendix A: The Rhumb Line Model	101
B	Appendix B: The Wind Problem	105
C	Appendix C: HMI ATCOs Questionnaire	107
D	Appendix D: Simulation Scenarios	109

List of Figures

Fig. 1: Number of the European passengers travelling by plane over time[1].	6
Fig. 2: Number of European passengers travelling by plane, with linear projection up to year 2030.	6
Fig. 3: Number of Italian passengers travelling by plane, with a linear projection up to 2030 [2].	7
Fig. 4: Number of Italy passengers in Milan Malpensa and Rome Fiumicino, the two main Italian international hubs [2].	8
Fig. 5: Average daily arrival flight delays in 2023 at Milan Malpensa (MXP) and Rome Fiumicino (FCO)[3].	9
Fig. 6: Rome Fiumicino (LIRF) ATZ Airspace[9].	14
Fig. 7: Rome CTR Airspace[9], the different “zones” are drawn in blue.	15
Fig. 8: Rome TMA Airspace[9], the different “zones” are drawn in light blue.	16
Fig. 9: The three Italian FIRs and UIRs with the corresponding horizontal boundaries [9].	18
Fig. 10: Overview of the different airspace volumes.	19
Fig. 11: Public institutions and private companies involved in the SESAR programme [17].	26
Fig. 12: The innovation pipeline with a brief description of its three stages represented by the SESAR JU [19].	28
Fig. 13: The synthetic flow diagram of the AMAN system, highlighting its inputs and outputs.	33
Fig. 14: Conventional RDPS Architecture: the radar device, RDPS and display devices, represent the three subsystems [31].	34
Fig. 15: The logic breakdown beyond the Trajectory Prediction proposed by Eurocontrol [35].	37
Fig. 16: AMAN schematic flow diagram.	38
Fig. 17: Delay sharing example. Each sector presents a different capacity, written in blue. The flight “ITY123” has to gain 10 minutes while crossing sectors 1, 2 and 4.	40
Fig. 18: Complete AMAN flow diagram and algorithm.	42
Fig. 19: The Human Factors performance circle. The main elements contributing to the human performance and workload are highlighted [38].	45
Fig. 20: The main factors determining the task load and the workload in the ATC environment [38].	45
Fig. 21: Scale used in the NASA-TLX for assigning the magnitude to each task [39].	47
Fig. 22: The Situational Awareness levels described according to Endsley et.al. [40]	49

Fig. 23: The Situational Awareness levels interconnected with the Decision-Making and Performance [40].	49
Fig. 24: The simulator compact algorithm; the inputs, given as Excel tables, are listed in the left. The two main computational blocks are resembling the real AMAN algorithm.	55
Fig. 25: The trajectory prediction algorithm; the inputs are represented as green blocks, the functions as blue blocks and the outputs are in black. The main output (ELDT) is highlighted in yellow.	56
Fig. 26: Schematic representation of the “GetRoutes” function; the inputs and the outputs are presented.	57
Fig. 27: Route of the flight “ITY123”. In black the route starting from the entry airway waypoint, in blue the STAR procedure and in green the ILS approach.	58
Fig. 28: The schematic representation of the “GetTAScruise” function; the inputs and the outputs are shown.	62
Fig. 29: Wind forecast over Europe, issued by WAFC London [43].	64
Fig. 30: Discretization of the Italian airspace into “weather sectors” for modelling the wind in the skies.	65
Fig. 31: The “GetWX” function represented along with the “GetRoutes” and “GetTAScruise” function. The function outputs are highlighted in yellow.	68
Fig. 32: The “GetTOD” function in the algorithm, the outputs are highlighted in yellow.	70
Fig. 33: Runway spacing (in nautical miles) according to the computed Estimated Landing Times ELDTs.	75
Fig. 34: Runway spacing (in nautical miles) according to the computed Target Landing Times TLDTs. The Time To Lose or Time To Gain is shown in green and red respectively. In cyan the neutral delay advice.	76
Fig. 35: The designed baseline interface; on the right-hand side, the radar screen with the traffic and the corresponding label is shown. On the left-hand side the AMAN timeline is presented.	79
Fig. 36: The designed solution interface; on the right side, the radar screen with the traffic and the corresponding label is shown. On the left side the AMAN timeline is presented.	82
Fig. 37: The color gradient used for positive delay advices.	83
Fig. 38: The color gradient used for negative delay advices.	83
Fig. 39: Questionnaire answers provided by the two questioned subjects involved in the test. Highlighted in green the personal anonymous questions, in light blue the data accessibility questions and in light orange, the situational awareness questions.	94

Fig. 40: Representation of a generic rhumb line in the global sphere; it is possible to see how the angle between the meridians and the route (true course TC) is constant [45]. 101

Fig. 41: Representation of the Latitude and Longitude in the earth's sphere. 102

Fig. 42: The rhumb line triangle in the earth sphere model. 103

Fig. 43: The rhumb line triangle. 103

Fig. 44: The wind triangle with the vectors $\overrightarrow{TC/GS}$, $\overrightarrow{TH/TAS}$ and $\overrightarrow{WD/WV}$ 105

List of Tables

Tab. 1: Average quarterly arrival flight delays (in minutes) at Rome FCO and Milan MXP compared to the national average in 2023.	9
Tab. 2: Average quarterly arrival delays (in minutes) in Italy compared to the European average in 2023.	10
Tab. 3: Example of scheduled arriving flights and their corresponding flight plan details. .	51
Tab. 4: Example of the Base of Aircraft Data (BADA) information arranged in an input table, using an Airbus A320 as an example.	52
Tab. 5: Separation (in nautical miles) between consecutive landing aircraft according to the wake turbulence category and to the LIRF standard operations in runway 16L.	53
Tab. 6: Geographical coordinates of waypoints in the Italian airspace [9], ϕ represents the latitude and λ the longitude.	53
Tab. 7: Rome Fiumicino “LAT3A” standard arrival procedure (STAR) for runway 16L [9].	54
Tab. 8: Rome Fiumicino runway 16L ILS procedure [9].	54
Tab. 9: Scheduled arriving flights with the corresponding flight plans information.	57
Tab. 10: Limits, expressed as longitude and latitude in degrees, of the different sectors shown in Fig. 30.	64
Tab. 11: Wind velocity in knots for each sector at different flight levels, according to the meteorological charts.	66
Tab. 12: Wind direction in degrees for each sector at different flight levels, according to the meteorological charts.	66
Tab. 13: Aerodrome wind velocity in knots and direction in degrees. The data is obtained by the METAR aerodrome message.	67
Tab. 14: Human Factors model to understand the controller critical thoughts about the presented solution.	85
Tab. 15: Traffic Scenario 1 Results. The Sequence Number, Estimated Landing Time (ELDT), Target Landing Time (TLDT), Delay Advice and Separation are provided for each aircraft in the scheduled arrivals. The simulation starting time is 12:00:00.	87
Tab. 16: Traffic Scenario 2 Results. The Sequence Number, Estimated Landing Time (ELDT), Target Landing Time (TLDT), Delay Advice and Separation are provided for each aircraft in the scheduled arrivals. The simulation starting time is 10:15:00.	87

Tab. 17: Traffic Scenario 3 Results. The Sequence Number, Estimated Landing Time (ELDT), Target Landing Time (TLDT), Delay Advice and Separation are provided for each aircraft in the scheduled arrivals. The simulation starting time is 17:00:00. 87

Tab. 18: Traffic Scenario 4 Results. The Sequence Number, Estimated Landing Time (ELDT), Target Landing Time (TLDT), Delay Advice and Separation are provided for each aircraft in the scheduled arrivals. The simulation starting time is 15:45:00. 88

Tab. 19: Traffic Scenario 5 Results. The Sequence Number, Estimated Landing Time (ELDT), Target Landing Time (TLDT), Delay Advice and Separation are provided for each aircraft in the scheduled arrivals. The simulation starting time is 21:30:00. 88

Tab. 20: Human Factors model to understand the controller’s critical thoughts about the presented solution: the answers of the two subjects are presented. The (2) at the end of the sentence means both the ATCOs have provided that answer. 93

Tab. 21: Traffic Scenario 1. Scheduled arriving flights and the corresponding flight plan details. 109

Tab. 22: Traffic Scenario 2. Scheduled arriving flights and the corresponding flight plan details. 109

Tab. 23: Traffic Scenario 3. Scheduled arriving flights and the corresponding flight plan details. 109

Tab. 24: Traffic Scenario 4. Scheduled arriving flights and the corresponding flight plan details. 110

Tab. 25: Traffic Scenario 5. Scheduled arriving flights and the corresponding flight plan details. 110

Acronyms

ACC Area Control Center

A-CDM Airport Collaborative Decision Making

ADS-B Automatic Dependent Surveillance-Broadcast

AIP Aeronautical Information Publication

ALRS Alerting Service

AMAN Arrival Manager

ANSPs Air Navigation Service Providers

APP Approach

ASM Airspace Management

ATC Air Traffic Control

ATCOs Air Traffic Control Officers

ATCS Air Traffic Control Service

ATFM Air Traffic Flow Management

ATM Air Traffic Management

ATS Air Traffic Service

ATZ Aerodrome Traffic Zone

BADA Base of Aircraft Data

CDO Continuous Descend Operations

CTOT Calculated Take-Off Time

CTR Control Zone

CWP Controller Working Position

DAPs Downlinked Airborne Parameters

DMAN Departure Manager

DME Distance Measuring Equipment

E-AMAN Extended AMAN

ELDT Estimated Landing Time

ENAC Ente Nazionale Aviazione Civile

ENAV Ente Nazionale di Assistenza al Volo

EOBT Estimated Off-Block Time

ETO Estimated Time Over

EU European Union

FIS Flight Information Service

FCFS First Come First Serve

FDPS Flight Data Processing System

FIC Flight Information Center

FIR Flight Information Region

FL Flight Level

FLDT Forecasted Landing Time

FMS Flight Management System

FRAIT Free Route Italy

FT Flight Time

FTOT Forecasted Take-Off Time

GPS Global Positioning System

GS Ground Speed

HF Human Factors

HMIs Human Machine Interfaces

IAF Initial Approach Fix

ICAO International Civil Aviation Organization

ILS Instrumental Landing System

IMC Instrumental Meteorological Conditions

IFR Instrumental Flight Rules

KPIs Key Performance Indicators

METAR Meteorological Terminal Air Report

MTOW Maximum Take-Off Weight

NASA National Aeronautics and Space Administration

NSAs National Supervisory Authorities

NWPs Numerical Weather Predictions

PANS Procedures for Air Navigation Services

PRB Performance Review Body

PRC Performance Review Commission

PSR Primary Surveillance Radar

RDPS Radar Data Processing System

RMAN Runway Manager

RO-CAT Reduced Separation Based on Local Runway Occupancy Time Characterisation

SA Situational Awareness

SARPs Standard And Recommended Practices

SES Single European Sky

SESAR Single European Sky ATM Research

SID Standard Instrument Departure

SSR Secondary Surveillance Radar

STAR Standard Arrival

TAS True Air Speed

TC True Course

TD Total Delay

TFCI Traffic Information

TH True Heading

TLDT Target Landing Time

TLX Task Load Index

TMA Terminal Control Area

TOBT Target Off-Block Time

TOC Top of Climb

TOD Top of Descend

TP Trajectory Prediction

TRL Technology Readiness Level

TSV Tactical Speed Vector

TTG Time To Gain

TTL Time To Lose

TTO Target Time Over

TTOT Target Take-Off Time

TWR Tower

UIR Upper Information Region

UNL Unlimited

VFR Visual Flight Rules

VMC Visual Meteorological Conditions

VOR Very High Frequency (VHF) Omnidirectional Range

VS Vertical Speed

WAFCs World Area Forecast Centers

WD Wind Direction

WPTs Waypoints

WV Wind Velocity

Introduction

Air transport is becoming increasingly popular with passengers travelling around the world. Statistical data shows that the number of passengers at airports is growing [1]-[2], leading to an increase in the number of flights. As a result, the infrastructure of airports, airlines, ground operators, air traffic control services, and all other parts involved in air transport must adapt and improve efficiency to meet this increasing demand. After the COVID-19 pandemic, air traffic has returned to pre-pandemic levels, reaching numbers never seen before and still exhibiting increasing trends.

The demand must also be managed efficiently to provide good quality services. A particularly important issue is indeed given by the delays caused by this high demand, which is especially noticeable in international hubs around the world, where delays often occur because the whole infrastructure is close to full capacity.

Statistical data shows that the management of arriving air traffic in international hubs contributes to the increase in delays. In Italy, the terminal areas of Milan and Rome are highly congested, and therefore, improvements in efficiency and capacity are needed.

In addition to improving efficiency, the environmental sustainability is playing a crucial role in the air transport network. Aircraft emissions and aeronautical systems are contributing to air pollution and environmental health. For this reason, more and more effort is put into finding solutions that balance both efficiency and environmental sustainability in air transport.

Furthermore, one crucial point that should never be forgotten is safety. All the operations, technological systems and solutions in air transport, must follow the principle *“safety first”*.

Among the different parts involved in air transport, the air traffic management (ATM) plays a crucial role in finding an equilibrium among these elements and handling the high demand. Indeed, the proper management of air traffic is essential for finding the right balance.

In this context, national institutions, private companies, and research groups are collaborating to develop new advanced solutions for air traffic management. To facilitate this cooperation, they have united in a collaborative framework known as Single European Sky (SES), which enhances the interoperability among the different parts in the air transport network. Within the SES, the Single European Sky ATM Research (SESAR) programme was established to design and deliver new technological solutions in the field of air traffic management.

Among the various areas in which SESAR operates, the management of arriving air traffic has been a primary goal in these years.

For this reason, different solutions have been proposed. One of the most recent, developed and delivered after years of study, is the Arrival Manager (AMAN). This new technology assists air traffic controllers in sequencing arriving flights when there is a high volume of arriving flights in the terminal area. The software provides an optimized flight sequence that allows to reduce delays, decrease emissions, improve the service levels, increase efficiency and lower costs, all while ensuring safety.

Even if AMAN appears to be an optimal solution for air traffic management, the solution is still not completely accepted by the users and presents some criticalities. The use of the system is indeed currently limited in real-world air traffic control environments due to several aspect. The objective of this work is to analyse and understand the working principles of AMAN, as well as to investigate the Human Factors related issues that limits its use and the benefits it provides.

As support to the next chapters, in the first part the statistical data and forecast in the airports is presented to help understand the numbers related to the high demand in Air Traffic Management. Successively, the basic ATM and Air Navigation concepts are given and explained in order to provide the required definitions and contexts to future explanations.

In the third chapter, the AMAN software is studied in its working principles and definitions and both technical and Human Factors analysis are conducted to identify the critical points of the system.

The analysis starts with a deep study of the real AMAN software and the logic behind the system. Then, a simulator environment is created to provide a basis for understanding the issues and complexities of AMAN and to work as frame of reference for the Human Factors related studies.

Among the different critical points of AMAN, one of the main issues is the interaction between the system and the user. To address this, a Human Factors study and analysis is conducted to identify the criticalities related to this aspect.

A study on the current AMAN interface and its level of acceptance is carried out and a new solution aimed to solve the interface issues is proposed. The final part of the work focuses on further Human Factors analysis of the proposed solution, involving workload and Situational Awareness studies, helping to assess the acceptability and the safety of this new approach. The validation of this study is conducted through collaboration with air traffic controllers, who are involved in a guided Human Factors analysis.

1 Air Traffic Demand Analysis

This thesis work focuses on the arrival segment of high-density air traffic flow airports, addressing the challenges and opportunities in optimizing arrival processes. Particular attention is given to the technologies studied, developed, and implemented by SESAR (Single European Sky ATM Research) to meet the increasing demand in air traffic, reduce delays, and optimize the ATM system to ensure high safety levels and environmental benefits.

A brief statistical overview and forecast of air traffic conditions in Europe and Italy is first provided to contextualize and give numbers about the high demand in the Italian skies. The analysis highlights the growing demand for air travel and the need for innovative solutions to manage increased traffic volumes while maintaining safety and operational efficiency.

1.1 European Statistics and Demand

The EU air traffic data has been collected from the official “Eurostat” website [1]. In Fig. 1, the number of passengers in the European airports is plotted. The graph clearly shows an overall positive trend until 2020, where a sudden and sharp decline is observed due to the COVID-19 pandemic. Moreover, a moderate decrease can be noted after 2008, corresponding to the economic crisis faced by EU countries during that period.

Focusing on the long-term trend in passenger numbers, excluding the impact of the 2020 crisis, the data reveals a consistent increase over the years. In fact, with the reducing effects of the pandemic, air traffic movements, reflecting the growing passenger numbers, have reached unprecedented levels. In Fig. 2, the regression line calculated using data up to 2019 is shown. Based on Eq. 1, it is estimated that by 2030 the number of passengers in the EU will reach 1.26 billion, representing a 20% increase compared to 2023.

$$pax = 3 \cdot 10^7 \cdot (year - year_0) + 6 \cdot 10^8 \quad (1)$$

Since the regression demonstrates a good fit to the data ($R^2 = 0.9029$, indicating that the model explains 90.29% of the variance in passenger numbers), this simple linear forecast provides a reliable basis for analyzing the trend and projecting future passenger numbers in the EU.

The statistical analysis presented so far helps to clarify the rationale behind the SESAR programme, as well as the accelerating technological advancements in the aerospace industry. However, improvements in air traffic management efficiency alone are insufficient to meet the growing de-

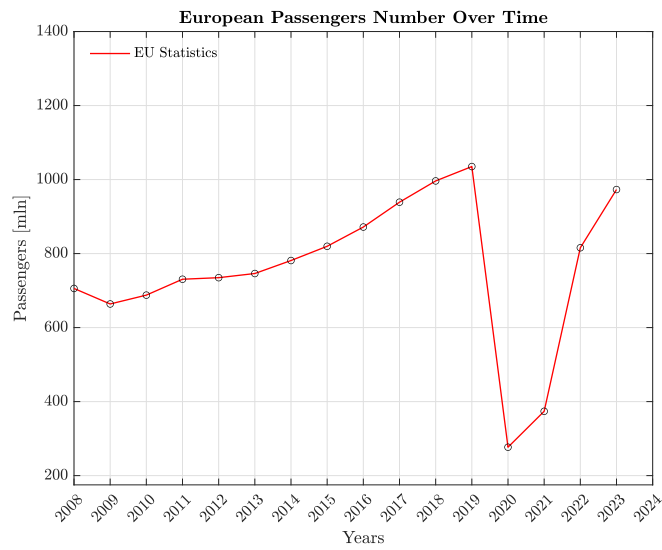


Figure 1: Number of the European passengers travelling by plane over time[1].

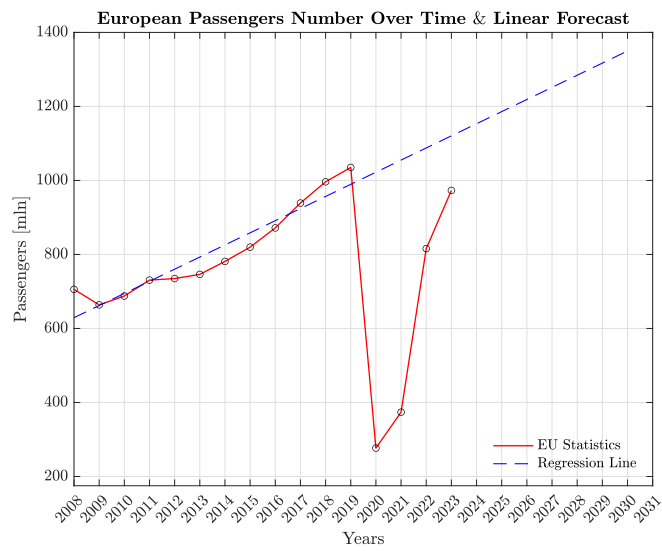


Figure 2: Number of European passengers travelling by plane, with linear projection up to year 2030.

mand illustrated in Fig. 2. Addressing this challenge requires the design of new airport layouts, the strengthening of logistics and transportation networks, and advancements in overall aeronautical technologies.

1.2 Italian Statistics and Demand

The statistics for the Italian airspace are now discussed and presented. The data from the previous section, in fact, is distributed unevenly among EU countries. Fig. 3 shows the passenger numbers and the related forecast for the Italian portion.

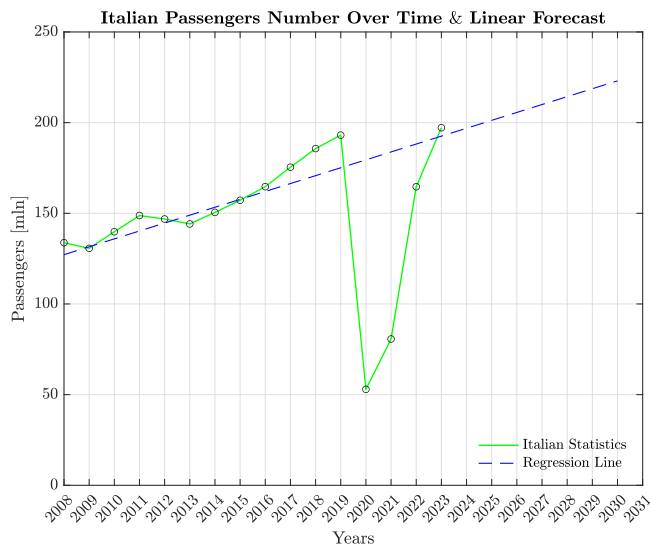


Figure 3: Number of Italian passengers travelling by plane, with a linear projection up to 2030 [2].

The regression equation estimates that by 2030 the number of Italian passengers will reach around 231 millions, representing a +17% increase compared to 2023. The two main hubs in Italy are Rome Fiumicino (FCO) and Milan Malpensa (MXP); Fig. 4 shows that about 40% of Italian passengers fly to or from one of these two international airports. The growing number of passengers travelling through Italian airports reflects an increasing demand, leading to a rise in flight movements and operations within Italian airspace. The main Italian airports, Rome FCO and Milan MXP, are likely to see flight volumes grow from current levels (approximately 267,000 and 202,000 flights per year for Rome and Milan, respectively) to pre-COVID levels (2019: 310,000 and 234,000 flights per year for FCO and MXP) or even higher.

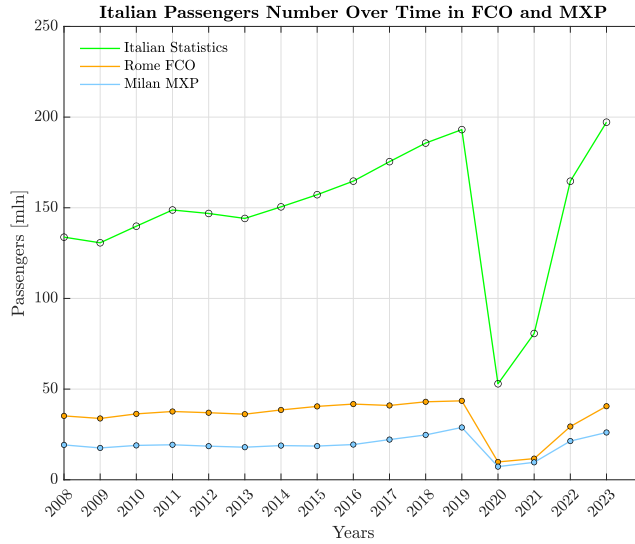


Figure 4: Number of Italy passengers in Milan Malpensa and Rome Fiumicino, the two main Italian international hubs [2].

This brief overview of statistics and forecasts for Italy’s main airports, and the previously discussed EU data, highlights the need to study, develop, and implement technological solutions for optimizing the air traffic management (ATM) system. As mentioned earlier, the SESAR programme was designed for this purpose and among the various areas SESAR addresses, this thesis focuses on technological solutions for the arrival segment.

Indeed, managing air traffic flow at major airports during peak hours and peak months is one of the most critical challenges for the ATM system, as it represents the time when most of the delay occurs. In Fig. 5, the arrival flight delays at Rome and Malpensa airports during 2023 are shown. The delay distribution shows an increase starting in spring and finishing in September; this is probably due to the the sharp rise in passenger numbers during the vacation season.

This recurring delay pattern is observed every year, even if local peaks can appear due to exceptional events such as bad weather, staff strikes, and similar occasional issues.

To highlight the seasonal effects on delays, a quarterly segmentation is provided in Tab. 1, where a comparison between Rome FCO, Milan MXP, and the overall arrival delays in Italian airspace is shown.

It is evident that the arrival delays at Milan Malpensa are consistently several percentage points higher than the Italian average. Even though the Italian airspace is among the most efficient ones in Europe for managing arriving flights (Tab. 2), further reductions in delays and optimization of

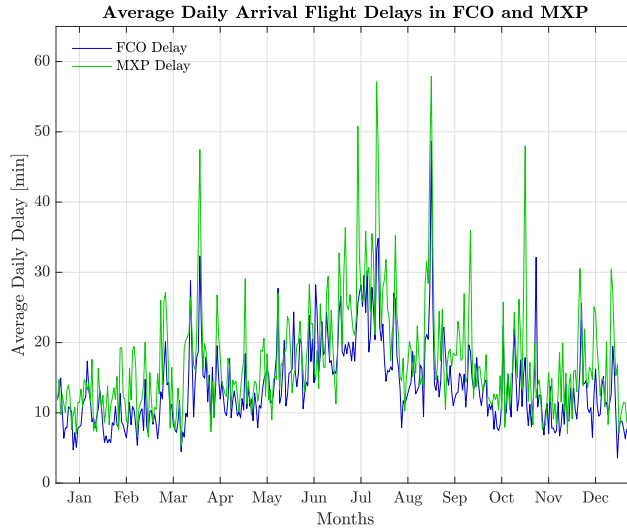


Figure 5: Average daily arrival flight delays in 2023 at Milan Malpensa (MXP) and Rome Fiumicino (FCO)[3].

trajectories and arrival sequences in the major hubs can significantly decrease fuel consumption and pollutant emissions. While the savings for a single flight may seem minimal, the impact becomes important when high-density air traffic areas are considered.

Table 1: Average quarterly arrival flight delays (in minutes) at Rome FCO and Milan MXP compared to the national average in 2023.

Average Quarterly Arriving Flight Delays [min] at FCO and MXP								
/	Jan-Mar	%	Apr-Jun	%	Jul-Sep	%	Oct-Dec	%
Italian Airspace	10.9	—	15.9	—	19.7	—	12.6	—
Rome FCO	10.1	-7.2%	15.4	-3.3%	18.3	-7.2%	11.7	-7.2%
Milan MXP	13.5	+24.3%	17.7	+11.1%	23.5	+19.2%	15.4	+22.0%

For this reason, new technological tools for handling the arriving traffic and helping the air traffic control officers (ATCOs) in minimizing delays, have been developed by SESAR. Among the different systems, this thesis focuses on the “Arrival Manager” called AMAN; this has been implemented at major airports across Europe and, in Italy, AMAN is currently operative in the Rome TMA (for Ciampino and Fiumicino Airports) and the Milan TMA (covering Malpensa, Linate, and Orio al Serio Airports).

The benefits of AMAN will be discussed in more details in the following sections. However, an initial estimation by ENAV SpA [4] highlights its impact: for Malpensa Airport alone, the system

Table 2: Average quarterly arrival delays (in minutes) in Italy compared to the European average in 2023.

Average Quarterly Arriving Flight Delays [min] in Europe and Italy								
/	Jan-Mar	%	Apr-Jun	%	Jul-Sep	%	Oct-Dec	%
European Airspace	14.2	–	16.8	–	19.3	–	15.7	–
Italian Airspace	10.9	–23.5%	15.9	–5.3%	19.7	+2.3%	12.6	–19.9%

achieves an average reduction of 30 seconds per flight, equivalent to about 2.6 NM less flown, resulting in a 30 kg fuel saving (93 kg of CO₂ emissions) per flight [4].

If AMAN were fully operational at EU hubs every day, the yearly fuel savings would increase significantly, leading to strong reductions in CO₂ emissions. This, would bring multiple benefits, including reduced delays, improved airline efficiency, enhanced passenger comfort, better environmental health, increased safety, and overall system efficiency.

2 Air Traffic Management (ATM) - Frame of Reference

Before going into the detailed analysis of the AMAN technology, it is important to first understand the basic concepts of air law and the key principles of air traffic management. These elements are essential to fully understand how the AMAN technology is used and applied in air traffic operations. This chapter so, provides the necessary background by defining the system's framework and offering the context needed to understand the following discussions.

2.1 Fundamentals of ATM and Airspace Organization

2.1.1 International Civil Aviation Organization (ICAO)

In 1944, the Chicago Convention on International Civil Aviation established a new aeronautical agency called ICAO (International Civil Aviation Organization) with the purpose of ensuring safe and efficient management of flights in the skies around the world. It is ICAO that has established the rules for the growth of air transport in order to guarantee the highest level of uniformity among the different Nations. These technical rules are described in the “*Annexes*”, regulatory documents provided to the different members; the annexes contain the *Standard and Recommended Practices (SARPs)* (the *standard practices* must be mandatorily adopted by the members, while the *recommended practices* are norms for improving safety and regularity in air navigation for which members are invited to adhere without any obligation).

Along with the SARPs, ICAO is also providing the *Procedures for Air Navigation Services (PANS)* explained in *DOCs*, documents that are complementary to the annexes and contain operative norms for the implementation of the SARPs rules.

Finally, ICAO defines the *Supplementary Procedures*; these are rules and norms for a specific ICAO region aiming to better adopt the standard rules according to the different local meteorological and orographic situations and local needs.

The ICAO annexes transposition for each member is the responsibility of each unique regulatory institution, which in Italy is represented by ENAC (Ente Nazionale Aviazione Civile); it has the role of inspecting, controlling, regulating, and monitoring national aeronautical activities. It is responsible for issuing and certifying licenses and managing all goods in the aeronautical State properties [5].

Going through some of the ICAO annexes and the regulatory instruments explained above, an overview of air traffic management and services along with the sky volume organization and classification is now provided.

2.1.2 Air Traffic Management (ATM)

Being the air traffic management the central topic of this thesis, a strict definition given by the ICAO Doc. 4444 [6] is provided: *“The dynamic, integrated management of air traffic and airspace including air traffic services, airspace management and air traffic flow management — safely, economically and efficiently — through the provision of facilities and seamless services in collaboration with all parties and involving airborne and ground-based functions.”*

The ATM provides the following three services:

- Air Traffic Service (ATS). The primary role is to prevent collisions and ensure an organized flow of air traffic. ATS depends on tactical interventions by controllers and direct communication with flight crews, typically throughout the entire flight.
- Air Traffic Flow Management (ATFM). With this service, the efforts is placed to balance supply and demand by spreading traffic over time and space and improving control capacity planning. This includes setting restrictions on traffics and airspaces as well as increasing supply by managing sectors.
- Airspace Management (ASM). This service has as main goal to manage the airspace as efficiently as possible to meet the needs of its diverse users, both civil and military. This service involves both the allocation of airspace to different users (via routes, zones, flight levels, etc.) and the organization of airspace to ensure the delivery of air traffic services.

2.1.3 Air Traffic Services

Among the 19 annexes provided by the ICAO, Annex 11 [7] gives the norms and rules about air traffic services, airspace foundation, and air service authorities.

As defined in Annex 11, the objectives of the air traffic services shall be:

1. prevent collision between aircraft
2. prevent collision between aircraft on the maneuvering area and obstructions on that area
3. expedite and maintain an ordered flow of air traffic
4. provide advice and information useful for the safe and efficient conduct of flights
5. notify appropriate organizations regarding aircraft in need of search and rescue aid, and assist such organizations as required

The air traffic services are divided into three blocks:

- **ATCS** (Air Traffic Control Service). This service aims to accomplish objectives 1, 2 and 3 stated above and it will be further divided into more parts:
 - i. Area Control Service
 - ii. Approach Control Service
 - iii. Aerodrome Control Service.
- **FIS** (Flight Information Service). This service accomplishes the objective 4 presented above.
- **ALRS** (Alerting Service). This service accomplishes the objective 5 presented above.

2.1.4 Airspace Volumes

Annex 11, in addition to the ATS services, presents a description of the division into blocks of a Nation's airspace; indeed, the air services previously discussed are delivered according to the portion of airspace and the corresponding classification.

Before listing and describing the different volumes of air, the definition of *controlled* and *uncontrolled* airspace is provided:

- **Controlled Airspace**. A controlled airspace refers to those air portions where the **ATCS** service is provided (along with FIS and ALRS) to IFR flights (it can also be applied to VFR flights according to airspace class; this will be explained later).
- **Uncontrolled Airspace**. A not controlled airspace instead applies to the airspaces where the **ATCS** service is not provided neither to IFR flights nor to VFR flights. Only flight information (TFCI ¹), FIS and ALRS service can be delivered (according to the airspace class).

The airspace is divided in the following volumes:

1. **ATZ (Aerodrome Traffic Zone)**. This is a cylinder of radius 5 *NM* centered in the aerodrome; its lower limit is the ground and its upper limit corresponds to 2000 *ft* (there might be cases of non-conventional ATZs with different height limits and shapes). The ATZ is a *controlled* airspace aiming to protect the aerodrome, manage the air traffic around the airport, and handle all the operations on the ground and on the runway (take-offs, landings and

¹Traffic Information - TFCI. It is a service provided by an ATS organization. Pilots receiving this service are informed of any known or observed traffic that may be in a position relative to their aircraft or planned flight route that requires their particular attention.

crossings).

The operative authority designed to operate in the ATZ is the control **Tower (TWR)**; it can present a single position in small airports (where the tower is capable of handling all the traffic) or it can be segmented into more positions (*Ground* and *Tower*) in larger airports.

The *Ground* manages the movements in the apron and on the taxiways, provides the IFR clearances². The *Tower* instead manages the aerodrome flying traffic (touch and go procedures, traffic patterns, airspace crossings, take-offs, landings and so on).

In particularly congested airports and hubs, in order to lighten the *Ground* load, a further position can be opened and it takes the name of *Delivery*; it has the role to provide IFR clearances and engine start-up authorizations to aircraft [8].

An example of Rome Fiumicino ATZ is given in Fig. 6.

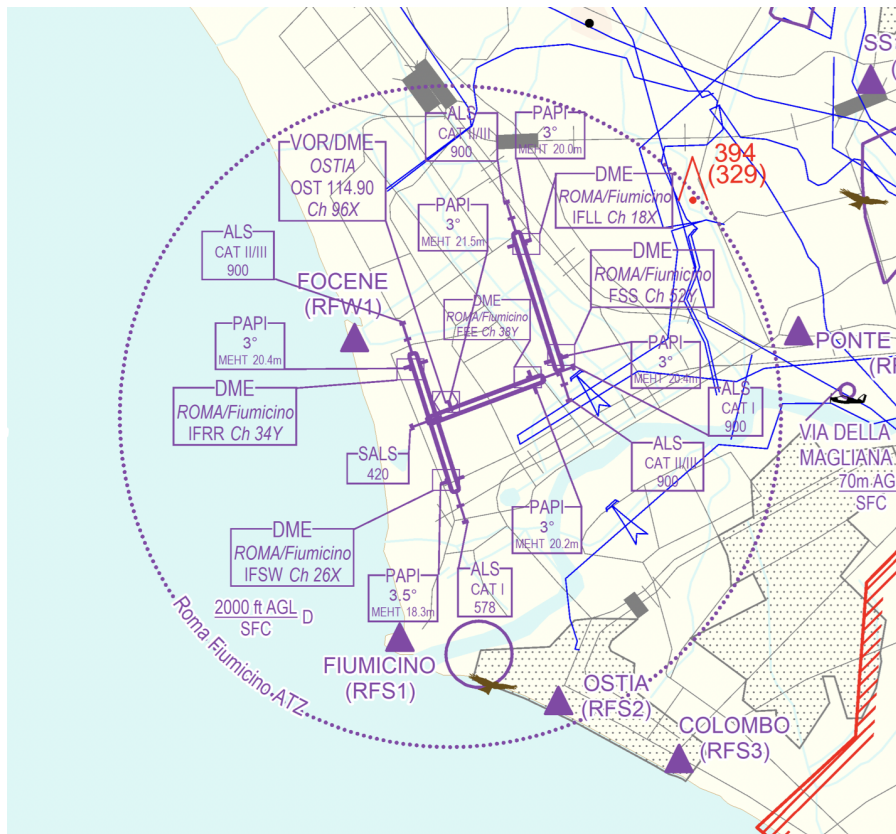


Figure 6: Rome Fiumicino (LIRF) ATZ Airspace[9].

²IFR Clearance. It is an authorization given by air traffic controllers for an aircraft to proceed in controlled airspace under IFR (see § 2.1.5) conditions.

2. **CTR (Control Zone)**. This *controlled* airspace is established in order to protect and manage the air traffic during their approach and initial climb phases to and from the destination airport respectively. A single CTR can be further divided into “zones” (each with a different boundary and lower/upper limit) and can handle flights operating in different aerodromes; the air traffic control is possible using surveillance systems such as radars. The CTR typically includes the ATZs within its boundaries and vertical limits as shown in Fig. 7. Indeed, in the figure, it is possible to appreciate that the “Rome CTR” with its division into “zones” gathers more than one single ATZ (in this case Fiumicino, Ciampino, and Urbe). The authority in charge of the CTR is called **Approach (APP)**; it can be made up of a single sector or divided into more sectors according to the airport and area.



Figure 7: Rome CTR Airspace[9], the different “zones” are drawn in blue.

3. **TMA (Terminal Control Area)**. The TMA is a *controlled* airspace designed to further segment the sky and assist in managing flights in the main National hubs (in Italy, Rome and Milan) where high volumes of traffic are handled every day. The TMA can be seen as a connection between the CTR (handling the final phase of approach/first phase of climb) and the AWYs (Airways) where aircraft are typically at the end of their climb/beginning of their

descent phase. As for the CTR, the TMA is divided into “zones” to help direct flights in the airports included in the terminal area; for instance, taking Rome as an example, the TMA helps in handling traffic flying to/from Fiumicino and Ciampino.

The TMA includes the CTR and the ATZ inside; its lower vertical limit typically corresponds to the CTR’s higher vertical limit, but it can vary from case to case and zone to zone.

An example of the Rome TMA is shown in Fig. 8 (light blue areas).

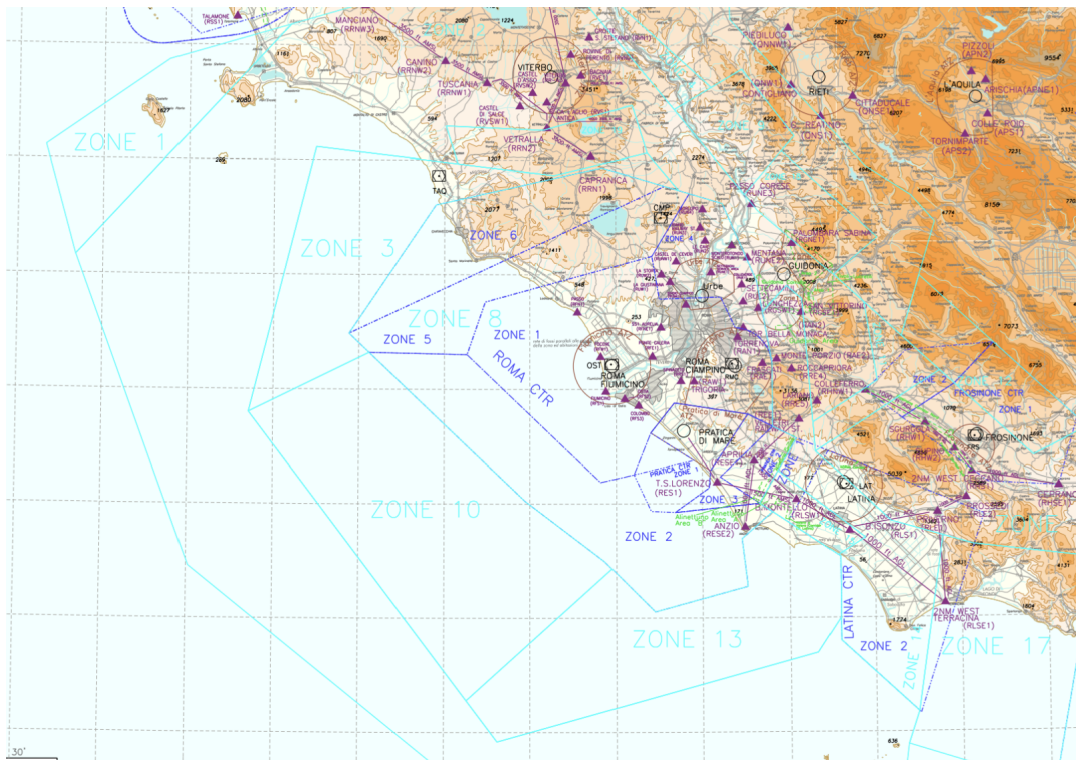


Figure 8: Rome TMA Airspace[9], the different “zones” are drawn in light blue.

4. **AWYs (Airways)**. The airways are defined as *controlled* “corridors” where flights operate in cruise or in their final phase of climb/initial phase of descent. They are identified by a name (e.g. *M726*) and they connect route waypoints (WPTs) below FL195³. Along with the concept of airways, a relatively new routing system, called **FRAIT** (Free Route Italy), is adopted in the Italian skies above flight level FL195; in this airspace, the traffic is allowed to

³Flight Level - FL. It is the pressure altitude in feet, divided by 1000. The pressure altitude represents the height from the isobaric level 1013.25 hPa (International Standard Atmosphere (ISA) pressure at mean sea level) and the aircraft. Using flight levels is necessary to provide the same barometric references to all flights avoiding the danger of collisions.

plan direct routes from an entry point to an exit point.

The authority managing the flights in the airways and in the FRAIT airspace is the **Area Control Center (ACC)**, responsible for delivering the ATS services in these areas. The ACC is divided into different operative sectors that change according to the needs; each configuration is called “sectorization”. One sector can, for instance, be split into two vertical sectors when the traffic demand exceeds the single sector’s capacity; this allows avoiding delays and issuing slots⁴.

5. **FIR (Flight Information Region)**. This *uncontrolled* airspace goes from the ground to FL195 and fills the gaps where the other airspaces (ATZ, CTR, TMA, AWY) are not present. It can be seen as the large box containing all the above-mentioned volumes below FL195. The operative authority managing the FIR is called **Flight Information Center (FIC)**; in Italy, there are three FIRs (Rome, Milan, and Brindisi) but four FICs: Rome, Milan, Brindisi, and Padova. The Milan FIR is controlled by two operative centers: Padova FIC and Milan FIC. To better explain the division, an image of the FIR (and UIR) boundaries is provided in Fig. 9.

Aircraft flying in the FIR are provided with the FIS and ALRS services, but the ATCS service is not delivered since the FIR is a uncontrolled airspace.

6. **UIR (Upper Information Region)**. The UIR airspace has the same FIR horizontal limits but extends from FL195 to unlimited (UNL). The UIR is further divided into two sectors: the first goes from FL195 to FL660 and is a *controlled* airspace (class C), while from FL660 to UNL (unlimited) it is *uncontrolled* airspace (class G), and the FIC will be the in-charge authority.

To facilitate the comprehension and sum-up the different concepts explained before, a vertical overview of the sky segmentation is provided in Fig.10.

⁴If capacity is less than demand, then the demand needs to be managed by giving the aircraft a slot stating when it can take off – the “Calculated Time of Take Off” (CTOT). Usually, an aircraft is allowed to take off within five minutes before and ten minutes after the CTOT. If the aircraft can’t achieve this take-off time, it has to wait for a new slot [10].

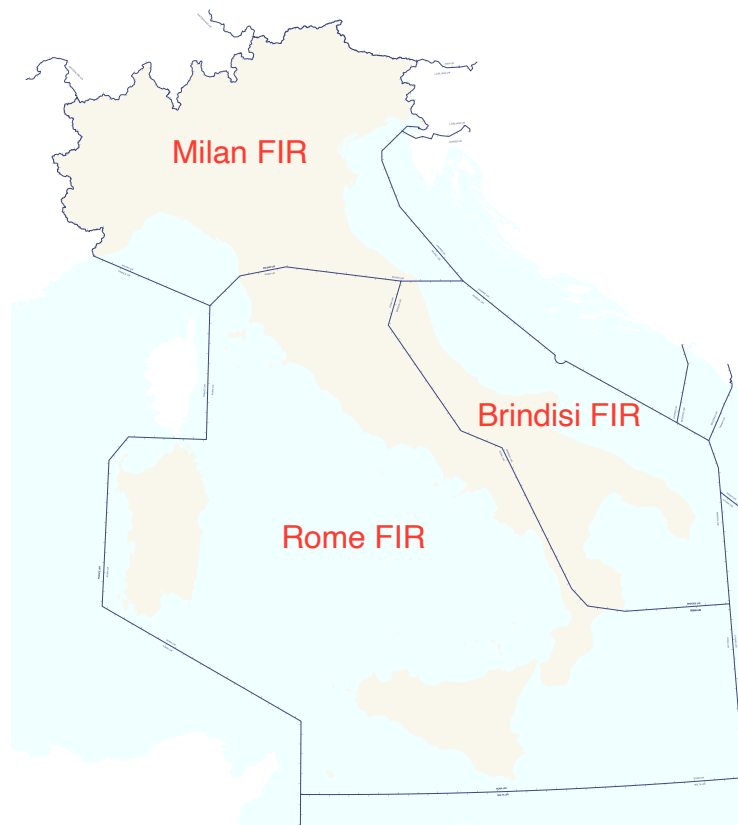


Figure 9: The three Italian FIRs and UIRs with the corresponding horizontal boundaries [9].

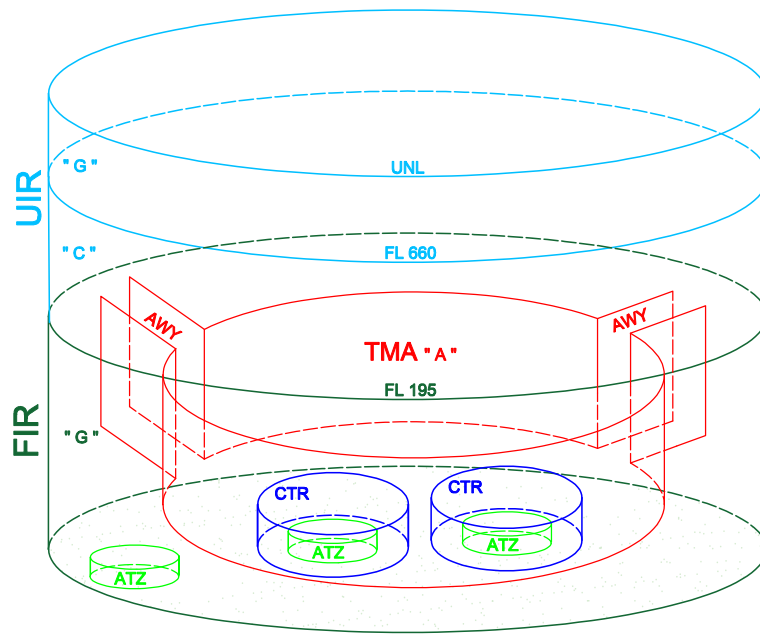


Figure 10: Overview of the different airspace volumes.

2.1.5 Airspace Classification

Having defined the various airspace volumes, the primary structure of airspace management and the division of the sky into blocks should now be clear. Beyond this segmentation of national airspace, it is crucial to discuss the classification of each block; indeed, each of them is assigned a specific “class” based on its strategic importance and intended use. Each class corresponds to a set of rules that are applied to the airspace itself.

In Italy, the classes range from **A** to **G** excluding the letter B and F.

The *controlled* airspaces are classified **A**, **C**, **D**, **E** while the *uncontrolled* airspace is the **G** airspace.

The rules applied to each class involve the two categories of flight rules: IFR and VFR flights:

- **Visual Flight Rules (VFR)**. The VFR flights follow the theorem “SEE AND TO BE SEEN”.

Traffics flying VFR are responsible of maintaining visual separation with obstacles and other traffics (except in airspaces where ATCS is provided to VFR flights).

They can only fly under **VMC** conditions⁵.

- **Instrumental Flight Rules (IFR)**. The IFR flights are those traffics operating with the assistance of on board instruments.

The separation with other traffics is provided by the ATC authority if flying in controlled airspaces while the obstacle separation is pilot’s responsibility (except if the aircraft is vectored).

The IFR flights can operate both in **VMC** and **IMC** conditions⁶.

The classification rules applied to each class are described in detail in the national service provider AIP (Aeronautical Information Publication) website [9].

2.1.6 Air Navigation Aids

In order to give context and understand future discussions in the next chapters of this work, a brief explanation about the air navigation aids (NavAids) is given.

NavAids refer to any visual or electronic systems, either airborne or on the ground, that provides directional guidance or location information to aircraft during flight.

Among the different NavAids, the most widely used are listed below.

⁵Visual Meteorological Conditions - VMC. They are the meteorological conditions expressed in terms of visibility, distance from the clouds, and ceiling equal to or better than the specified minima [11].

⁶Instrument Meteorological Conditions - IMC. They are meteorological conditions expressed in terms of visibility, distance from the clouds, and ceiling, less than the minima specified for VMC [11].

1. *Very High Frequency Omnidirectional Range (VOR)*. This NavAid, helps in providing the direction information with respect to the point in which the VOR is located. This means the VOR is giving the angle between the magnetic north and the segment starting in the station (VOR) and ending in the aircraft. This angle is called *radial*.
2. *Distance Measuring Equipment (DME)*. This NavAid, helps in providing the distance from the DME position to the aircraft. The distance is called *slant distance* being calculated as the straight line distance between the aircraft and the station.
3. *Instrumental Landing System (ILS)*. This NavAid, is used by the pilots during the landing phase. It allows to be perfectly aligned with the runway center line and at the correct altitude during the landing. This is possible through two subsystems: the *glide slope*, ensuring the aircraft flies at the correct altitude, and the *localizer*, providing the horizontal alignment information.
4. *Automatic Dependent Surveillance-Broadcast (ADS-B)*. The ADS-B is a surveillance technology where the aircraft determines its position via satellite navigation. It works by broadcasting information about an aircraft's location, altitude, ground speed and other data to ground stations and other aircraft, once per second.

When the DME is placed in the same position of the VOR, the NavAid is also called VOR-DME. This allows to get the aircraft position by measuring the distance using the DME and the radial using the VOR. Alternatively, the position fix of an aircraft can be determined using two radials of two different VOR stations. Finally, the more modern way to determine the position is using satellite data or GPS (Global Positioning System).

These NavAids, that are just some of the navigation aids nowadays used, play a crucial role in ensuring safe and efficient air navigation by providing accurate and reliable information to both pilots and air traffic controllers.

2.1.7 Flight Phases and Procedures

In the next chapters, a deep analysis of the different flight's phases in the AMAN context is done; particularly on the descend and approach phase. For this reason a quick insight on the different flight phases and procedures is now given.

The flight phases are defined from the take-off to the landing and can be divided into three main parts: the climb, the cruise and the descend.

Climb Phase

The climb phase refers to the trajectory the aircraft follows from the runway (just after lift-off) to the point at which the ascending phase stops. This point is known as “*Top of Climb - TOC*”.

During this phase, the aircraft follows the so called “*Standard Instrument Departure - SID*” procedure. This is defined as a designed trajectory ensuring safe horizontal and vertical separation with the ground and obstacles during the climbing phase. The point in which the SID terminates, the airway starts. It is remarked that the ending point of the SID is not the TOC. Today, in the Italian airspace the airways are defined up to flight level 195, then the FRAIT airspace starts; in this volume the aircraft can proceed to follow direct routes from an entry point to an exit point.

Cruise Phase

The cruise phase refers to the part of route flown at constant flight level. This route goes from the TOC to the point in which the descend starts, called “*Top of Descend - TOD*”. The route may be direct from the TOC to the TOD or it can presents more intermediate points in which the track changes.

Descend Phase

This last phase begins at the TOD point, where the aircraft starts losing altitude. During the descend phase the aircraft will reach a particular point called “*STAR Entry Waypoint*”. In this point, the aircraft will begin the “*Standard Arrival - STAR*” procedure, which is defined as the designed trajectory guiding the aircraft from the airway exit point (coinciding with the STAR entry waypoint) to the “*Initial Approach Fix - IAF*”. This route ensures safe vertical and horizontal separation with obstacles and the ground. Once the flight reaches the IAF, the approach procedure starts. It is defined as the sequence of maneuvers that will guide the aircraft from the IAF to the touchdown. The instrumental procedures can change from case to case and can be either *Precision Approach Procedure* or *Non Precision Approach Procedure*. In the first case, both vertical and horizontal guidance are provided, hence systems as the ILS system are necessary. In the second case instead, the vertical guidance is not provided and only horizontal information are given; in this case systems like the VOR can be used.

All the above mentioned procedures are published in the national service provider AIP (Aeronautical Information Publication) website [9].

2.1.8 Separation and Separation Minima

During the different phases of a flight, the separation with the other traffics must be guaranteed by the air traffic controllers. The separation rules are described in details and for the different scenarios, by the ICAO Doc. 4444 [6].

The separation is defined both as *vertical separation* and *horizontal separation*. The first one is given in feet or flight levels while the second one in nautical miles.

The **separation minima** corresponds to the minimum separation (in feet for vertical and nautical miles for horizontal) that must be ensured among the different flights. This values change from case to case and are described in the ICAO Doc. 4444.

In addition to the traffic separation standards applied to en-route aircraft, restrictive separation minima are defined for flights landing or departing from the same or closely spaced runways. This more strict separation minima are established to ensure that trailing aircraft, are not endangered by the wake vortex turbulence created by the preceding aircraft. For this reason, a classification according to the Maximum Take-Off Weight (MTOW)⁷ is made.

Wake Turbulence Categories.

1. **Light - L.** MTOW < 7000 kg
2. **Medium - M.** 7000 kg < MTOW < 136000 kg
3. **Heavy - H.** MTOW > 136000 kg
4. **Super - J.** MTOW in the order of 560000 kg (only Airbus A380)

According to the category of the preceding aircraft and the following one in a runway, different minimum spacings are defined by the ICAO. The separation minima are defined for the case of single runway (with departing flights only, arriving flights only or mixed operations) and for multiple runway use.

This short discussion on separation and separation minima is necessary to understand the further discussions on the AMAN system that, even though it is not responsible for ensuring the separation among in flight aircraft, it must provide outputs respecting the separation minima at the runway.

⁷Maximum Take-Off Weight - MTOW. It represents the maximum mass at which the aircraft is certified to take-off.

This brief introduction about the air traffic management in the skies is helpful to contextualize the working scenario for the AMAN technology and fully understand its operational environment. The AMAN system is implemented in the main hubs all over Europe, where the airspace is highly congested and the arriving traffics must be carefully managed ensuring efficiency and safety. In Italy, AMAN is deployed at two of the country’s busiest airports: Milan and Rome.

AMAN is primarily focused on IFR traffic management, so those flights presenting a scheduled plan; indeed, both Rome and Milan terminal area are classified as **A**. In this airspace class, according to the regulations, only IFR flights are allowed to operate and VFR traffics are prohibited.

To conclude, the AMAN system performs sequencing calculations from the en-route phase all the way down to the touchdown involving more than one airspace and extending beyond the TMA and CTR. For example, the system also involves air volumes such as Flight Information Regions (FRAITs) and Airways (AWYs), which are part of the airspace network.

In relation to the ICAO objectives described in § 2.1.3, the AMAN technology specifically addresses objective 3, which focuses on the safety and efficiency improvement of air traffic flows.

2.2 Single European Sky ATM Research

The negative effects of fragmentation in European Air Traffic Management have been a persistent concern for EU countries over the years. Several studies have examined the impact of fragmentation on the European ATM network. For instance, the Eurocontrol Performance Review Commission (PRC) published a detailed report in 2006, analyzing the consequences of a fragmented EU service in terms of communication, navigation, and surveillance [12]. The report also provided a definition of fragmentation: *“the division of air navigation service provision into smaller decision-making or operational units than would result from considerations of optimum scale.”* Similarly, the University of Dresden conducted a study on fragmentation, highlighting different types such as financial (charges and taxes), technical (procedures and operations), structural (airspace management) and others. The researchers concluded that while the current fragmentation strategies have generally performed adequately over the past decade, they are not sufficiently equipped to efficiently accommodate future traffic growth and therefore require further optimization [13].

To face the fragmentation related issues and address the projected growth in air traffic, in 2004 the European Union launched the **SES (Single European Sky)** initiative. The aim was to unify the fragmented European airspace by enhancing safety, efficiency, and interoperability among different service providers, while ensuring full respect for environmental considerations.

To achieve these goals, new technologies are essential. As a result, the EU has placed significant efforts into supporting research in air traffic management and improving system performance. To guide this progress, the SES initiative introduces a performance and charging scheme (regulatory instruments) monitored by the European Commission, focusing on the four key areas listed below [14].

1. Safety
2. Environment
3. Airspace Capacity
4. Cost Efficiency

The Commission works in cooperation with the Member States, their National Supervisory Authorities (NSAs - in Italy, “Ente Nazionale Aviazione Civile ENAC”) and Air Navigation Service Providers (ANSPs - in Italy, “Ente Nazionale Assistenza al Volo ENAV”). The NSAs are responsible for the development and monitoring of the performance targets. A PRB (Performance Review Body) is designed by the Commission; it has the role to assist the Commission itself and the NSAs in the development of the charging and performance scheme. The PRB is providing an annual review monitoring report including summaries on the traffic situation, on the key points stated above, and possible future developments and recommendations [15].

In the SES initiative, an important role for the improvement of the ATM efficiency is played by the **SESAR (Single European Sky ATM Research)** programme that aims to define, develop and deploy the ATM technological solutions [16].

Different public and private partners (see Fig. 11) are involved in the programme such as EU, Eurocontrol, Universities, ANSPs (ENAV, ENAIRE, etc) and industries that play an important role in the later stages of a system’s project, when most of the funding comes from private companies.

Among them, Eurocontrol has been identified as the responsible organization to address the problem of increasing delays in Europe and provide possible solutions within 2029 [18].

To facilitate this task, the European Union and Eurocontrol, as part of the SESAR programme, founded in 2007 a unique public-private partnership called SESAR Joint Undertaking (JU).



Figure 11: Public institutions and private companies involved in the SESAR programme [17].

The SESAR JU and its members have taken the ATM research onto real systems and real-life air traffic operations, accelerating through research and innovation the delivery of the objectives related to the ATM technological transformation in its 10-year mandate (2021-2031); the on going mandate started in 2021, set up the partnership that takes the name of SESAR 3 JU.

To define the developments of a solution from the early stages to the end, the SESAR defined an **innovation pipeline**, a process that guides the progression of new technologies to the deployment. This process is divided into three main phases:

- **Exploratory Research:** in this first stage new solutions, ideas and concepts addressing the actual challenges in the ATM branch are thought and developed. The research is mainly done by universities, research centers and innovators and it is mostly funded by public investments.
- **Industrial Research and Validation:** in this intermediate stage, the assessments, refinements and adjustments along with the simulations and first validations are done in real environments. Since it is in this step that the idea is acquiring commercial interest, the funds are provided by both public institutions and private companies.
- **Digital Sky Demonstrators:** in this final stage the tests in real operations are done; the industry takes an important role since the investments are mainly private being the solution more likely to become a real service that can be sold hence generating profit. Indeed, this step aims to demonstrate the performance and reliability of the proposed solution as well as its integration within existing systems, ensuring it meets both technical and economic requirements.

The innovation pipeline described above is deeply described in the SESAR website and a visual representation is presented in Fig. 12. Aviation projects often involve sophisticated technologies or methods that require iterative improvements. Each stage of development may present new challenges, necessitating updates to designs and validation strategies. For this reason, when an innovative solution is studied, a continuous update in the maturity of ongoing work is necessary; in aviation indeed, it is fundamental to quantify the readiness state of a solution in order to understand whether it is ready (mainly in terms of safety) to be introduced in the industry and become operative or not. For this purpose, the NASA agency divided in a clear way the progress of an assignment into different stages called “TRL (Technology Readiness Levels)” [20], defined as follows:

- **TRL1:** basic principles observed and reported.
- **TRL2:** technology concept and/or application formulated
- **TRL3:** analytical and experimental critical function and/or characteristic proof of concept

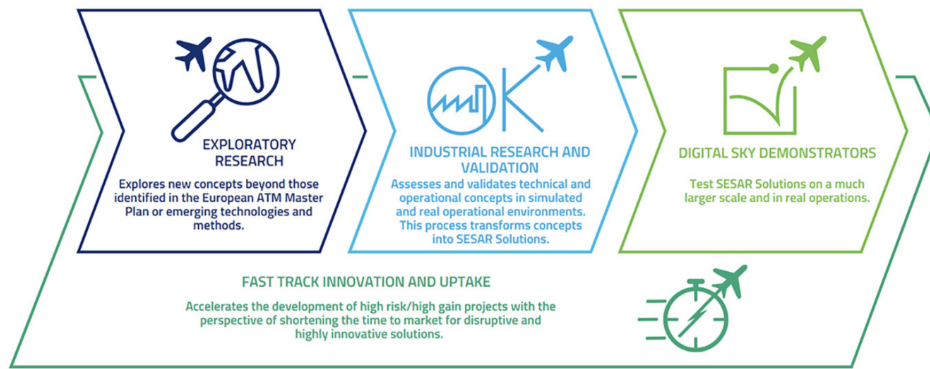


Figure 12: The innovation pipeline with a brief description of its three stages represented by the SESAR JU [19].

- **TRL4:** component and/or breadboard validation in laboratory environment
- **TRL5:** component and/or breadboard validation in relevant environment
- **TRL6:** system/subsystem model or prototype demonstration in a relevant environment (ground or space)
- **TRL7:** system prototype demonstration in a space environment
- **TRL8:** actual system completed and “flight qualified” through test and demonstration (ground or space)
- **TRL9:** actual system “flight proven” through successful mission operations

The TRL scale presented above is the original one written by the NASA and it regards the space environment and aeronautical components but it can be generalized according to the aim of the project.

Grouping the different levels in macro-areas; *TRL1* to *TRL3* are levels in which the solution is still being studied deeply in terms of theoretical formulations and possible ways of developing. *TRL4* to *TRL6*, instead, are stages representing a good maturity level that is reached when the solution is considered to be worthy enough and for which the involved private and public institutions are ready to invest in experiments. Finally, from *TRL7* to *TRL9*, the work is experiencing real tests and the product is about to be deployed.

As an analogy to the NASA TRL reference system, SESAR has developed its own strategy to assess the progress of a solution. In particular, the development of a work occurs in a progressive way by doing different checks (through periodic yearly reports) summarizing the maturity level of a solution and the achievement of the related Key Performance Parameters (KPIs). The KPIs are a unity of measurement of a new solution impact in the SESAR's objectives (such as safety, environmental impact, cost efficiency and others). The periodical assessments are called validation phases (V-phases) and they are defined as follows [21]:

- **V0**: identification of potential benefits and risks.
- **V1**: potential benefits, impact mechanisms and influence factors, initial assessment on the primarily affected KPIs.
- **V2**: quantitative intermediate assessment on all KPIs .
- **V3**: complete assessment including final quantitative results on all KPIs.

To provide an analogy, the *V0* level corresponds to *TRL1*, *V1* to *TRL2*, *V2* to *TRL4*, and *V3* maps to *TRL6* [21].

All the SESAR solutions with the corresponding level of maturity are gathered in the so-called "Solution Catalogs". They are collections of yearly reports giving an overview of the different technological solutions and the corresponding state of progress. An example of the 2021 solution catalogue is provided in the references [22].

3 The Arrival Manager (AMAN): a Human Factors Perspective

3.1 State of Work

Because of the increasing demand and congestion in the terminal areas, the SESAR JU partnership and its members have been focusing on new advanced concepts and solutions. Different technologies have been discussed and implemented so far to match the requirements and targets for the next years; particularly, in relation with the increasing density of air traffic and the need to meet the safety, efficiency and environmental sustainability targets, the following techniques are emerging for the optimization of the air traffic flow in the TMAs.

1. **Continuous descent operations (CDO) using point merge [23]**. This solution has already been deployed (maturity level V3, § 2.2) and consists in evaluating flight paths in order to follow a smooth descent to the runway threshold instead of a traditional stepped approach. The CDO along with the point merge (where aircraft are vectored to a common point merge from where they proceed to fly following RNAV⁸ procedures and then intercepting the ILS) can be applied to dense air traffic areas resulting in several benefits:
 - (a) Reduced fuel consumption and emissions
 - (b) Reduced environmental impact of airports on their neighbouring communities
 - (c) Noise reduction

This solution has already been deployed in Austria, France, Turkey and United Kingdom.

2. **Optimised use of runway configuration for multiple runway airports [25]**. The already existing RMAN (Runway Manager) is a tool that allows the air traffic controller to determine the optimal runway configuration according to the capacity, the demand and the airport's constraints by computing the forecasted landing time (FLDT) and the forecasted take-off time (FTOT). This new solution (maturity level V3) is an improved technology that combines the RMAN with an integrated runway sequence tool (that considers the runway occupancy time, capacity, demand and other factors) in order to minimize the delay and maximize the efficiency and capacity, hence optimising the sequence and reducing fuel emissions. The solution has been validated in Barcelona El-Prat Airport.

⁸“A method of navigation which permits aircraft operation on any desired flight path within the coverage of station-referenced navigation aids or within the limits of the capability of self-contained navigation aids, or a combination of these” [24].

3. **Reduced separation based on local runway occupancy time characterisation (RO-CAT)** [26]. This deployed (maturity level V3) solution aims to optimise the runway throughput by reducing the separation between successive aircraft. This is possible by predicting with minimal errors the runway occupancy times; indeed, this represents the major constraint on the landing separation along with wake turbulence. This technology is one hundred percent operative in London Heathrow and Helsinki Airport where an increased in the productivity, safety and efficiency has already been experienced.
4. **Arrival and Departure Manager (AMAN/DMAN)**. The arrival/departure manager (AMAN/DMAN) is a tool improving traffic predictability and cost efficiency ensuring safety and environmental sustainability.

The **DMAN** provides the optimal departing sequence taking into account the scheduled departure times, slot constraints, runway capacity and airport factors. In order to do this computations, DMAN requires access to the Airport Collaborative Decision Making A-CDM⁹ and other inputs such as the TOBT¹⁰ (Target Off-Block Time, given by the ground operator), the TTOT¹¹ (Target Take-Off Time, from the control tower), the CTOT (Calculated Take-Off Time, it represents the calculated time at which a flight is required to become airborne according to its slot). The DMAN contributed to an average reduction of 14.6 kg of fuel per flight, a decrease in the average taxi time of around 9 % and a better estimation of the EOBT¹² time by 7.8 %, allowing aircraft to depart within the allocated slot window, avoiding issuing further delays [27].

Along with DMAN, the arrival manager **AMAN** has been studied and developed. This tool provides an optimised sequence of arriving aircraft in particularly congested airports and hubs. It takes into account several factors and constraints such as wake turbulence separation, runway capacity, speed limits, aircraft performance, meteorology and so on. The tool allows to strongly reduce the fuel consumption and CO2 emissions, improve the predictability, reduce holding times and delays and enhance the safety.

Both AMAN and DMAN technologies are already deployed in most of the European hubs; in Italy, they are operative in Rome and Milan terminal areas.

The aforementioned solutions are just a few examples of the solutions developed by SESAR for

⁹Airport Collaborative Decision Making - A-CDM. It is a platform providing flights information exchange among the air traffic controllers, airlines, airport operators, ground handlers and other parts involved in the air traffic management.

¹⁰Target Off-Block Time - TOBT. It is the time that an aircraft operator expects to be ready to leave their stand.

¹¹Target Take-Off Time - TTOT. It is the time the air traffic controller expects the aircraft to take-off, this is computed by means of tables where different taxi times are indicated.

¹²Estimated Off Block Time - EOBT. It is the estimated time for which an aircraft will start moving from the stand.

optimizing the air traffic flows and capacity. Beyond this examples, giving context to the thesis topic, many other initiatives at different maturity stages can be found in the official SESAR solutions catalogue website [28].

This work provides an in-depth examination of the AMAN solution, proposing, through the help of a simulator, new concepts and updates to facilitate the air traffic controllers to familiarize and trust this powerful aid to the ATM system. In the next section, the actual AMAN working principle is explained and discussed. The next chapter will then describe how a simulator replicating the AMAN behaviour was constructed in order to perform further Human Factors studies and test some technical improvements, as presented at the end of the thesis.

3.2 AMAN Structure and Logic

The main AMAN software purpose is to provide assistance to air traffic controllers in the management of the arriving air traffic flow to particular points (for instance runway threshold or metering points); the objective function for AMAN is to optimise the sequence (according to the runway capacity), reducing delays (and so eliminating holding patterns¹³ when possible), fuel consumptions (lowering environmental impact) and providing an increased efficiency and cost savings. The AMAN software indeed, represents a technology allowing to balance conflicting aviation requirements [29]:

- i. Capacity
- ii. Safety
- iii. Efficiency
- iv. Environmental Sustainability

The system provides the aircraft sequence at the runway and the corresponding estimated time at the runway (or at a certain metering point); this automatic sequencing problem solution provides, according to Eurocontrol[29], a *reduction in the air traffic controller's workload* (this is a fundamental point for the analysis that will be presented later in this work).

The AMAN processing principle is the **linear delay absorption**; the software is thought to avoid the aircraft delay accumulation that has to be consumed all at once close to the arrival airport by performing holding patterns or vectoring routes. Indeed, the system allows to distribute and smooth out the delay along the route, in the airspace sectors crossed by the flight during its cruise, descend and approach phase.

This translates in the possibility of providing to the air traffic controller an optimised sequence at

¹³A racetrack-shaped route that it repeats for a certain period to delay the aircraft descent toward the runway.

the runway that maximizes its capacity. Indeed, by properly distributing delays to the arriving aircraft, a sequence with standard separation at the runway (respecting the constraints such as wake turbulence and minima) will be computed.

To respect the output sequence, AMAN talks with the ATCOs through a delay advice for each scheduled arriving flight; the delay represents the minutes the aircraft have to gain or to lose in order to respect the optimised calculated sequence. The total delay is then distributed among different sectors crossed by the flight; each ATCO task is to ensure the flight absorbs or dissipates the corresponding sector delay by applying appropriate measures, such as speed adjustments or vectoring.

To understand the AMAN logic and algorithm, a block diagram will be used as representation. However, before digging into the details of the flow chart and the processing steps, an overview of the inputs and outputs [29] is given in Fig. 13 and subsequently discussed.

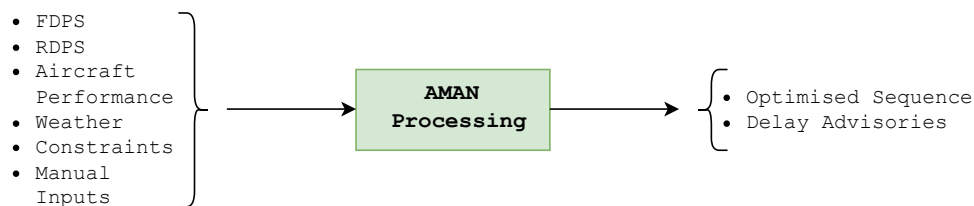


Figure 13: The synthetic flow diagram of the AMAN system, highlighting its inputs and outputs.

3.2.1 Inputs

1. **FDPS** (Flight Data Processing System). This is a software that processes flight plans (hence it gives all the required information about flight plans) and track the aircraft movements with the help of surveillance systems such as radars. The FDPS indeed, allows the ATCOs to manage and update flight information, performing calculations (such as trajectory predictions and conflict detection) of on going flights and sharing the real-time data on the network. By processing dynamic real-time flight data, it allows the air traffic controllers to continuously monitor and manage the air traffic in an efficient and safe way [30].
2. **RDPS** (Radar Data Processing System). This input processes the radar data, meaning it decodes and elaborate signals in order to provide real-time information about aircraft position. This system relies on the surveillance data extracted from the PSR/SSR (Primary/Secondary Surveillance Radar), ADS-B (Automatic Dependent Surveillance-Broadcast), multilatera-

tion¹⁴ and so on. As shown in Fig. 14, the conventional ATC radar system includes a radar device, the RDPS system and different display stations (ATCOs screens). Through an antenna, a transmitter and a receiver, the radar device allows to detect the traffic and/or gather the signals sent from the aircraft transponder¹⁵. The RDPS, that is an high performance software, allows to elaborate and decode the radar signals, perform tracking calculations and control operations; the RDPS system provides the processed information to the ATCOs displays and, on the other way, it controls the radar according to the operators' actions [31].

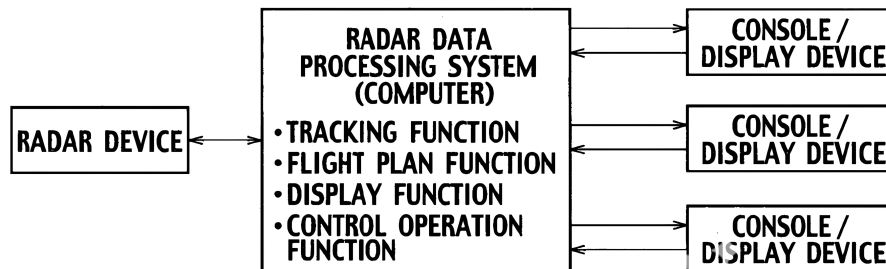


Figure 14: Conventional RDPS Architecture: the radar device, RDPS and display devices, represent the three subsystems [31].

3. **Aircraft Performance Model.** An effective ATM system depends on the planning of traffic flows, which relies on precise estimation of aircraft performance. An aircraft performance model is thus a crucial element for trajectory computations and plays a central role in the development of ATM systems. There are several ways and techniques to model and simulate the aircraft performances such as kinetic or kinematic approaches. An example, that will be used in the next chapter, is the Base of Aircraft Data (BADA) provided by Eurocontrol; this is an aircraft performance database calculated using a kinetic approach. In the context of AMAN, the aircraft behavior is necessary to make calculations of trajectories and time in relation to the aircraft typology [32].

4. **Weather Information.** The meteorological data play a crucial role in the computations carried out by AMAN, particularly the real-time wind data used to calculate speed corrections. The weather information is provided by different sources such as Numerical Weather

¹⁴Multilateration - It is a technique used in ATM to track aircraft by measuring the time difference between signals received at several ground stations.

¹⁵A transponder (XPDR) is an on board receiver/transmitter equipment which will generate a reply signal upon proper interrogation. The signal will contain identification information (Mode A) and additional flight data, depending on the selected mode (C or S).

Predictions (NWPs), radar data and ground based sensors. AMAN systems use this weather information to dynamically adjust sequencing and delay predictions.

5. **Constraints.** In the AMAN system, limits such as the speed (e.g. 250 kts below FL100), airspace restrictions and flight constraints are fundamental to provide reliable results. Indeed, in the trajectory prediction calculations the software must know the boundary conditions affecting the problem. By considering these limits, the system can accurately forecast arrival times and provide the best sequencing solution.
6. **Manual Inputs.** In addition to the above listed inputs, manual criteria have to be added as well; indeed, the software must be capable of adapting to the different possible runway configuration and procedures. The typical degrees of freedom left to the ATCO supervisor (that are boundary conditions for the AMAN software) are the spacing expressed in NM at the runway threshold (or at the Initial Approach Fix-IAF), the landing rate (number of landings per hour), a particular optimization criteria (for instance, wake category grouping, first come first serve, and others that can vary according to the airport needs), the runway configuration [29].

3.2.2 Outputs

1. **Optimised Sequence.** AMAN provides as main output an optimised sequence of landing aircraft according to the selected criteria. The resulting information is presented to the air traffic controller on the radar screen in a vertical timeline of flights, displaying the target arrival times and the order in which the aircraft should land.
2. **Delay Advisories.** Along with the provided sequence, AMAN computes the required delay absorption or recovery for each flight in order to match the position (and the target landing time) in the sequence. The advisories are displayed as TTG (Time To Gain, positive) or TTL (Time To Lose, negative) and they are distributed among all the different ACC sectors crossed by the flight. The delay that each ATCO sees in its screen for each flight represents the time that the aircraft has to lose or gain in that sector jurisdiction. The air traffic controller task so is to apply control actions (at his own discretion) to make the aircraft absorbing/dissipating the delay and bringing the corresponding advisory to zero prior transferring the flight to the next sector.

3.2.3 Processing

After describing inputs and outputs of the system, this section focuses on its central block, the core system of the algorithm, that is the **processing**, meaning all the required computations to map

the inputs into the outputs.

This core phase will be described in a general way without digging into the details of calculations because of a lack of information (due to restricted access) about the real AMAN algorithm. Nevertheless, in the next chapter an AMAN simulator that replicates as much as possible the real software is studied and explained in details.

The AMAN processing phase is split into two main blocks: the **trajectory prediction** and the **sequencer**.

Trajectory Prediction (TP)

This first module of the system elaborates the input data and provides for each flight an estimated time (unconstrained) at a particular point (for instance at the runway threshold, the IAF or a metering point). This prediction is obtained by computing dynamically the aircraft performance elaborating the flight plans using the FDPS data, integrating the weather information and real-time updates retrieved by the RDPS. The calculated time can be referred to the runway threshold (in this case it is called **ELDT** - Estimated Landing Time), particular metering points, initial approach fixes (IAFs) and other waypoints (in these cases it is indicated as **ETO** - Estimated Time Over).

As a trajectory prediction software, the system can use a model developed by external companies or the internal AMAN algorithm. A lot of effort in the ATM research is placed in the possibility of combining the AMAN software with an optimised trajectory predictor tuned according to the local terminal area needs. In particular, the SESAR Joint Undertaking community along with the private companies and public institutions are evaluating the possibility of integrating 4D trajectory predictions in the ATM solutions [33].

The trajectory prediction is not only used for the air traffic management solutions but also for estimating the aircraft future behavior directly on-board during flight. In that case, the calculations are done by the Flight Management System (FMS) that is generally using the *Point Mass Model*, hence a set of differential algebraic equations integrated over time. For the on board predictions, most of the inputs (as the aircraft mass at each time instant, the thrust, the wind and temperature, climb rate and so on) are directly provided by the sensors and aircraft equipments. Instead, when the same model is applied to ground based systems as AMAN, it is not easy to have that data with a great accuracy; for this reason, the trajectory prediction is sometimes more complex than expected and can vary from case to case. Nowadays, ground based trajectory predictions are generally using the point mass model integrated with the BADA database used to provide the aircraft performance [34].

In addition to the discussion above, Eurocontrol explains in a detailed report about the TP specifications [35], how the software is actually divided in two main sub functions (see Fig. 15): first, the *intent function* constructs the aircraft future behavior using a combination of declared intents (flight plan, ATC procedures and others) and undeclared intents (operator thrust and speed for instance). Then, using the aircraft performance model and integrating the weather information, the undeclared intent gaps are filled with the estimation of a *trajectory function*.

As stated before, it is highlighted how, in the case of AMAN, the calculations provided by the TP model are providing the Estimated Landing Time (ELDT) for each arriving aircraft.

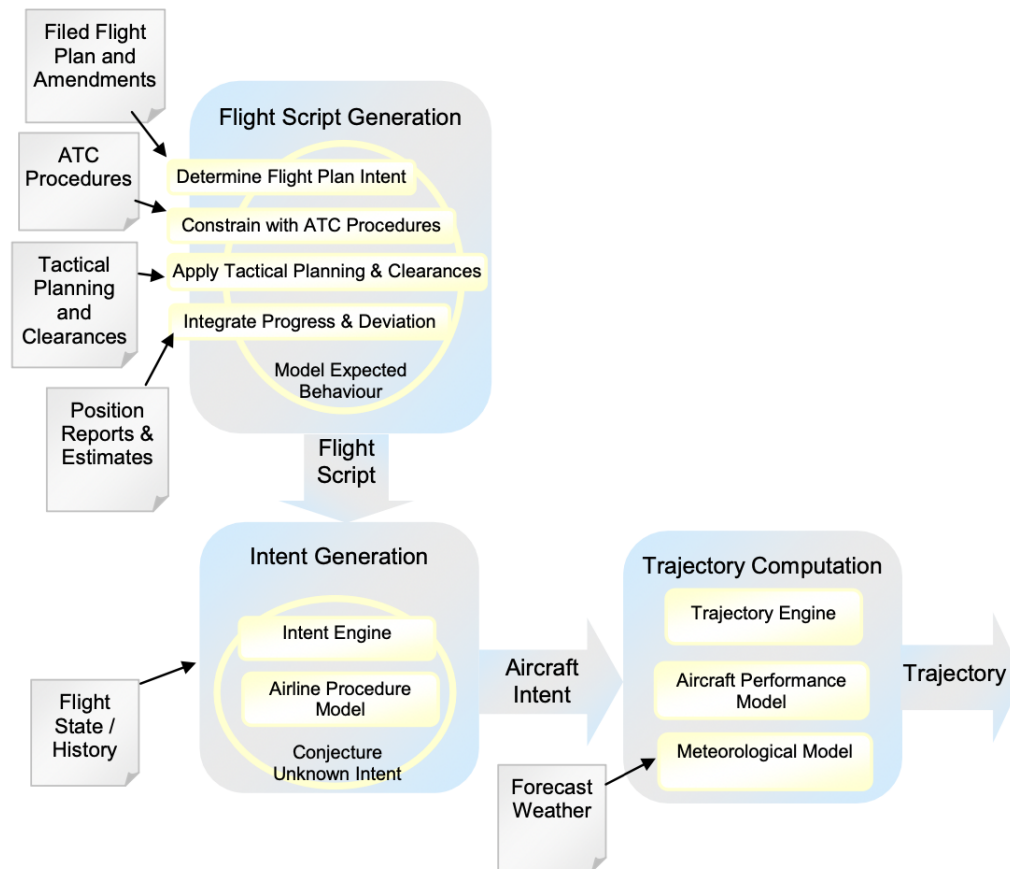


Figure 15: The logic breakdown beyond the Trajectory Prediction proposed by Eurocontrol [35].

Sequencer

The sequencer block provides, according to the given constraints and manual inputs, the optimised flow of flights at the runway based on the adopted maximization principle. In most cases the FCFS (First Come First Serve) theory is used; this states that the sequence is calculated according to the ELDTs (this means the order is dictated by the estimated landing time). Other principles can be also applied such as wake category grouping and others [29].

Along with the sequence of landing aircraft, the sequencer computes the **TLDT** - Target Landing Time, meaning the time at which a flight should be at the runway threshold in order to optimize the sequence; this time is computed knowing the trajectory prediction outputs, the manual input constraints (such as the landing rate) and the external limits (wake turbulence and speed limits). If the time refers to a particular waypoint or IAF it takes the name of **TTO** - Target Time Over. The objective function to be optimized, allowing for the TLDT calculation, can change from case to case according to the needs. In the next chapter a proposed solution for calculating the TLDT is implemented and explained in details.

Once the unconstrained time (ELDT) and the constrained time (TLDT) have been calculated, the total delay at the runway (TD - Total Delay) for each flight can be easily calculated:

$$TD_i = TLDT_i - ELDT_i \quad (2)$$

The delay information (G - Gain if positive, L - Lose if negative) is then shared among the upstream physical sectors interested by the flight. To clarify, a schematic flow diagram representation is given in Fig. 16.

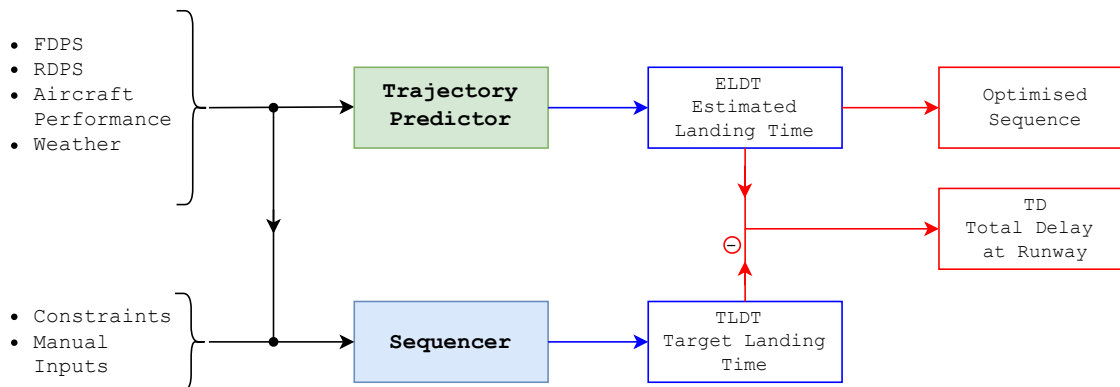


Figure 16: AMAN schematic flow diagram.

After describing the overall working principle, it is important to underline that AMAN presents a finite distance horizon beyond which flights are not captured and sequenced; nowadays extended AMANs (E-AMANs) have ranges around 200 NM and more [36].

Since the AMAN software is designed as a **dynamic system** able to capture any air traffic controller action by iterating the algorithm for each flight at different discrete time instants and continuously updating the delay advice, another important distance is defined and it takes the name of **stable horizon**. This represents the radius of the circle centered in the runway touchdown zone, delimiting an area inside which flights can not be re-sequenced, hence called **frozen area**. This zone avoids continuous sequence updates in the final approach phase, confusing the air traffic controller and increasing its workload during this delicate stage of flight.

Delay Sharing

Once that AMAN calculates (at each discrete time instant) the delay advice, this has to be distributed among the different sectors crossed by the flight within the AMAN range capability. The delay sharing is done following precise rules:

- i) calculation of the sectors crossed by the flight
- ii) delay distribution starting from the outer sectors
- iii) evaluation of each sector's capacity
- iv) delay advice for each sector and/or holding advice (just in the case in which the total delay advice exceeds the sum of the sectors' capacity)

The third point can seem trivial but actually it is quite complex: indeed, this requires to know what the capacity (in terms of number of aircraft) is for each sector and evaluate, according to the expected crossing flight trajectories, what is the maximum sector delay capacity for which the air traffic controller can handle the traffic.

To better understand the complete process let's take the 2D (not considering the vertical airspace fragmentation) example in Fig. 17; in this case the flight *ITY123* has a delay advice of 10' and the sectors capacities are given as shown in Fig. 17.

In this case no holdings are required, since the total delay advice (10') is not exceeding the sum of the sectors capacity (18').

Moreover, in this trivial example, no other traffics are considered. In the real case the delay distribution takes into account both the sectors capacity and the air traffics. The description of how capacity is computed lies beyond the purposes of this work.

To conclude, an overall picture of the AMAN working principle and algorithm is presented in the flow diagram in Fig. 18 that represents an extension of what has been presented in Fig. 16. The complete scheme indeed, includes the dynamic effects (continuous updates) and the delay sharing process explained before; it is underlined that the represented case holds for flights that have not entered the frozen area (in there, the sequence is indeed frozen).

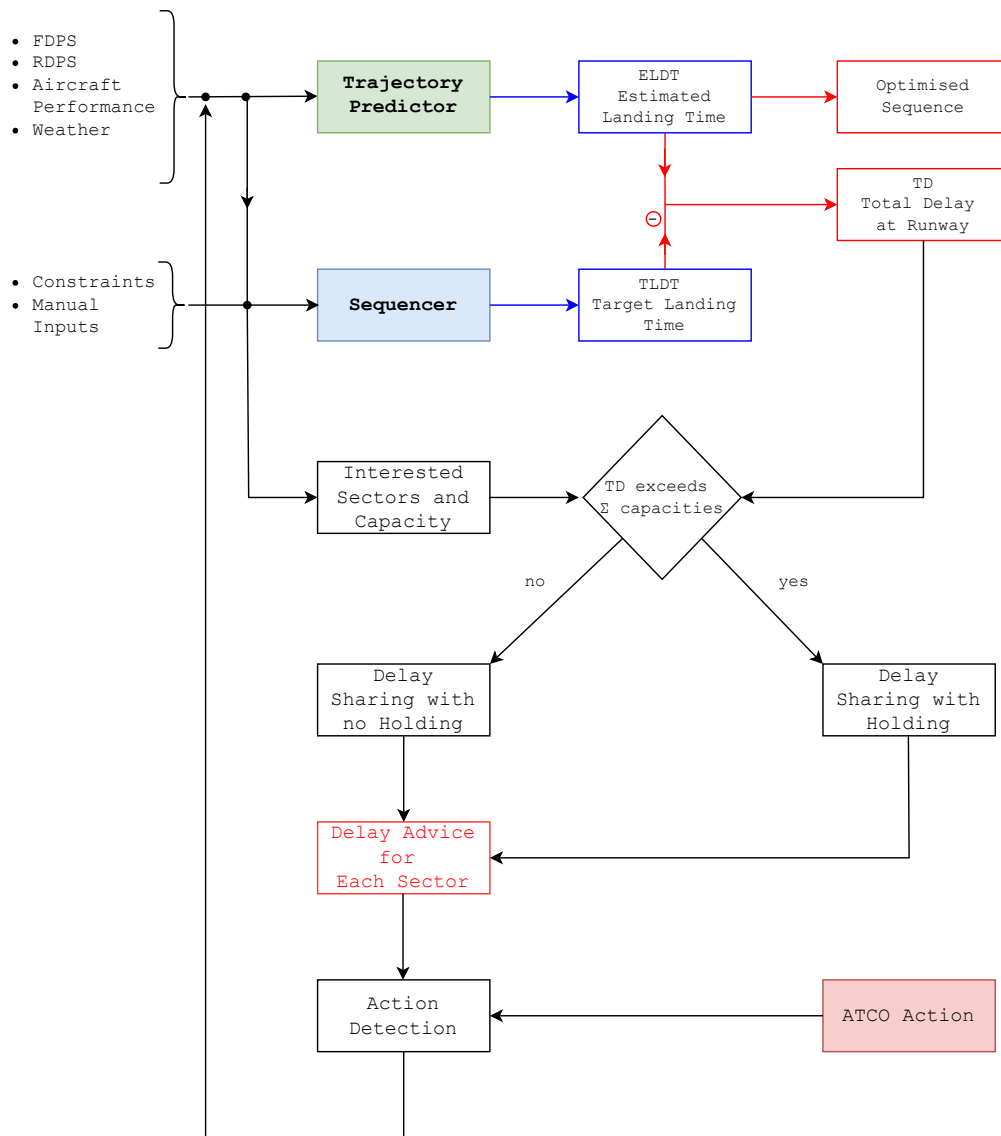


Figure 18: Complete AMAN flow diagram and algorithm.

3.3 Human Factors Limitations in AMAN

Despite the AMAN technology offers significant potential to address challenges in the ATM domain and improve efficiency, its operational use remains quite limited. This limitation is linked to the low acceptance of the system by air traffic controllers. An important factor contributing to this lack of confidence is observed to be the design of the interface. When developing a Human-Machine Interface (HMI), it is indeed essential to consider the interaction between the system and its users, as well as the corresponding human limitations.

The discipline of Human Factors focuses on understanding and optimizing the interaction between humans and systems to ensure efficient and safe operations. Human Factors studies are therefore critically important in the aviation sector, where the safety is the priority and Human-Machine Interfaces are widely used.

Because of the limited acceptance of the AMAN system, particularly its interface, this thesis conducts a Human Factors study to analyse its usability and propose improvements.

3.3.1 Human Factors in Air Traffic Management

In this work, a Human Factors analysis is conducted to investigate the issues related to low acceptance of the AMAN system, particular attention is given to its interface. To contextualize and provide the necessary background, this section gives the main definition of the Human Factors discipline in the context of Air Traffic Management. Particular attention is placed in the definitions of *workload* and *situational awareness*, being the main areas in which the Human Factors investigations about AMAN will take place in this work.

The global ATM system is considered one of the most complex human-machine systems ever created. The new technologies introduced to improve the performance and the system capabilities, are sometimes critical for the mental effort required by the operators. These technologies often require workers to manage large amounts of information, understand rapidly changing situations, make quick decisions, and plan their actions carefully. This added workload can increase stress and even compromise the safety in the routine operations if not managed properly. For this reason, the technologies are analysed not only from a technical perspective, but also from an ergonomic point of view, with particular attention to the human limitations. These studies are included in the **Human Factors** discipline that is defined as the study of the interaction between humans and machines. The primary goal of the Human Factors experts is to enhance performance, efficiency, comfort, and safety in this interaction.

Various elements are studied by the Human Factors discipline, focusing on the interaction between humans and systems. Human Factors considers cognitive, physical, and organizational aspects that affect the daily operations of pilots, air traffic controllers, maintenance crews and other staff.

The main disciplines are listed below [37].

- *Cognitive Load*. It studies how the tasks and the amount of information being processed, impact the cognitive performance.
- *Perception and Attention*. It examines how individuals perceive and respond to inputs in the operational environment.
- *Teamwork and Communication*. It represents the study of the effective collaboration between individuals, especially in high pressure environments. Human Factors investigates team dynamics and possible communication barriers.
- *Training and Skill Development*. These studies are carried out to understand how training programs can be designed to face human limits.
- *Stress Management*. Since most of the operations in aviation are taking place in high stress environments, the stress management techniques are studied to help the individuals to cope with the stress.
- *Workload Management*. The workload studies are crucial to prevent overloads or underloads in the cognitive sense, which can affect performance.
- *Situational Awareness*. The situational awareness is addressing the perception, understanding and future projection of the current environment.

In this work, the *workload* and the *situational awareness* are addressed for the Human Factors studies applied to the AMAN technology. For this reason a more in depth discussion about these two subjects is now made.

3.3.2 Workload

The workload is intended to be the mental demand placed on an operator while performing a task. This factor is strictly linked to other inputs that can influence the operator.

In Fig. 19, the *performance circle* shows the main elements that influence human workload in Air Traffic Management [38]. These elements include the *experience* and *ability* of the operators, which

can be improved through training, as well as the *task load*, which is defined as the measurement of human performance and depends on the design of the equipment, on the interfaces and on the complexity of the problem. These factors are interconnected and have a strong impact on the operators' performance, efficiency and the overall safety of the ATM system [38].

The *task load* shown in Fig. 19 is the main input that helps in defining the **workload** along with the *experience* and the *ability*.

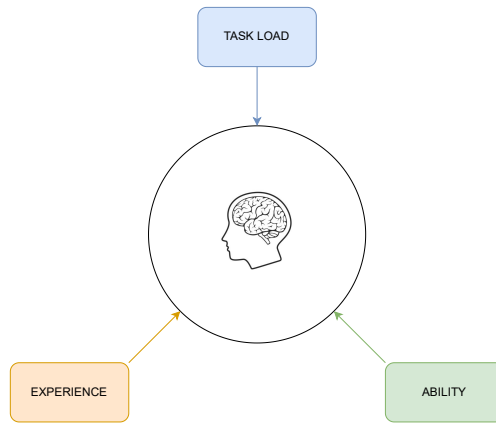


Figure 19: The Human Factors performance circle. The main elements contributing to the human performance and workload are highlighted [38].

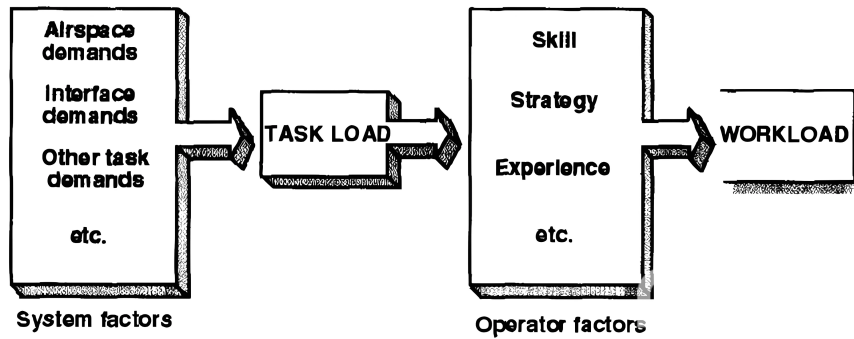


Figure 20: The main factors determining the task load and the workload in the ATC environment [38].

In Fig. 20, the factors contributing to the task load and the workload in the ATC environment are highlighted. It is possible to divide them in “systems factors” and “operator factors”. The first are those elements defining the *task load*. They define the required human effort to handle the work (it is in this step that the proper design of airspaces, interfaces, and ATM technologies play a crucial role). The operator factors are instead represented by the *experience* and *ability* of the operator which depend on its training and skills.

The interconnection of the different elements in the performance circle is defining the workload.

The **task load** and **workload** have been investigated carefully in the years; the NASA defined an index allowing to quantify and measure them. This methodology takes the name of *NASA Task Load Index (NASA-TLX)* [39].

The NASA-TLX index, represents a multi-dimensional rating procedure that provides a workload number calculated as a weighted average of six Human Factors tasks:

- **Mental Demand.** This represents how much mental activity is demanded (e.g. calculating, thinking, deciding and so on).
- **Physical Demand.** This represents how much physical activity is demanded (e.g. visual focus and scanning, pushing buttons, moving and so on).
- **Temporal Demand.** This helps in investigating how much the time stress is felt by the subject (e.g. if the activity is slow or fast).
- **Performance.** It measures the level of success and satisfaction for accomplishing the goals.
- **Effort.** It measures how hard is the activity (both mental and physical) for the subject to deliver the level of the performance.
- **Frustration.** This represents how much irritated, stressed, annoyed, relaxed, happy (and so on) is the subject during the test.

The index is computed in three phases [39]:

1. *Weight Definition.* Since the importance of each task to the workload is different from case to case, a number weighting the relevance of each task is defined. The way the NASA calculates the weight is the following: there are 15 possible pair-wise comparisons of the six tasks. A computer program shows each pair to the subject on the screen. The subject chooses which factor contributed more to the workload for that task between the two. This process is performed for the 15 pairs and by counting how many times each factor is chosen it is possible

to determine the importance of the task. The counts can range from 0 (not important) to 5 (the most important factor).

2. *Rating Definition.* The rating helps in defining the magnitude of the task. It allows to understand how much each task is challenging for the operator during the work. The magnitude can be evaluated using a linear scale divided into 20 equal parts ranging from 0 (low) to 20 (high). The official NASA layout for determining the rating is shown in Fig. 21.
3. *Combine.* The third and last step consists in computing the weighted average of the two indicators (Weight and Rating) described above. This will provide a single index that takes into account the previously listed six dimensions.

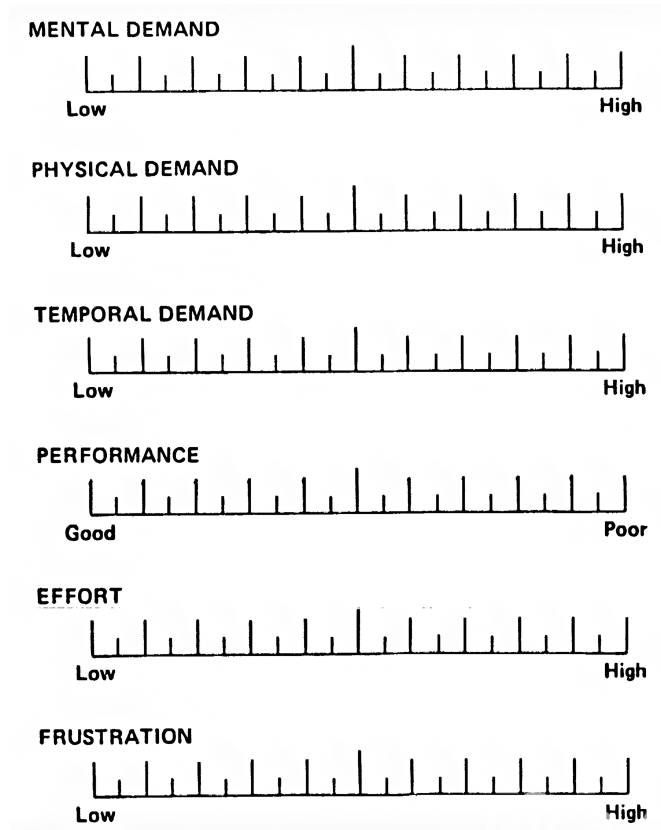


Figure 21: Scale used in the NASA-TLX for assigning the magnitude to each task [39].

3.3.3 Situational Awareness

In the context of air traffic control and air traffic management technologies, the **Situational Awareness (SA)** plays a crucial role.

It is defined as the clear understanding of the current and evolving state of a situation or system, along with the ability to predict future changes or developments in the system or environment. Endsley et.al. [40] simply defines the SA as “*knowing what is going on around you*”.

Improving operator situational awareness has become a key design objective for those creating operator interfaces in the ATM field. For the air traffic controller, understanding the traffic being managed, knowing the current positions of aircraft, and predicting future situations to identify and anticipate potential conflicts or unexpected changes, are all essential elements of the situational awareness process that occur in their mind.

In the context of human-machine interfaces (HMIs), the challenge is providing the SA by finding the necessary information to be displayed when they are needed. Endsley underlines that *more data do not mean more information*, so the decision in what elements communicate to the subject is crucial.

Since the elements change from study to study, a general methodology helping in investigating the SA was developed by Endsley et.al. This consists in analysing three different levels of situational awareness (see Fig. 22) [40]-[41]:

1. **Perception.** This refers to perceiving the current state of the environment using the senses, identifying the most important factors and information quickly.
2. **Comprehension.** This level is about the understanding of the information perceived and it is not just about the design but also about the personal knowledge and training. Misinterpretations due to uncorrect information display are lacks in this level of SA.
3. **Projection.** It investigates the ability of the subject to project in the future the environment based on the provided information (which have been perceived and understood). The completeness of data is crucial to build a mental model able to draw a clear environmental image in the future horizon.

The situational awareness is strongly interconnected with the *decision making*. Indeed, basing on the understanding provided by the controller’s SA, the operators can decide how to manage the situation and take the required actions.

Situational awareness is therefore seen as the mental step before decision-making. Once the decision is taken the following element that comes into play is the *performance*, meaning how well the task

is handled (see Fig. 23). Both the decision-making and performance require further studies and analysis that are beyond the purpose of this project. In this thesis a Human Factors investigation

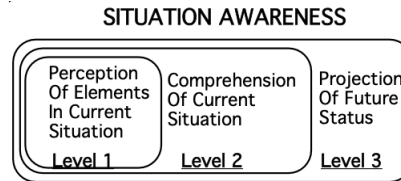


Figure 22: The Situational Awareness levels described according to Endsley et.al. [40]

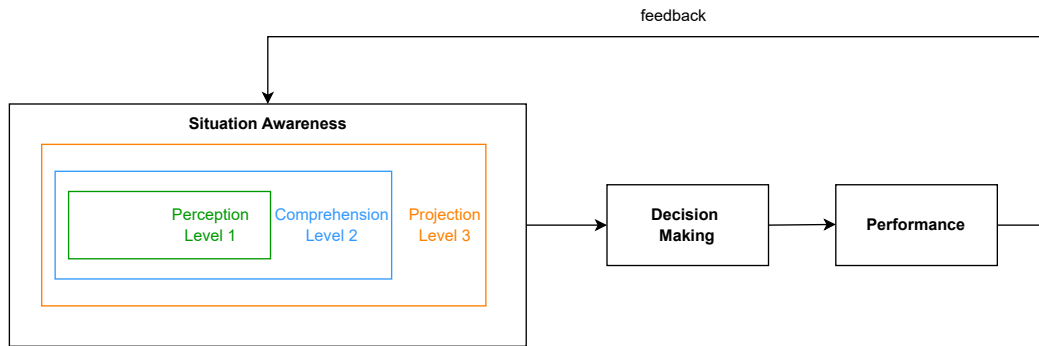


Figure 23: The Situational Awareness levels interconnected with the Decision-Making and Performance [40].

based on a conventional AMAN interface and on a proposed solution is done. The study will be further explained in Chapter 5 and 6 and it mainly covers the interface usability, information accessibility and situational awareness.

4 AMAN Simulator - Methodology and Simulation Model

Introduction

In order to analyse the strong and weak points of the AMAN system and carry out an advanced study for future developments, a simulator that replicates the reality as much as possible is built.

This chapter highlights the methodology used to mimic the software algorithm and the connected necessary assumptions. The model can be applied to different scenarios and with different boundary conditions; in this thesis work, it is applied to Rome Fiumicino Airport for the case of single runway landing operations. In reality, Fiumicino typically operates dual runways for landings (runways 16L/R) and uses runway 25 for departures, which intersects with runway 16R. The intersection consists in an additional constraint since landings in runway 16R have to be managed considering the departures in runway 25, hence an integration with the Departure Manager (DMAN) is necessary. To avoid increasing the complexity in this first stage of study the single runway landing operations are considered; nevertheless, the same methodology can be further adapted and modified to handle different scenarios.

4.1 Hypothesis

As specified and discussed for the standard AMAN algorithm, the necessary inputs are derived from various air navigation subsystems, including the RDPS, FDPS, and meteorological radars. For this reason, obtaining all the required data is challenging and making assumptions (as close to reality as possible) becomes necessary.

1. It is assumed that the aircraft will strictly follow their flight plan route without ATCO vectoring or route shortening (this is the strongest hypothesis that is nevertheless required for trajectory estimations being the RDPS and FDPS data not accessible). In practice, a *static scenario* is built, where the simulator is not detecting the ATCO actions (red block in Fig. 18) and so is not iterating and updating continuously the delay advice and sequence. Under this hypothesis, the trajectory prediction coincides with the planned route in the horizontal plane while calculations considering the aircraft performance are required to predict the vertical trajectory profile and flight times.
2. It is assumed that the aircraft will fly their planned STAR procedure in its completeness, without shortenings and cuts in the route.
3. The simulator is issuing the total delay advice without being concerned about how it is distributed among the sectors according to their capacity. In the real model, the delay distri-

bution is happening as described in § 3.2.3. This assumption implies the simulator will stop its calculations to the total delay for each flight.

4. The meteorological model is built in average terms due to the lack of punctual measurements and the complexity of numerical weather models that are behind the aim of this work. Nevertheless, the proposed methodology (further discussed in § 4.3.1) is taking into account the wind effect in a model that balances the precision (and so complexity) and the practicality required for the scope of this thesis. Moreover, in terms of flight mechanics, small flight path angles and roll angles are considered, thus allowing to calculate the ground speeds by treating the wind problem in a 2D dimension. This further approximation along with the details about the weather model are discussed in details in the dedicated section (§ 4.3.1).
5. To estimate the aircraft performance, the BADA model is used; the airlines’ operating policies are assumed to be equal. Hence an aircraft model presents the same performances regardless of the operating airline company.

4.2 Inputs

The AMAN simulator is built in Matlab-Simulink environment. Because of the missing real-time data, the corresponding required inputs are simplified and stored in tables or when possible neglected. For instance, the FDPS and RDPS data are not taken into consideration since, as explained above, the simulator proposes a static model not presenting dynamic updates and continuous trajectory computations.

The following list of inputs is representing the way in which the required information is stored and then analysed. The data inside the tables is referred for explanatory purposes, to example scenarios used in the simulations.

- **Traffic Scenario.** To simulate the arriving traffic over a given period of time, different scenarios are developed. Each static simulation consists in analysing the uploaded scenario containing the information about the scheduled arriving flights (and the corresponding flight plans data), stored as represented in Tab. 3.

Table 3: Example of scheduled arriving flights and their corresponding flight plan details.

Traffic								
ID	Flight	Aircraft	Departure	Exit WPT	Route	STAR	Entry WPT	FL
1	ITY123	A320	LICJ	LURON	LURON M726 LAT	LAT3A	LAT	320
2	BAW456	E190	EGKK	PELEG	PELEG ... RITEB	RITEB3A	RITEB	350
...

Not all the information in Tab. 3 is required for the computations; anyway, for purposes of

completeness, all the standard information is reported. The details not presenting importance for the calculus are called “aesthetic” information and they are the Departure Airport and the Exit Waypoint (WPT).

- **Aircraft Performance.** The characteristics of an aircraft model represent a fundamental input that allows to compute the performances. A widely used model for taking into account the aircraft behavior is the BADA model provided by Eurocontrol [42]; this database is used in both simulation and real environments. The necessary data for the purpose of this work is extracted and summarized in an input table represented in Tab. 4.

Table 4: Example of the Base of Aircraft Data (BADA) information arranged in an input table, using an Airbus A320 as an example.

A320						
Cruise			Descend			
FL	TAS (<i>kts</i>)	Fuel Flow ($\frac{Kg}{min}$)	FL	ROD ($\frac{ft}{min}$)	TAS (<i>kts</i>)	Fuel Flow ($\frac{Kg}{min}$)
0	0	0	0	710	136	36
...
100	289	34.2	100	2374	345	8
...
390	447	36.5	390	2374	453	4.7

Since p different aircraft types will be simulated as arriving traffics, p input tables will be necessary to simulate their performances.

- **Separation Minima.** The separation minima input in the simulation model, corresponds to the “*Manual Inputs*” and “*Constraints*” blocks of the real AMAN. Indeed, this input takes into account the wake turbulence separation minima between different landing aircraft’s categories and the runway minimum (and optimal since optimises the capacity) spacing between successive landing aircraft¹⁶. This information is summarised in Tab. 5 which contains in the rows the following aircraft and in the column the preceding one; the separation is expressed in NM.

To clarify let’s take an example: position $(3, 2) = 4$ NM means that the preceding aircraft is category “H” and the following one is category “M”; hence, because of the wake turbulence restriction, at least 4 NM of separation is required at the threshold.

¹⁶This data is provided by Rome Fiumicino operations documents, which are not publicly available; for runway 16L, it corresponds to 2.5 NM.

Table 5: Separation (in nautical miles) between consecutive landing aircraft according to the wake turbulence category and to the LIRF standard operations in runway 16L.

Separation				
	L	M	H	J
L	2.5	2.5	2.5	2.5
M	4	2.5	2.5	2.5
H	5	4	2.5	2.5
J	6	5	4	2.5

- **Coordinates.** This input is a database containing all the waypoints geographical coordinates (including NavAids such as VORs) retrieved from the ENAV AIP website [9]. The input is given in a unique file arranged as in Tab. 6 where ϕ represents the latitude and λ the longitude.

Table 6: Geographical coordinates of waypoints in the Italian airspace [9], ϕ represents the latitude and λ the longitude.

Waypoints Coordinates						
Name	ϕ°	ϕ'	ϕ''	λ°	λ'	λ''
LAT	41	32	28	12	55	5
...

- **STAR Procedure.** Since the trajectory estimation is done according to the planned route, in the final approach phase it is assumed that the flights will strictly follow their assigned STAR procedure (given in Tab. 3). To do the calculations in that phase it is necessary to know how the arrival procedure is designed. Each existing STAR procedure in Rome Fiumicino is then described as shown in Tab. 7, containing information about the distance and true course¹⁷ between successive legs, and the corresponding flight level at which the aircraft should be in that point. The first higher FL is a fundamental number used for calculating the TOD position.

The table should be read as follows: “The landing aircraft must be at “LAT” VOR at FL160 and proceed for 11 NM/TC 317° to waypoint “RF414” where it must be FL140; then from “RF414” it proceeds for 11 NM/TC 317° to “RMC” VOR where it must fly at FL120; and so on until the last STAR waypoint, that corresponds to the initial approach fix (IAF)”.

¹⁷True Course - TC. It is the angle (clockwise positively defined) between the geographical north and the route segment starting from a point A and ending in a point B.

Table 7: Rome Fiumicino “LAT3A” standard arrival procedure (STAR) for runway 16L [9].

STAR LAT3A Procedure			
Name	D (NM)	TC (°)	Flight Level FL
LAT	11	317	160
RF414	11	317	140
RMC	8	315	120
...
IRBES	-	-	030

- **ILS Procedure.** As for the STAR procedure, the final approach phase must be defined in terms of route and altitude. For this reason, the ILS procedure is described in Tab. 8. In the same way as for the STAR, the procedure is retrieved by the ENAV AIP [9] official publication.

Table 8: Rome Fiumicino runway 16L ILS procedure [9].

ILS16L Procedure			
Name	D (NM)	TC (°)	Altitude (ft)
IRBES	3	162	3000
OXERU	3.1	162	2500
FAF	3.6	162	2500
OM	3.5	162	1350
MM	0.7	162	230
RWY	-	-	14

The table should be read in the following way: “*The landing aircraft must be at “IRBES” at 3000 ft and proceed for 3 NM/TC 162° to “OXERU” where its altitude must be 2500 ft; then from “OXERU” it proceeds for 3.1 NM/TC 162° to final approach fix (FAF) where it must be at 2500 ft; and so on until the touchdown at 14 ft (runway elevation)*”.

- **Weather Wind Data.** Since the simulation model is taking into account the wind effect on the aircraft speed, the corresponding weather input must be present. It is specified that the simulator only takes into account the wind effect and neglects any other weather phenomena that can occur and affect the problem.

The integration of the weather model into the AMAN simulation algorithm is described in a dedicated section (§ 4.3.1).

4.3 Processing & Outputs

In this section, a detailed description of the calculations and iterative steps required for the analysis of the given inputs and their mapping into the outputs is provided.

The algorithm is built to resemble the real AMAN flow chart (presented in § 3.2.3) and since the process contains different functions, a block diagram will be used for the sake of clarity.

The simulator AMAN algorithm is very similar to the one presented in Fig. 16, representing the real AMAN flow chart. Indeed, in Fig. 24 it is possible to observe how the simulator processing takes place in the two main blocks: **Trajectory Prediction** and **Sequencer**. The main outputs are described by the *Estimated Landing Time (ELDT)*, the *Target Landing Time (TLDT)*, the *Optimised Sequence* and the *Delay Advice* (that can be either Time To Gain (TTG) if positive, or Time To Lose (TTL) if negative).

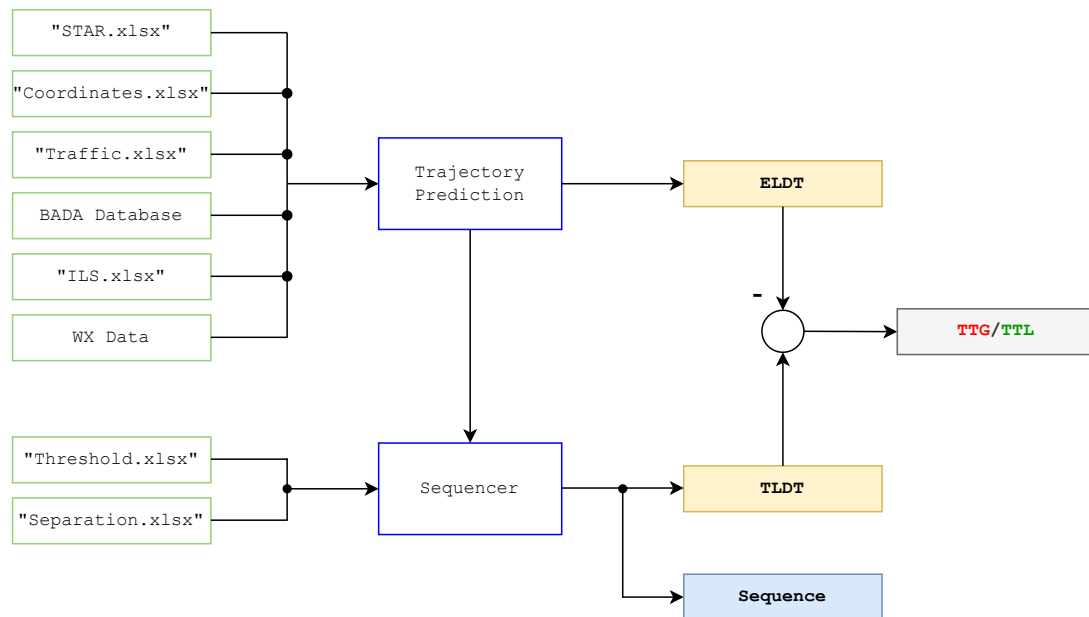


Figure 24: The simulator compact algorithm; the inputs, given as Excel tables, are listed in the left. The two main computational blocks are resembling the real AMAN algorithm.

4.3.1 Trajectory Prediction

The Trajectory Prediction (TP) block contains a set of functions necessary to compute the Estimated Landing Time (ELDT) for each aircraft in the scheduled arriving table.

The main algorithm architecture of the TP module is shown in Fig. 25. The functioning of each block is now explained along with the meaning and the structure of its outputs.

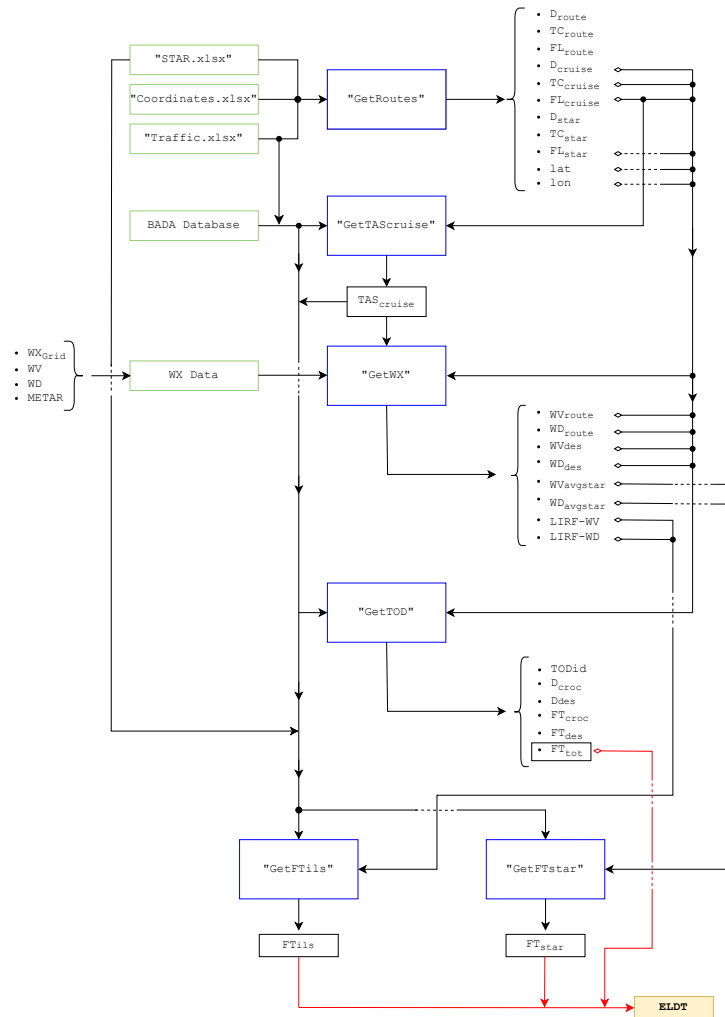


Figure 25: The trajectory prediction algorithm; the inputs are represented as green blocks, the functions as blue blocks and the outputs are in black. The main output (ELDT) is highlighted in yellow.

For the sake of clarity in explaining the functions and the corresponding outputs, the first flight in the schedule, “ITY123”, is taken as an example; the flight presents the characteristics highlighted in Tab. 9 and represented in Fig. 27.

Table 9: Scheduled arriving flights with the corresponding flight plans information.

Traffic									
ID	Flight	Aircraft	Exit WPT	Departure	Route	STAR	Entry WPT	FL	
1	ITY123	A320	LICJ	LURON	LURON M726 PNZ M726 NEKPI M726 LAT	LAT3A	LAT	320	
2	RYR456	B738	LIBD	TOPNO	TOPNO L995 TEA Z803 LAT	LAT3A	LAT	300	
...

“GetRoutes” Function

The first function the TP block calls, is the “GetRoutes” function. This function takes as input the scheduled traffic scenario (Tab. 3), the coordinates database (Tab. 6) and all the possible STARs procedures applied at the arriving airport (each procedure represented by a single file as shown in Tab. 7).

The function, analyses the different flight plans and provides the navigation parameters (in terms of distance, course and altitude) for each flight in the cruise and descend phase. The computed outputs are represented in Fig. 26 and explained below.

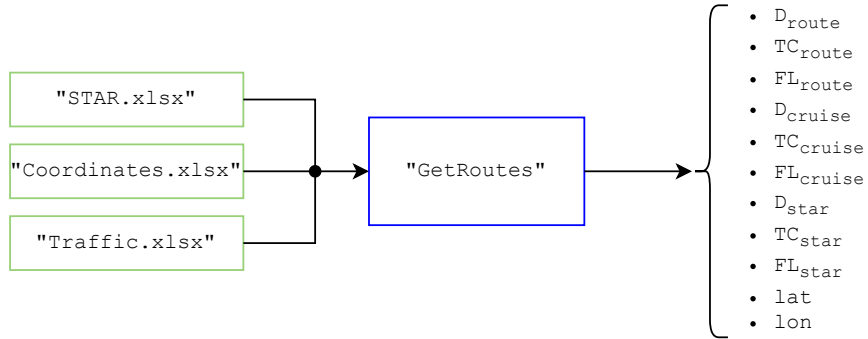


Figure 26: Schematic representation of the “GetRoutes” function; the inputs and the outputs are presented.

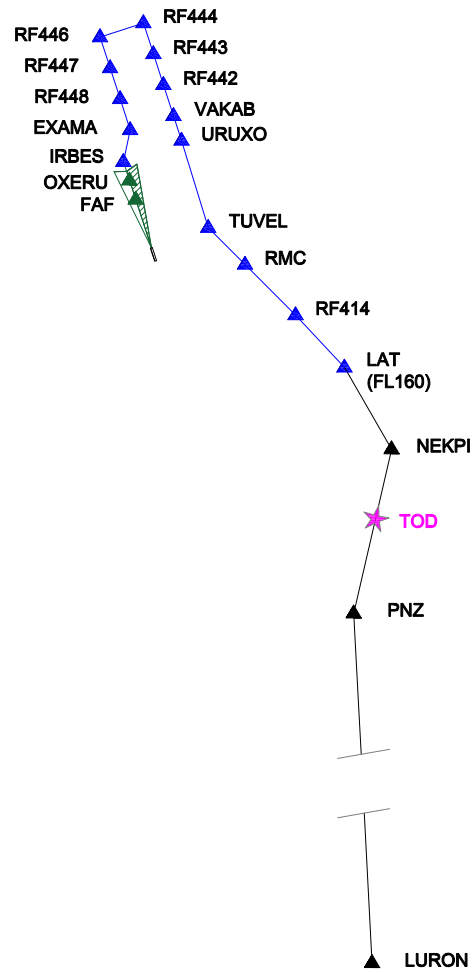


Figure 27: Route of the flight "ITY123". In black the route starting from the entry airway waypoint, in blue the STAR procedure and in green the ILS approach.

- **FLcruise.** This vector stores the cruise FL of each traffic in the list:

$$\text{FLcruise} = \left[\text{FL}_1^{(c)} \quad \text{FL}_2^{(c)} \quad \dots \quad \text{FL}_j^{(c)} \quad \dots \quad \text{FL}_n^{(c)} \right]$$

The flight “ITY123” is represented by $\text{FL}_1^{(c)} = 320$.

- **FLstar.** This output is expressed as a matrix and contains, in the first row, the flight level at which each traffic (represented by a column) should be at the corresponding entry STAR waypoint. The following rows will store the flight levels at which the traffics must be in the STAR intermediate waypoints until the last one (initial approach fix). In the case, a flight flies a STAR procedure presenting a number of segments lower than k (that is, the number of legs of the longest STAR procedure followed by any of the traffics considered in the simulation) the column will be filled with zeros in the gaps.

$$\text{FLstar} = \begin{bmatrix} \text{FL}_{11}^{(s)} & \text{FL}_{12}^{(s)} & \dots & \text{FL}_{1i}^{(s)} & \dots & \text{FL}_{1n}^{(s)} \\ \text{FL}_{21}^{(s)} & \text{FL}_{22}^{(s)} & \dots & \text{FL}_{2i}^{(s)} & \dots & \text{FL}_{2n}^{(s)} \\ \dots & \dots & \dots & \dots & \dots & \dots \\ \text{FL}_{k1}^{(s)} & \text{FL}_{k2}^{(s)} & \dots & \text{FL}_{ki}^{(s)} & \dots & \text{FL}_{kn}^{(s)} \end{bmatrix}$$

The flight “ITY123” must pass by “LAT” at FL160; the following waypoint, “RF414”, must be overflown at FL140 and so on until the last waypoint “IRBES” that must be passed over at 3000 ft.

$$\text{FLstar} = \begin{bmatrix} 160 & 150 & \dots \\ 140 & 140 & \dots \\ \dots & \dots & \dots \\ 030 & 0 & \dots \end{bmatrix}$$

- **Dcruise.** This output is represented by a matrix where each column corresponds to a traffic j , and each row corresponds to the distance (in NM) of the $i - th$ route segment. The total number of traffics is denoted by n and the maximum number of segments in a route among the different flights is called m . In case, a flight has a number of segments lower than m the column will be filled with zeros in the gaps.

$$\mathbf{D}_{\text{cruise}} = \begin{bmatrix} D_{11} & D_{12} & \dots & D_{1,j} & \dots & D_{1,n} \\ D_{21} & D_{22} & \dots & D_{2,j} & \dots & D_{2,n} \\ \dots & \dots & \dots & \dots & \dots & \dots \\ D_{i1} & D_{i2} & \dots & D_{i,j} & \dots & D_{i,n} \\ \dots & \dots & \dots & \dots & \dots & \dots \\ D_{m1} & D_{m2} & \dots & D_{m,j} & \dots & D_{m,n} \end{bmatrix}$$

The first column is then related to the first flight in the list (“ITY123”) and provides the length from “LURON” to “PNZ” in the first row, from “PNZ” to “NEKPI” in the second row, and from “NEKPI” to “LAT” in the third; so it includes the distances between successive route waypoints until the first star waypoint (“LAT” for the flight “ITY123”). The final zero is necessary for dimensional reasons since the third flight (third column) presents four segments.

$$\mathbf{D}_{\text{cruise}} = \begin{bmatrix} 123.4 & 98.8 & 98.5 & \dots \\ 25.9 & 49.6 & 97.3 & \dots \\ 14.5 & 0 & 25.9 & \dots \\ 0 & 0 & 14.5 & \dots \end{bmatrix}$$

- **TCcruise.** This output matrix is organized in the same way as **Dcruise**, but it stores the true courses (in degrees) for the different routes’ segments.

$$\mathbf{TC}_{\text{cruise}} = \begin{bmatrix} TC_{11} & TC_{12} & \dots & TC_{1,j} & \dots & TC_{1,n} \\ TC_{21} & TC_{22} & \dots & TC_{2,j} & \dots & TC_{2,n} \\ \dots & \dots & \dots & \dots & \dots & \dots \\ TC_{i1} & TC_{i2} & \dots & TC_{i,j} & \dots & TC_{i,n} \\ \dots & \dots & \dots & \dots & \dots & \dots \\ TC_{m1} & TC_{m2} & \dots & TC_{m,j} & \dots & TC_{m,n} \end{bmatrix}$$

The first column represents the true courses related to the flight “ITY123”.

$$\mathbf{TC}_{\text{cruise}} = \begin{bmatrix} 356.6 & 282.1 & 334.9 & \dots \\ 12.7 & 287.2 & 336.7 & \dots \\ 329.2 & 0 & 12.7 & \dots \\ 0 & 0 & 329.2 & \dots \end{bmatrix}$$

- **Lat.** This output is a matrix containing the latitude (in degrees) of the different route points for each flight. Each column is representing a flight and each row a waypoint (e.g. first row

first column will be the first route waypoint latitude of the first flight).

$$lat = \begin{bmatrix} \phi_{11} & \phi_{12} & \dots & \phi_{1,j} & \dots & \phi_{1,n} \\ \phi_{21} & \phi_{22} & \dots & \phi_{2,j} & \dots & \phi_{2,n} \\ \dots & \dots & \dots & \dots & \dots & \dots \\ \phi_{i1} & \phi_{i2} & \dots & \phi_{i,j} & \dots & \phi_{i,n} \\ \dots & \dots & \dots & \dots & \dots & \dots \\ \phi_{m1} & \phi_{m2} & \dots & \phi_{m,j} & \dots & \phi_{m,n} \end{bmatrix}$$

In the first column, the latitude of the route’s points for the first flight “ITY123”, is stored. The first column then will be: $[\phi_{LURON}, \phi_{PNZ}, \phi_{NEKPI}, \phi_{LAT}]^T$:

$$lat = \begin{bmatrix} 38.86 & 40.95 & 37.94 & \dots \\ 40.91 & 41.30 & 39.42 & \dots \\ 41.33 & 41.54 & 40.91 & \dots \\ 41.54 & 0 & 41.33 & \dots \\ 0 & 0 & 41.54 & \dots \end{bmatrix}$$

- **Lon.** This matrix is identical to **Lat**, but refers to the longitude (in degrees) of the points.

$$lon = \begin{bmatrix} \lambda_{11} & \lambda_{12} & \dots & \lambda_{1,j} & \dots & \lambda_{1,n} \\ \lambda_{21} & \lambda_{22} & \dots & \lambda_{2,j} & \dots & \lambda_{2,n} \\ \dots & \dots & \dots & \dots & \dots & \dots \\ \lambda_{i1} & \lambda_{i2} & \dots & \lambda_{i,j} & \dots & \lambda_{i,n} \\ \dots & \dots & \dots & \dots & \dots & \dots \\ \lambda_{m1} & \lambda_{m2} & \dots & \lambda_{m,j} & \dots & \lambda_{m,n} \end{bmatrix}$$

The air navigation parameters, true course and distance, are computed by the function with the knowledge of the waypoints geographical coordinates. This calculation process relies on the *rhumb line* route and is explained in details in Appendix A.

“GetTAScruise” Function

The FL_{cruise} output of the “GetRoutes” Function is used along with the BADA aircraft database to extract the cruise speed of each aircraft according to the corresponding cruise flight level (see Fig. 28). The function is simply analysing each traffic in the schedule and extracting the corresponding aircraft type and the relative BADA table (arranged as shown in Tab. 4).

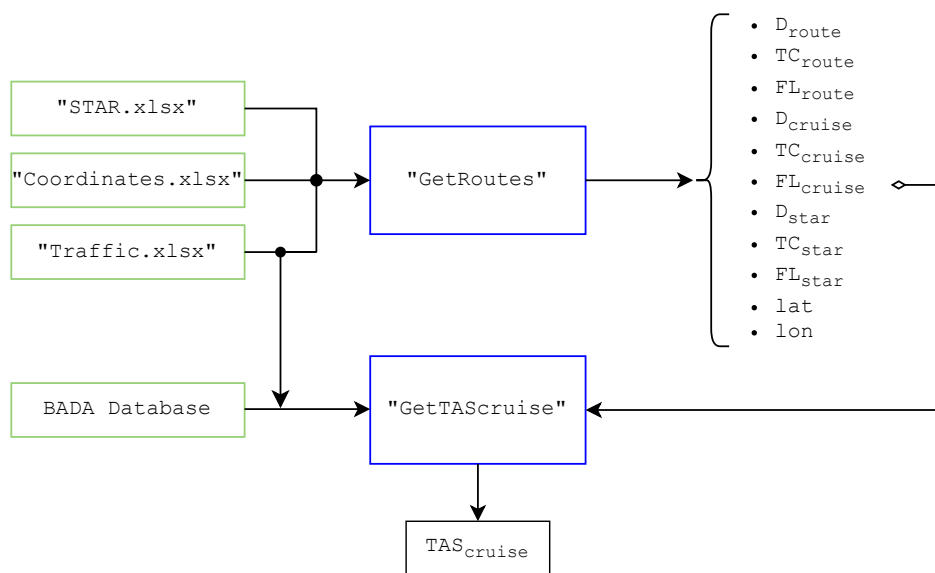


Figure 28: The schematic representation of the “GetTASCruise” function; the inputs and the outputs are shown.

Then, by knowing each flight FL_{cruise} , it is easy to extract from the performance table the corresponding true air speed (TAS)¹⁸. It may happen that the cruise flight level is not present in the performance table; in that case a linear interpolation is done.

TAScruise. This vector represents the cruise TAS (in knots) for each flight.

$$\text{TAScruise} = \left[\text{TAS}_1^{(c)} \quad \text{TAS}_2^{(c)} \quad \dots \quad \text{TAS}_j^{(c)} \quad \dots \quad \text{TAS}_n^{(c)} \right]$$

The flight “ITY123”, flying at FL320, presents $\text{TAS}_1^{(c)} = 456$ kts.

“GetWX” Function

Some of the “GetRoutes” and “GetTAScruise” outputs are further processed in the weather block, whose purpose is to obtain the meteorological data on the simulation domain related to each traffic. Before digging into the details of the function, the simulation weather model is explained.

The main input required to proceed with the analysis, is the wind velocity and direction in the skies and on the airport runway. This data can be obtained using meteorological wind charts [43] as the one represented in Fig. 29. The charts provide a wind forecast at a given time and flight level; they are generally issued every 6 hours.

In the chart below each arrow indicates the main wind direction (from where it blows) and the corresponding intensity (triangle = 50 kts, line = 10 kts and half line = 5 kts).

To provide a reasonable input to the function, the chart below must be converted into a set of data. This is done by dividing the Italian airspace into different weather sectors as shown in Fig. 30.

The grid is more relaxed in the areas far from the arriving airport and more tightened in the skies interested by the Rome terminal area, where most of the arriving flights are.

This segmentation helps in discretizing the wind; indeed, in each sector, an average wind (derived from London WAFC¹⁹ weather charts or different meteorological sources) for different flight levels is defined. This information is translated into data in Tab. 10, Tab. 11 and Tab. 12, where the horizontal and vertical wind in the fragmented Italian airspace is stored.

¹⁸True Air Speed - TAS. It is the aircraft velocity compared to the surrounding air mass; it does not take into consideration any wind effect.

¹⁹World Area Forecast Centers - WAFCs. They provide global aviation weather forecasts, including upper winds, temperatures, turbulence, and significant weather phenomena.

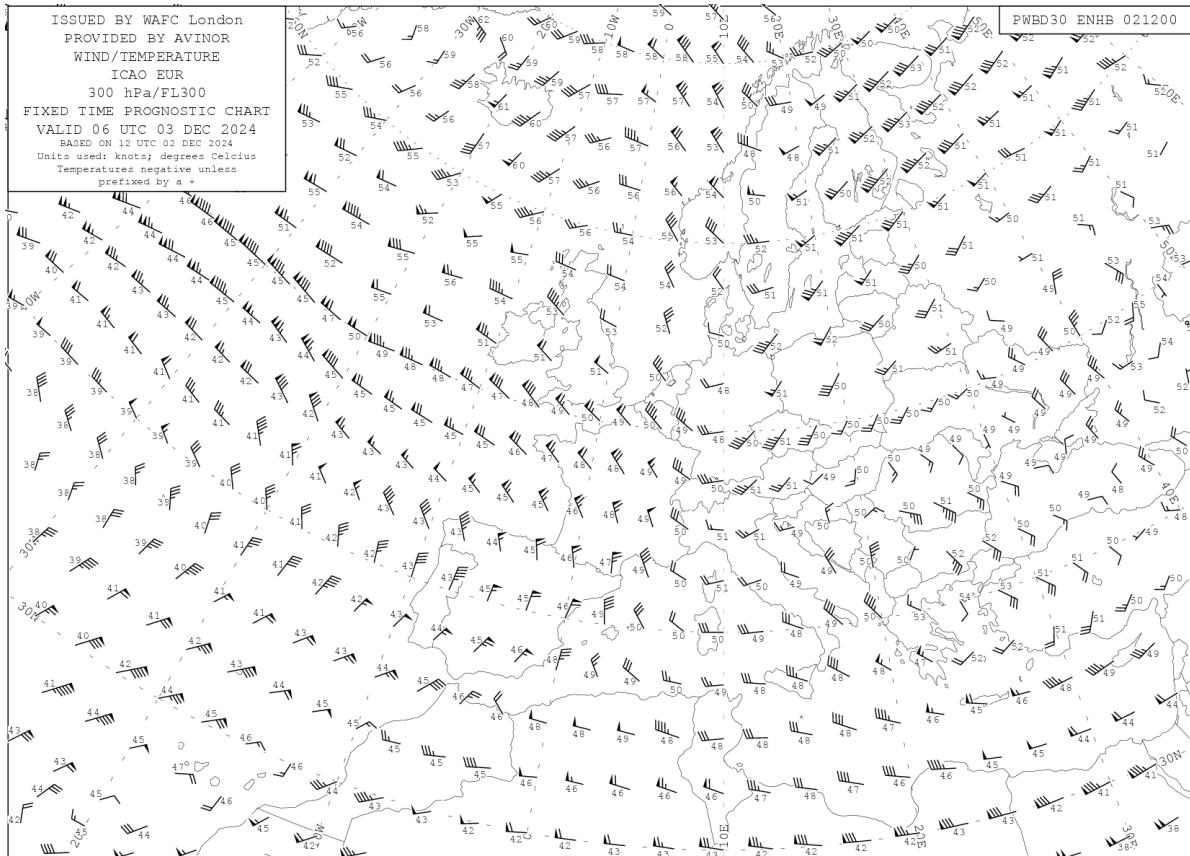


Figure 29: Wind forecast over Europe, issued by WAFC London [43].

Table 10: Limits, expressed as longitude and latitude in degrees, of the different sectors shown in Fig. 30.

Weather Grid Input				
Sector	ϕ_1	ϕ_2	λ_1	λ_2
1	45	47	6	14
2	43	45	7	15
3	38	43	7	11
4	36	40	11	15
5	36	43	15	19
6	41	42	13	15
7	40	41	11	13
8	40	41	13	15
9	42	43	11	13
10	42	43	11	13
11	42	43	13	15

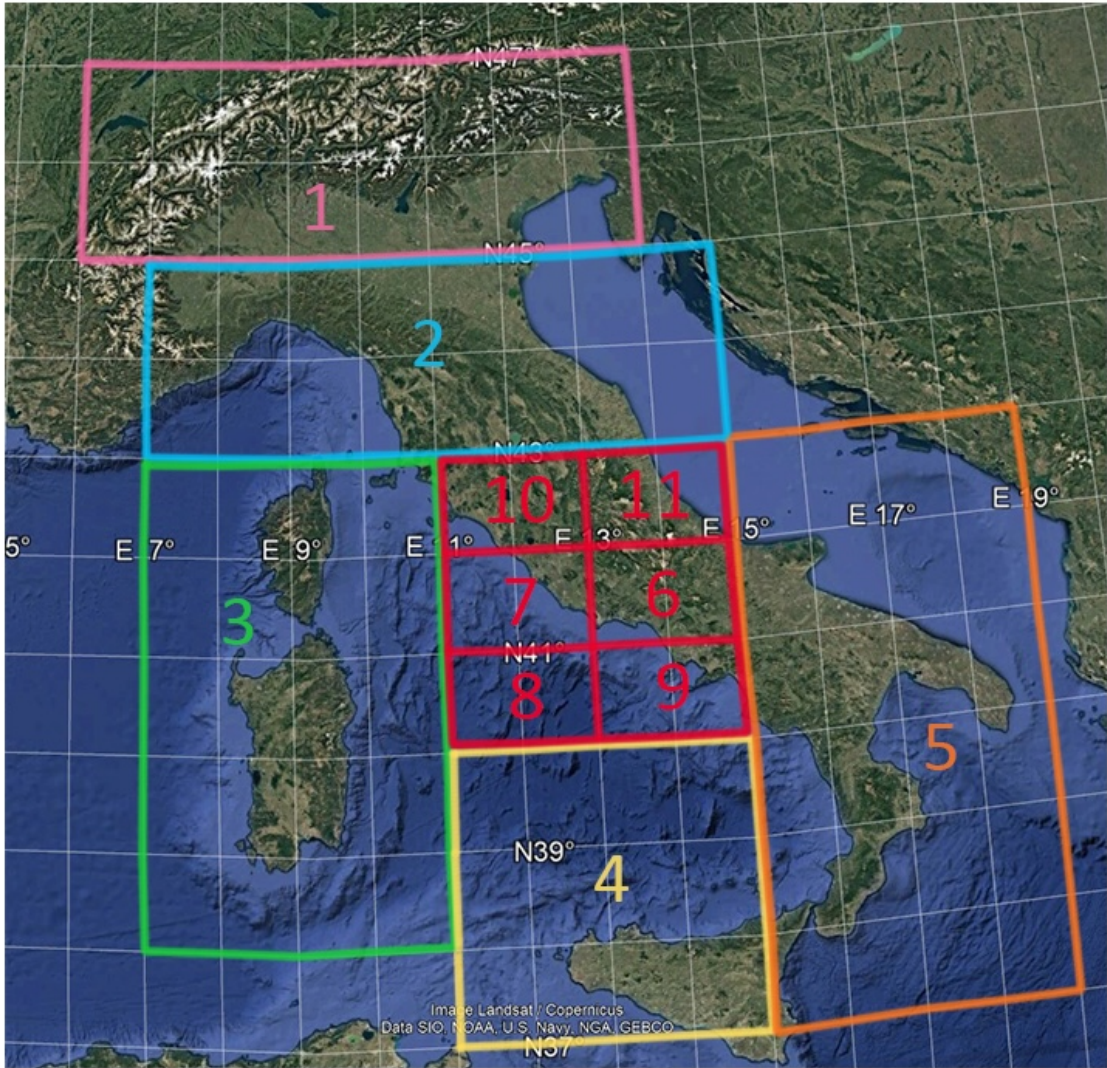


Figure 30: Discretization of the Italian airspace into “weather sectors” for modelling the wind in the skies.

Table 11: Wind velocity in knots for each sector at different flight levels, according to the meteorological charts.

Wind Velocity Input				
FL	Sec1	Sec2	...	Sec11
390	35	30	...	20
360	35	30	...	25
340	40	30	...	25
320	40	40	...	25
300	45	25	...	20
270	45	20	...	20
240	40	20	...	20
180	30	20	...	15
140	25	15	...	15
100	5	10	...	15
50	5	5	...	10

Table 12: Wind direction in degrees for each sector at different flight levels, according to the meteorological charts.

Wind Direction Input				
FL	Sec1	Sec2	...	Sec11
390	290	300	...	290
360	315	350	...	300
340	315	10	...	290
320	315	20	...	275
300	315	20	...	20
270	340	10	...	10
240	330	350	...	350
180	330	350	...	330
140	315	350	...	350
100	330	10	...	350
50	330	360	...	360

The last required weather input, is the aerodrome wind. This can be derived from the METAR²⁰ messages and expressed in a simple input file as in Tab. 13.

Table 13: Aerodrome wind velocity in knots and direction in degrees. The data is obtained by the METAR aerodrome message.

Aerodrome Wind	
Velocity	Direction
20	150

The above weather inputs, are stored in the input module *WX Data*.

As shown in Fig. 31 the *WX Data* along with the other required parameters (that are most of the other functions' outputs) allow to compute the highlighted weather outputs explained below.

- **WVroute.** This output is a matrix where each row corresponds to a flight. The first column represents the cruise FL of each flight, the second column is the wind velocity (in knots) at that cruise FL in sector 1, the third column is the wind velocity at that cruise FL in sector 2, and so on, until sector 11.

$$WV_{route} = \begin{bmatrix} FL_1^{(c)} & WV_1^{(1)} & \dots & WV_1^{(j)} & \dots & WV_1^{(11)} \\ FL_2^{(c)} & WV_1^{(2)} & \dots & WV_2^{(j)} & \dots & WV_2^{(11)} \\ \dots & \dots & \dots & \dots & \dots & \dots \end{bmatrix}$$

- **WDroute.** This matrix presents the same structure as WV_{route} , but it provides the wind direction (in degrees) for each sector.

$$WD_{route} = \begin{bmatrix} FL_1^{(c)} & WD_1^{(1)} & \dots & WD_1^{(j)} & \dots & WD_1^{(11)} \\ FL_2^{(c)} & WD_2^{(1)} & \dots & WD_2^{(j)} & \dots & WD_2^{(11)} \\ \dots & \dots & \dots & \dots & \dots & \dots \end{bmatrix}$$

- **WVdes.** This vector, contains the average descend wind velocity (in knots) for each flight. In row 1, it stores the average descend wind velocity for the first flight (it refers to flight "ITY123") in each sector. This average wind, is computed taking into account the weather sectors the flight will cross during its descent until the STAR entry waypoint ("LAT" for flight "ITY123").

$$WV_{des} = \left[WV_1^{(des)} \quad WV_2^{(des)} \quad \dots \quad WV_j^{(des)} \quad \dots \quad WV_n^{(des)} \right]$$

²⁰Meteorological Terminal Air Report - METAR. It is an aviation weather report providing real-time information about current weather conditions at an airport. It is usually issued every 30 minutes (depending on the airport) [44].

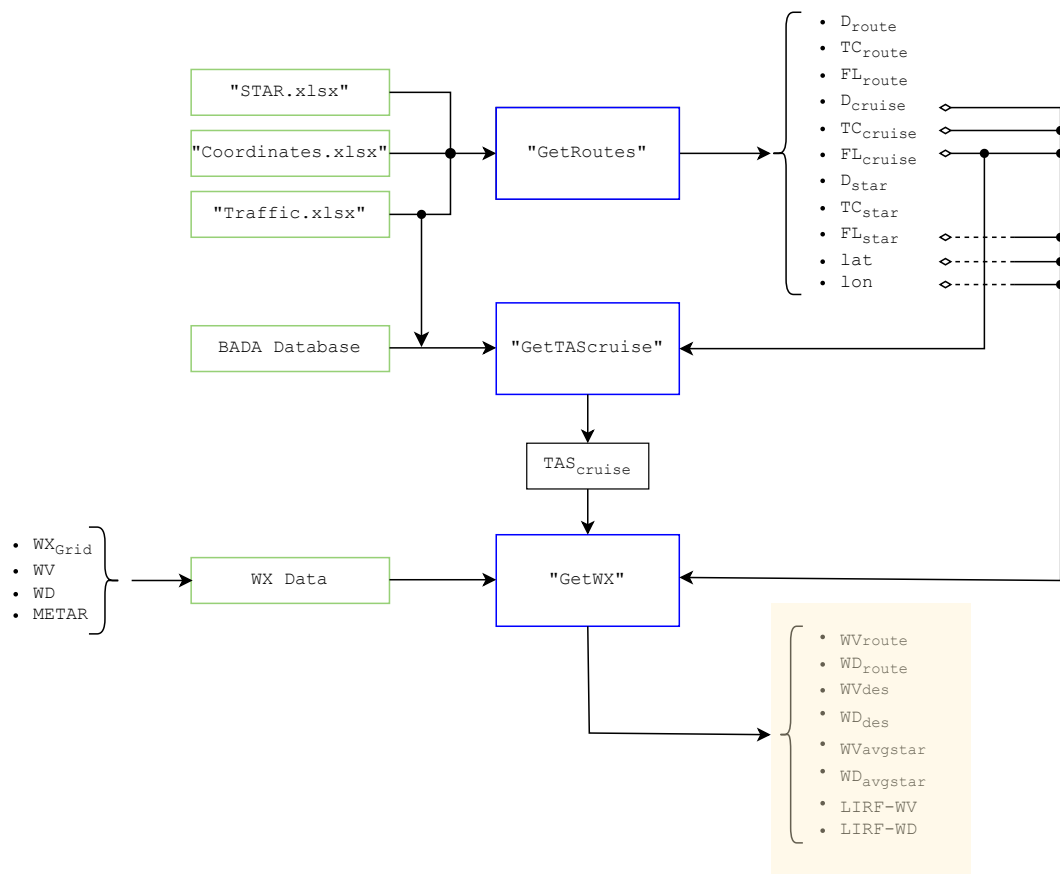


Figure 31: The “GetWX” function represented along with the “GetRoutes” and “GetTAScruise” function. The function outputs are highlighted in yellow.

- **WDdes**. This vector contains the average descend wind direction (in degrees) for each flight, arranged as for WV_{des} .

$$WD_{des} = \left[WD_1^{(des)} \quad WD_2^{(des)} \quad \dots \quad WD_j^{(des)} \quad \dots \quad WD_n^{(des)} \right]$$

- **WVstar**. This vector contains the average STAR wind velocity (in knots) for each flight. In row 1, it gives the average STAR wind velocity for the first flight (“ITY123”).

$$WV_{star} = \left[WV_1^{(star)} \quad WV_2^{(star)} \quad \dots \quad WV_j^{(star)} \quad \dots \quad WV_n^{(star)} \right]$$

- **WDstar**. Identically to WV_{star} , this vector contains the average star wind direction (in degrees) for each flight.

$$WD_{star} = \left[WD_1^{(star)} \quad WD_2^{(star)} \quad \dots \quad WD_j^{(star)} \quad \dots \quad WD_n^{(star)} \right]$$

- **LIRFWV**. This is the aerodrome wind velocity given by the METAR message and it is a single value expressed in knots (given as input in Tab. 13).
- **LIRFWD**. This is the aerodrome wind direction given by the METAR message and it is a single value expressed in degrees (given as input in Tab. 13).

“GetTOD” Function

In order to provide the flight times in each route’s leg, the top of descent (TOD) position is calculated. The function, computes the TOD position and the flight times and distances for the cruise phase until the TOD, and the descend phase until the STAR entry waypoint. In addition, since each flight presents a different TOD position, the function is run iteratively for each traffic. The outputs are highlighted in Fig. 32 and explained below.

- **TODid**. This output is a vector containing the position of the TOD in the route starting from the first route fix to the STAR entry waypoint (for flight “ITY123”, they are “LURON” and “LAT” respectively). $TOD_1^{(id)} = 2$ means the TOD is in the route leg number two (“PNZ” → “NEKPI” for flight “ITY123”).

The vector, for n flights will be:

$$TOD_{id} = \left[TOD_1^{(id)} \quad TOD_2^{(id)} \quad \dots \quad TOD_n^{(id)} \right]$$

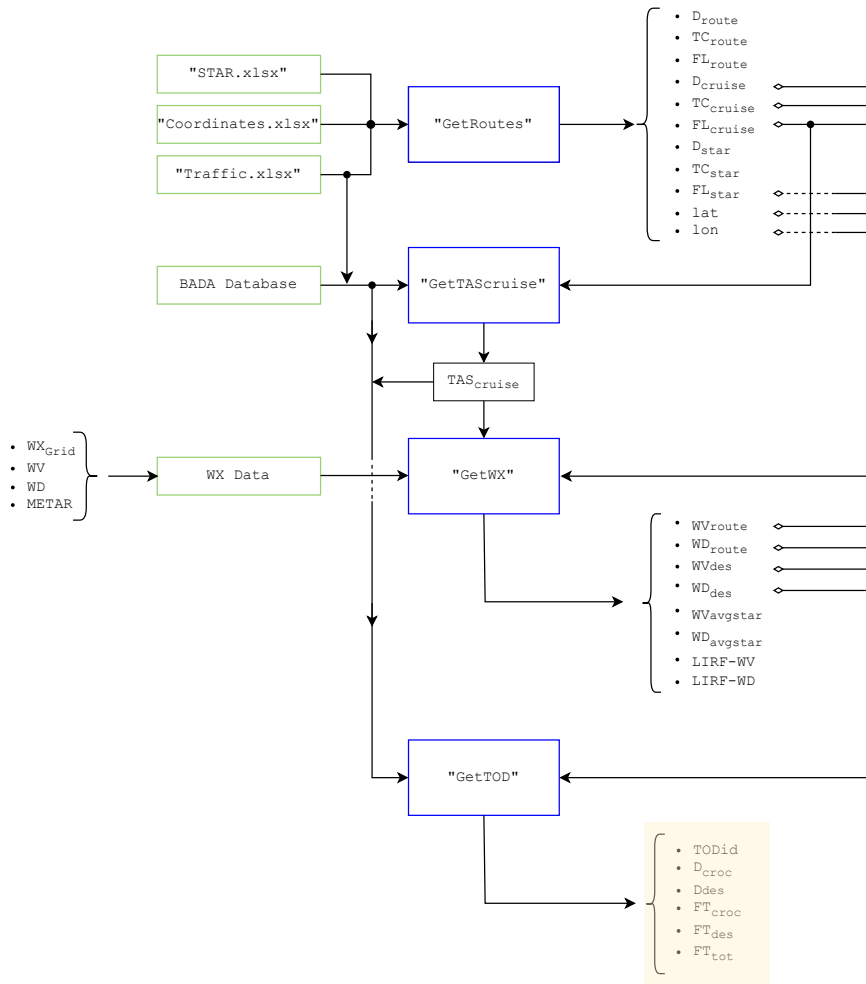


Figure 32: The "GetTOD" function in the algorithm, the outputs are highlighted in yellow.

- **Dcroc.** This matrix, is arranged in the same way as D_{cruise} but, while D_{cruise} contains in each column (representing each flight) the legs' distances from the first route fix to the entry STAR waypoint, D_{croc} contains the legs' distances from the first route fix to the top of descent point. As for D_{cruise} , the total number of traffics is denoted by n while the maximum number of segments from the first fix to the TOD, among the different flights, is called p . In the case in which a flight has a number of segments lower than p , the column will be filled with zeros in the gaps.

$$D_{croc} = \begin{bmatrix} D_{11} & D_{12} & \dots & D_{1,j} & \dots & D_{1,n} \\ D_{21} & D_{22} & \dots & D_{2,j} & \dots & D_{2,n} \\ \dots & \dots & \dots & \dots & \dots & \dots \\ D_{i1} & D_{i2} & \dots & D_{i,j} & \dots & D_{i,n} \\ \dots & \dots & \dots & \dots & \dots & \dots \\ D_{p1} & D_{p2} & \dots & D_{p,j} & \dots & D_{p,n} \end{bmatrix}$$

In the illustrative example, the first column is related to the first flight in the list, "ITY123", and provides the length from "LURON" to "PNZ" in the first row and from "PNZ" to the "TOD" in the second row; so it includes the distances between successive route waypoints until the top of descend point for the flight "ITY123".

The next row zero is necessary for dimensional reasons since the maximum number of legs (until the TOD) among the different flights is $p = 3$ (meaning the TOD for that particular flight is in the third route leg).

$$D_{croc} = \begin{bmatrix} 123.4 & 98.8 & 98.5 & \dots \\ 12.5 & 30.1 & 70.8 & \dots \\ 0 & 0 & 5.6 & \dots \end{bmatrix}$$

- **Ddes.** Also this output matrix is arranged in the same way as D_{croc} . However, it stores the legs' distances from the top of descend point to the entry STAR waypoint. The total number of traffics is denoted by n while the maximum number of segments from the TOD to the first STAR entry waypoint, among the different flights, is called t . In case a flight has a number of segments lower than t , the column will be filled with zeros in the gaps.

$$\text{Ddes} = \begin{bmatrix} D_{11} & D_{12} & \dots & D_{1,j} & \dots & D_{1,n} \\ D_{21} & D_{22} & \dots & D_{2,j} & \dots & D_{2,n} \\ \dots & \dots & \dots & \dots & \dots & \dots \\ D_{i1} & D_{i2} & \dots & D_{i,j} & \dots & D_{i,n} \\ \dots & \dots & \dots & \dots & \dots & \dots \\ D_{t1} & D_{t2} & \dots & D_{t,j} & \dots & D_{t,n} \end{bmatrix}$$

In the example below, the first column is related to the flight “ITY123” and provides the length from “TOD” to “NEKPI” in the first row and from “NEKPI” to the “LAT” in the second row. As explained before, the next row zero is necessary for dimensional reasons.

$$\text{Ddes} = \begin{bmatrix} 13.4 & 19.5 & 26.5 & \dots \\ 14.5 & 0 & 25.9 & \dots \\ 0 & 0 & 14.5 & \dots \end{bmatrix}$$

- **FTcroc.** This output vector contains the total cruise time (from first route fix to TOD) for each flight.

$$\text{FTcroc} = \left[FT_1^{(c)} \quad FT_2^{(c)} \quad \dots \quad FT_n^{(c)} \right]$$

This flight time is calculated by using the TAS_{cruise} of each flight, the corresponding cruise wind (WV_{route} and WD_{route}) and the true course of each leg until the top of descend. Since for the flight time computations, the ground speed (GS)²¹ is required, the function “GetGS”, defined inside “GetTOD”, allows to get the GS with the given data (see Appendix B).

It is underlined that the cruise wind used to calculate the ground speed, is not actually the one provided by WV_{route} and WD_{route} since it would not take into account the TOD position (indeed, that wind represents the average cruise flight level wind in the weather sectors crossed by the flight). To be precise, the wind should be defined as the average flight level wind in the sectors crossed by the flight until the TOD position. For this reason, now that the TOD position is known, an inside function called “GetWXcruise” is defined in order to provide the corrected $WV_{route}^{(*)}$ and $WD_{route}^{(*)}$ for each flight.

- **FTdes.** This output vector contains the total descend time (from TOD to the STAR entry waypoint) for each flight.

²¹Ground Speed - GS. It is the velocity of the aircraft with respect to the ground hence it is calculated by summing the wind effect to the true air speed (TAS).

$$FT_{des} = \left[FT_1^{(d)} \quad FT_2^{(d)} \quad \dots \quad FT_n^{(d)} \right]$$

This flight time is calculated using the descend performance of each flight, the corresponding descend wind (WV_{des} and WD_{des}) and the true course of each leg from the TOD until the STAR entry waypoint.

- **FTtot.** This vector stores the total flight time from the first route waypoint to the STAR entry waypoint for each traffic.

$$FT_{tot} = \left[FT_1^{(tot)} \quad FT_2^{(tot)} \quad \dots \quad FT_n^{(tot)} \right]$$

It is easily computed:

$$FT_j^{(tot)} = FT_j^{(d)} + FT_j^{(c)} \quad (3)$$

Now that the cruise and descend phase until the STAR entry waypoint have been analysed, the STAR and approach procedures are studied.

“GetFTstar” Function

This function allows to compute the flight time from the STAR entry waypoint until the initial approach fix (IAF), where the ILS begins. The function, shown in Fig. 25, calculates the flight time using the aircraft performance, the corresponding flight STAR procedure and the wind input. As for the descend and cruise computations, the function includes the calculation of the ground speed using the “GetGS” function (see Appendix B).

The output is expressed as a vector containing in each column (representing each traffic) the flight time from the STAR entry waypoint to the first approach waypoint (which corresponds to the IAF).

$$FT_{star} = \left[FT_1^{(s)} \quad FT_2^{(s)} \quad \dots \quad FT_n^{(s)} \right]$$

“GetFTils” Function

This function, simply computes the flight time required for each traffic to fly from the IAF to the runway. The inputs and the output are visible in the complete trajectory prediction module algorithm in Fig. 25. The function first calculates the average approach ground speed using the average approach TAS (that depends on the aircraft performances), the landing course and the

aerodrome wind. Knowing the approach distances it is then immediate to get the required approach time.

$$FTils = \left[FT_1^{(app)} \quad FT_2^{(app)} \quad \dots \quad FT_n^{(app)} \right]$$

To conclude, the calculation of the “Estimated Landing Time” (ELDT) for the j -th flight is given by Eq. 4.

$$ELDT_j = t_0 + FT_j^{tot} + FT_j^s + FT_j^{app} \quad (4)$$

Where t_0 represents the actual time.

4.3.2 Sequencer

The sequencer module calculates the “Target Landing Time” (TLDT) and determines the landing sequence based on the “First Come, First Serve” principle.

The sequence is determined by sorting (in increasing order) the ELDT times (and the corresponding flights) provided by the TP module.

To compute the target landing time, the following inputs (see Fig. 24) are required:

- **Separation Minima.** This input, described in § 4.2, represents the required spacing (in nautical miles) between two consecutive landings. It is determined by the wake turbulence category and other constraints, such as runway capacity.
- **ELDT:** This input, calculated by the TP module, represents the estimated landing time for each flight.
- **Wake Turbulence Category.** The wake turbulence categories of the flights are obtained from the “Traffic” input and sorted according to the landing sequence.
- **Approach Ground Speed.** This speed is computed inside the TP module and used to calculate the distance between consecutive aircraft. It is determined using the function “GetGS” (see Appendix B), which considers the approach TAS (from aircraft performance data), the approach course (as defined by the ILS procedure), and the aerodrome wind.
- **Threshold.** This defines the maximum allowable delay advice in minutes. It prevents cases where a flight is optimized in the sequence with an excessive Time To Lose (TTL, negative delay) or Time To Gain (TTG, positive delay), which the air traffic controller may not be able to handle. The threshold sets a limit the delay advice cannot exceed.

The sequencer module is represented by a single function that provides the TLDT for each aircraft.

First the spacing (in nautical miles) according to the ELDT is calculated using Eq. 5 as shown in the explanatory example in Fig. 33. Since it is an iterative process, the first iteration is initialized using $TLDT_1 = ELDT_1$.

$$\Delta D_{i+1} = (ELDT_{i+1} - TLDT_i) \cdot GS_{i+1}^{(app)} \quad (5)$$

For sake of clarity, let's take the example in Fig. 33. The flight "BAW147" is following the traffic "IBE556"; the ELDT are respectively $10^h38^m24^s$ and $10^h37^m56^s$. The spacing at which the following aircraft ("BAW147") will be:

$$\Delta D_2 = (ELDT_2 - TLDT_1) \cdot GS_2^{(app)} = (10^h38^m24^s - 10^h37^m56^s) \cdot 114kts = 0.9NM \quad (6)$$

With $TLDT_1 = ELDT_1$.

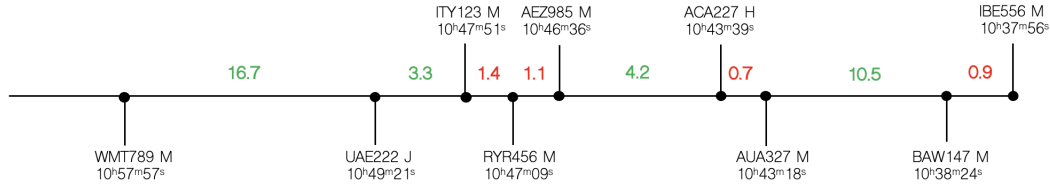


Figure 33: Runway spacing (in nautical miles) according to the computed Estimated Landing Times ELDTs.

Comparing the separation minima distances (input *separation minima* represented in Tab. 5) with the computed ΔD_{i+1} , it is possible to calculate with Eq. 7 the gain or loss requirements in distance terms.

$$\Delta D_{i+1}^{(*)} = sep - \Delta D_{i+1} \quad (7)$$

To understand and clarify, the previous example is extended.

Since the wake turbulence category of both "BAW147" and "IBE556" is "M", the input provides the minimum separation of 2.5 NM.

This means that the following flight should gain:

$$\Delta D_2^{(*)} = 2.5 - \Delta D_2 = 1.6NM \quad (8)$$

Translating in time, the quantity $\Delta D_{i+1}^{(*)}$ becomes:

$$\Delta t_{i+1}^{(*)} = \frac{\Delta D_{i+1}^{(*)}}{GS_{i+1}^{(app)}} \quad (9)$$

In the previous example, this corresponds to:

$$\Delta t_2^{(*)} = \frac{1.9}{114} = +0^m 50^s \quad (10)$$

This represents the exact delay the aircraft “BAW147” should gain in order to respect the separation minima distance with the preceding flight “IBE556”. The result is calculated with a precision of seconds; however, the delay information provided to the controller is expressed in minutes, as their sensitivity is not high enough to handle operations requiring second precision. For this reason the rounding to minutes is necessary (for flight “BAW147” it will be $+1^m$). It is remarked that the rounding must be such that the minimum separation is respected; for this reason, it is carried out in a conservative way as shown in Alg. 1.

The target landing time is then easily calculated:

$$TLDT_{i+1} = ELDT_{i+1} + \Delta t_{i+1}^{(*)} \quad (11)$$

This procedure is applied iteratively to all the landing aircraft in the sequence, producing the delay advices and target landing times for all the scheduled traffics.

Referring to the previous example, the final landing sequence looks like the one represented in Fig. 34. In the figure, the flight “IBE556” represents the first flight in the sequence.

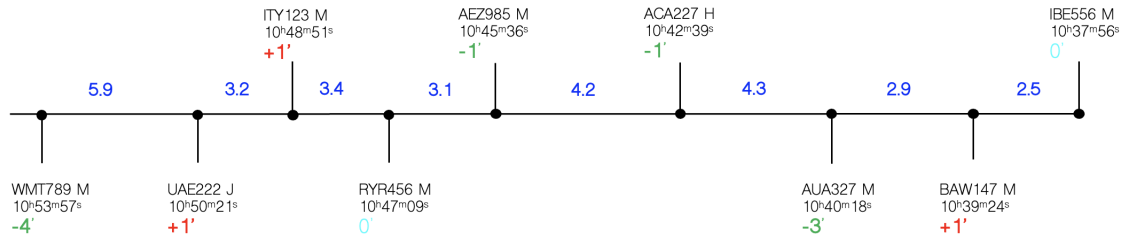


Figure 34: Runway spacing (in nautical miles) according to the computed Target Landing Times TLDTs. The Time To Lose or Time To Gain is shown in green and red respectively. In cyan the neutral delay advice.

In the computations explained above, an important remark must be done for the calculus of the delay advice (Eq. 9). The threshold limit must be taken into account for TTL and TTG delays. The threshold can be the same number for TTL and TTG or not, this is at user's discretion according to the needs. The software iterates for each flight (represented by i in the loop) the instructions reported in Alg. 1, allowing for the proper delay advice rounding and checking against the threshold. This process also updates the spacing and TLDT accordingly.

Algorithm 1 Pseudocode for Updating $\Delta t_{i+1}^{(*)}$

- 1: **if** $|\Delta t_{i+1}^{(*)}| > \text{threshold}$ **and** $\Delta t_{i+1}^{(*)} < 0$ **then** ▷ Case “TTL” larger than threshold
 - 2: $\Delta t_{i+1}^{(*)} = -\text{threshold}$ ▷ Maximum TTL the ATCO can handle
 - 3: $\Delta D_{i+1}^{(*)} = \Delta t_{i+1}^{(*)} \cdot GS_{i+1}^{(app)}$ ▷ Spacing update
 - 4: **else if** $|\Delta t_{i+1}^{(*)}| > \text{threshold}$ **and** $\Delta t_{i+1}^{(*)} > 0$ **then** ▷ Case “TTG” larger than threshold
 - 5: $\Delta t_{i+1}^{(*)} = +\text{threshold}$ ▷ Round to the higher minute
 - 6: $\Delta D_{i+1}^{(*)} = \Delta t_{i+1}^{(*)} \cdot GS_{i+1}^{(app)}$ ▷ Spacing update
 - 7: **else if** $|\Delta t_{i+1}^{(*)}| < \text{threshold}$ **and** $\Delta t_{i+1}^{(*)} < 0$ **then** ▷ Case “TTL” lower than threshold
 - 8: $\Delta t_{i+1}^{(*)} = \text{fix}(\Delta t_{i+1}^{(*)})$ ▷ Round to the lower minute
 - 9: $\Delta D_{i+1}^{(*)} = \Delta t_{i+1}^{(*)} \cdot GS_{i+1}^{(app)}$ ▷ Spacing update
 - 10: **else if** $|\Delta t_{i+1}^{(*)}| < \text{threshold}$ **and** $\Delta t_{i+1}^{(*)} > 0$ **then** ▷ Case “TTG” lower than threshold
 - 11: $\Delta t_{i+1}^{(*)} = \text{ceil}(\Delta t_{i+1}^{(*)})$ ▷ Round to the higher minute
 - 12: $\Delta D_{i+1}^{(*)} = \Delta t_{i+1}^{(*)} \cdot GS_{i+1}^{(app)}$ ▷ Spacing update
 - 13: **end if**
-

The results obtained by checking the simulator in different scenarios are discussed in the last chapter of this work. In the following chapter, particular attention is given to the visualization of the simulator outputs and on how these outputs are presented to the user, highlighting the importance of an efficient interface design.

5 Human Factors Study on the Solution AMAN Interface

5.1 AMAN and Radar Interface

The outputs produced by the AMAN simulator, explained in the previous chapter, need to be displayed to the user through an interface. This human-machine interface (HMI) should be easy to use and understand, providing good situational awareness and following the Human Factors principles outlined in § 3.3.

Based on the feedback from air traffic controllers, who have reported issues with the current AMAN HMI, a study is conducted to understand how the interface can be improved and better adapted to the operators' needs. Indeed, several aspects of the current HMI are not user-friendly for air traffic controllers which more importantly, *often report that the workload is increased rather than reduced*. These critical aspects are now investigated through an analysis of the current AMAN interface design. Subsequently, the development of a new HMI solution is proposed in order to enhance its usability.

Before describing the interfaces, it is important to highlight that AMAN is used by air traffic controllers operating in the ACC and managing arriving flights at a terminal hub. For this reason, they perform their tasks using radar systems.

The interface, known as CWP (Controller Working Position), can be split in two main parts: in the right, the controllers are provided by the radar screen while in the left, the AMAN interface is displayed.

Being the study conducted for Rome Fiumicino airport, the interfaces presented in this work are resembling as much as possible the real CWP HMIs installed in Rome and Milan ACC.

5.2 Baseline HMI

In this section, the current CWP HMI development is discussed. Each air navigation service provider presents its own interface design, for this reason it might be difficult to replicate with precision all the elements and features the HMI presents. Nevertheless, the information displayed to the air traffic controllers are more or less the same. As mentioned earlier, the interface is designed to resemble the Italian HMIs used in the ACCs, but still, it may differ from the real systems in use. Additionally, since the ATCO can manually select what kind of information associated to a flight he/she wants to see, the complete label is used in the interest of clearness and simplicity.

In Fig. 35, the developed **baseline** interface is shown. On the right-hand, the radar screen with one single traffic is presented, while on the left-hand the AMAN timeline is displayed.

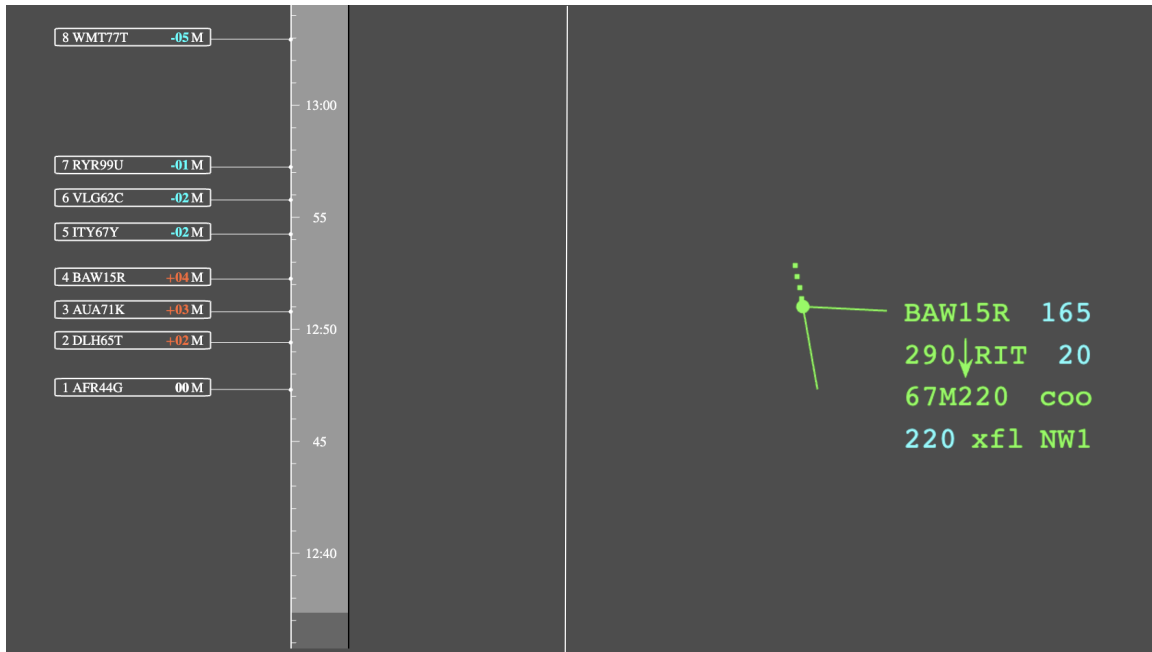


Figure 35: The designed **baseline** interface; on the right-hand side, the radar screen with the traffic and the corresponding label is shown. On the left-hand side the AMAN timeline is presented.

5.2.1 Radar Screen

The right side of the screen is first explained. As represented in the figure, two main sets of information are provided:

1. The radar track. This allows to detect the position and movements of an aircraft over time and three main information are given.
 - Aircraft Position. This is determined by the central green circle.
 - Aircraft History. The dots (squares), called “*history dots*”, are giving to the controller the idea of the path the aircraft followed in the previous n minutes (this number can be chosen by the controller according to the needs).
 - Aircraft Future Prediction. The green segment, known as “*tactical speed vector*” (TSV), allows the controller to predict where the aircraft will be in the next p minutes (that the ATCO can choose) based on the current speed and heading.
2. The label. This is a sort of matrix representing the set of crucial information about the aircraft and its status. The label is linked to the radar track through a segment. The information

in cyan color are the so called “*downlinked airborne parameters*” (DAPs), which are directly sourced from the aircraft. This data is available only when the aircraft is equipped with a Mode S transponder or ADS-B technology.

- Callsign. This is the flight name (“BAW15R”).
- Heading. This is the true heading of the aircraft, meaning the angle (positive clockwise) between the geographic north and the longitudinal axis. (“165” degrees).
- Flight Level. This is the flight level at which the aircraft is actually flying (“290”).
- Trend. The arrow is telling the ATCO if the aircraft is climbing, descending or cruising. It is intuitive, if pointing downward it is descending, if upward climbing, if absent the airplane is cruising.
- Exit Waypoint. This represents the waypoint (sometimes abbreviated) where the aircraft is leaving the ATCO’s jurisdiction airspace (“RIT” represents “RITEB”).
- Vertical Speed. This represents the vertical velocity of the aircraft in feet per minute. It is reported in the abbreviated form as $\frac{VS}{1000}$ (“20”- meaning 2000 feet per minute).
- Mach Number. This is the velocity expressed with the Mach Number²² (“67”, meaning Mach $N^\circ = 0.67$).
- Wake Turbulence Category. This is the wake turbulence category of the aircraft which depends on the maximum take-off weight (MTOW). It is important to know this information since, according to the category, the ATCO must respect a certain horizontal and vertical separation with other traffics (“M”).
- Authorized Flight Level. This represent the flight level the controller has authorized (“220”).
- Coordination. This text represents whether the authorized flight level is coordinated with next sector or not. The text “coo” means the authorized FL (“220”) is coordinated in the exit waypoint (“RIT”) between air traffic controllers.
- Selected Flight Level. This is giving an information about the selected FL in the on-board autopilot. This helps in checking the compatibility of the authorized flight level and selected flight level (“220”).
- Transfer Flight Level Coordination. In this field the ATCO can write the flight level at which the aircraft is transferred to next control sector. The controller of the next sector can accept or not the proposed flight level (“xfl”).

²²Mach Number. It is defined as the ratio $\frac{TAS}{a}$, where a represents the speed of sound at that altitude.

- Next Control Sector. This is giving an information about the next control sector the aircraft will be in contact with (“NW1”).

In addition to the information mentioned above, the color of the aircraft’s label and radar track changes based on its status within the sector.

5.2.2 AMAN Screen

On the left side of the CWP, the AMAN information is displayed. The interface provides a timeline where the different flights are positioned according to their corresponding target landing time (TLDT). This baseline interface is not providing all the information the real AMAN provides, in particular, for the sake of simplicity, two information are missing: the *reference fix* (representing the entry point in the STAR procedure) and the *distance to go* (representing the predicted nautical miles from the current position to the touchdown). The other crucial elements, present in the baseline interface (see Fig. 35), are explained below.

1. Timeline. This is the vertical grey band, with time markers indicated at intervals of 1 minute. Additionally, the time is specified in minutes at 5-minute intervals (e.g. “45” for 12:45), while the full format (hours and minutes) is displayed at 10-minute intervals (e.g. “12:50” for 12:50). In the baseline interface, the current time is typically indicated by the transition between the grey region of the band and the start of the dark grey region. In Fig. 35, the current time is around 12:37 and the flight “BAW15R” is supposed to land at 12:52.
2. Aircraft Tag. This is the left box connected to the timeline in the corresponding target landing time, containing different pieces of information.
 - Sequence Number. This represent the number the flight has in the landing sequence computed by AMAN (e.g. “4”, that corresponds to the flight “BAW15R”, means the aircraft will be the 4th in the sequence).
 - Aircraft Callsign. This is to identify the corresponding flight.
 - Delay Advice. This is the delay advice provided by AMAN and referred to that sector; it is represented in dark orange if positive (TTG), in cyan if negative (TTL) and in white if neutral.
 - Wake Turbulence Category. This is useful for the separation between successive landings (that is taken into account by AMAN).

The issues the air traffic controllers underlined are mainly referred to the absence of the AMAN information in the right part of the screen. Indeed, because the radar screen and and the AMAN

are not communicating, the information is not transferred between the two parts. This issue along with other operative problems (discussed in Chapter 6) contributes to an increased workload for air traffic controllers. To address these interface related problems, a new proposed solution is now presented.

5.3 Solution HMI

The primary goal of the proposed solution is to display the AMAN delay advice and sequence number directly in the label on the radar screen. Since the ATCO primarily manages air traffic by focusing on the radar screen (that is on the right), presenting the essential AMAN information in the label helps the ATCOs to avoid constantly shifting their focus from the right side of the screen to the left in order to access the AMAN details. Additionally, a color gradient is used to indicate the severity of the delay. This allows the ATCO to directly perceive the extent of the delay through the visual representation. In Fig. 36, the proposed solution is shown.

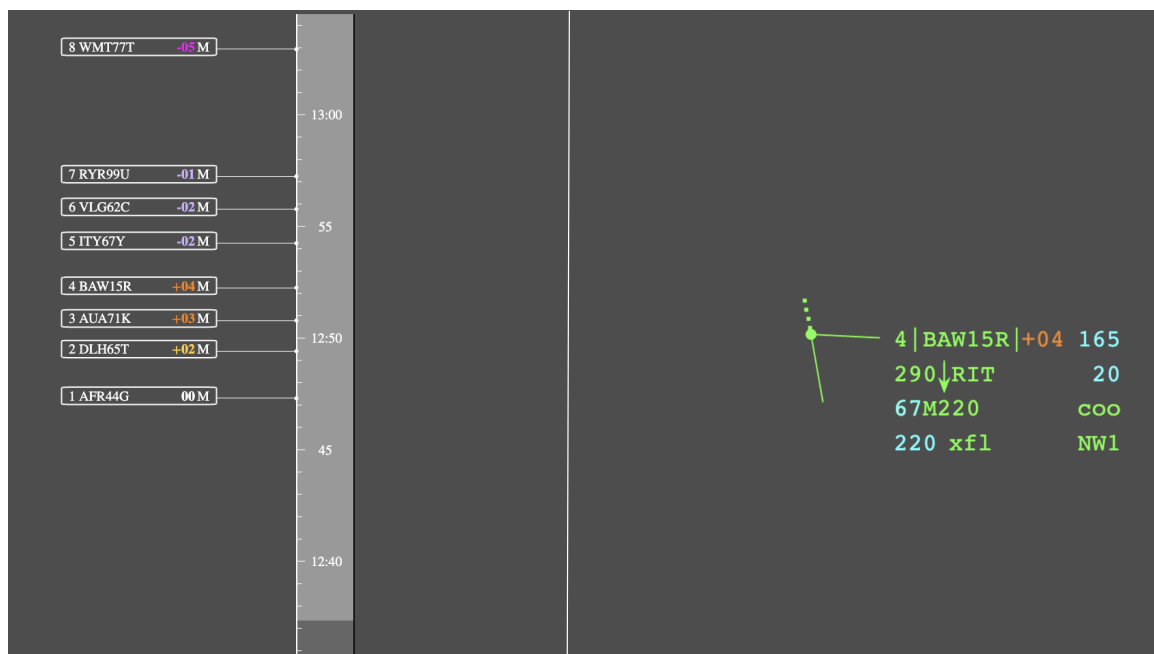


Figure 36: The designed **solution** interface; on the right side, the radar screen with the traffic and the corresponding label is shown. On the left side the AMAN timeline is presented.

The new HMI is including the following upgrades:

1. Sequence Number in the label. As shown in the figure, the sequence number is displayed on the left side of the callsign. This number provides the ATCO with the flight's position in the sequence; this allows the air traffic controller to avoid focusing on the timeline. The color of the number matches the default color of the label and radar track, which changes according to the flight's state.
2. Delay Advice in the label. The delay advice, is the second essential piece of information computed by AMAN. It is displayed just after the callsign, assisting the ATCO along with the sequence number. This value indicates the amount of delay the flight must either gain or lose (within the ATCO sector's jurisdiction) to meet the Target Landing Time (TLDT) presented in the optimized sequence, which is shown on the timeline on the left side of the screen. Unlike the sequence number, the delay advice changes color according to its severity. This helps the operator to instantly understand the magnitude. The positive delays range from dark yellow (indicating low delays) to dark orange (indicating high delays). If a dark orange number is shown in red, it means that a holding advice is proposed to the controller for delay absorption. The negative delays instead range from lilac (indicating low negative delays) to magenta (indicating high negative delays). Finally, the neutral delay (zero minutes) is depicted in white. Selecting suitable colors is a complex task as most of them are already designated for other purposes and features. Furthermore, the dark grey background requires colors that are sufficiently luminous to ensure visibility but not too much bright to minimize distractions.
3. Delay Advice Color in the AMAN screen. While the baseline solution used only two colors (one for delay loss and one for delay gain), this solution proposes applying the same color gradient explained in the previous point, to the information displayed on the left side of the screen (the AMAN interface) as well.

The color gradients explained before are shown in Fig. 37 and Fig. 38 for positive and negative delays respectively.



Figure 37: The color gradient used for positive delay advices.



Figure 38: The color gradient used for negative delay advices.

5.4 Human Factors Analysis

To evaluate the goodness of the proposed solution from a Human Factors perspective, a preliminary study is done. This study aims to analyse the impact of the new solution in its usability, workload, situational awareness and user satisfaction. By focusing on these factors, the study aims to determine if the proposed AMAN solution matches the needs of air traffic controllers.

The proposed study consists in receiving feedbacks from air traffic controllers who are asked to answer a structured questionnaire that aims to investigate the interface usability, data accessibility and situational awareness. The test is divided in three main parts, performed in sequence.

1. *Introduction to the problem.* In this initial part, the subject is requested to listen and understand the explanation about the investigation and the project. This introductory section is essential for providing context to the subject being questioned, ensuring he/she can respond to the questions accurately.

In this work, the brief introduction (around 10 minutes) is structured in order to highlight the following areas:

- Context and motivation. The choice of AMAN and Human Factors analysis is explained in the context of the Master's thesis.
 - The AMAN Simulator. The AMAN simulator, explained in Chapter 4, is briefly presented. The focus is set on the outputs and the limits of the simulator.
 - The Baseline HMI. The HMI design that mimics the current real interface is explained.
 - The Solution HMI. The different features of a new solution aiming to solve the problems emerged in the usability of the baseline interface, are explained.
2. *Questionnaire.* After the introduction, the investigation starts with some questions about the solution interface. The questionnaire is submitted in written form to avoid possible bias during oral interviews. The questions are based on the solution interface that the participants need to refer to in order to answer. To avoid them becoming too familiar with the information in the interface, different scenarios are shown randomly across the various questions. The questionnaire is divided into two parts, but the ATCOs are not informed about this.

- Data Accessibility Questions. These questions are designed to understand how easy it is for the subject to access certain data and they focus on evaluating the clarity of retrieving information as well as any potential obstacle to the data access.

In this study, the questions are structured in a guided format, using appropriate linear

scales or multiple-choice options. Open questions are avoided to simplify the analysis of the results. The proposed questions are in Appendix C.

- **Situational Awareness Questions.** These questions are instead designed as “operative questions” to assess the situational awareness offered by the interface. By focusing on SA, these questions aim to find out if the interface helps with critical thinking processes and improves the overall work performance.

Similarly to the data accessibility questions, multiple-choice options are used whenever possible and short open answers are used only for specific questions. The SA questions are in Appendix C.

3. *Discussion.* This last phase of the study, aims to understand what the controller thinks about the solution, in particular, what is necessary and what is redundant and superfluous.

This analysis is done using Tab. 14 that helps identifying possible developments and adjustments in the proposed solution.

Table 14: Human Factors model to understand the controller critical thoughts about the presented solution.

REMOVE (have but don't want)	PRESERVE (have and want)
AVOID (don't have and don't want)	ACHIEVE (don't have but want)

6 Results and Discussion

6.1 Simulation Results and Considerations

The simulator described in Chapter 4 is tested across various scenarios to evaluate the results and validate the model. Five different scenarios are provided in Appendix D.

These working scenarios depict traffic situations where there is a high volume of traffic arriving over a short period of time. This is because the AMAN system is most useful and effective when a large number of flights, close to the maximum airport's capacity, are arriving at the terminal hub. Considering that the airport capacity at Rome Fiumicino is approximately 45 arriving flights per hour (with multiple runway configuration), simulations involving 6 to 9 flights within about 20 minutes on a single runway represent a standard situation at Fiumicino.

For simulation purposes, at the start of the simulation the aircraft are overflying their first waypoint shown in the planned route. Therefore, the planned route indicated in the scheduled flight plans does not represent the actual first waypoint of the flight, but rather the waypoint where the flight is generated.

To clarify, let's take the example of the flight "BAW147" (see Scenario 1 in Appendix D). Its first route waypoint is "PELEG". However, this is surely not its first route waypoint, as the flight departs from London Gatwick, and "PELEG" is located in Italian airspace. In the simulation so, the flight originates in cruise in the point "PELEG" and at its cruise flight level.

The simulations are conducted with different thresholds (see § 4.3.2) for gaining and losing the delay. This approach is used because typically, TTG delays are easier to absorb compared to TTL delays. In fact, gaining delay can be managed through ATCO instructions such as holding patterns, vectoring, reducing speed and longer routes. In contrast, losing delays can be more difficult to be handled; indeed, the planned route is often close to the shortest possible, and increasing speed is not always possible in cruise due to aerodynamic or structural limitations.

The threshold values chosen for the simulation are:

- TTL Threshold = 5 minutes
- TTG Threshold = 10 minutes

The results are presented below.

Table 15: Traffic Scenario 1 Results. The Sequence Number, Estimated Landing Time (ELDT), Target Landing Time (TLDT), Delay Advice and Separation are provided for each aircraft in the scheduled arrivals. The simulation starting time is 12:00:00.

Traffic Scenario 1					
Sequence N°	Flight	ELDT	TLDT	Delay Advice (min)	Separation (NM)
1	IBE556	12:37:56	12:37:56	00	–
2	BAW147	12:38:15	12:39:15	+01	2.5
3	AUA327	12:43:18	12:40:18	-03	2.9
4	ACA227	12:43:39	12:42:39	-01	4.3
5	AEZ985	12:46:36	12:45:36	-01	4.2
6	RYR456	12:47:09	12:47:09	00	3.1
7	ITY123	12:47:51	12:48:51	+01	3.4
8	UAE222	12:49:21	12:50:21	+01	3.2
9	WMT789	12:57:57	12:53:57	-04	5.9

Table 16: Traffic Scenario 2 Results. The Sequence Number, Estimated Landing Time (ELDT), Target Landing Time (TLDT), Delay Advice and Separation are provided for each aircraft in the scheduled arrivals. The simulation starting time is 10:15:00.

Traffic Scenario 2					
Sequence N°	Flight	ELDT	TLDT	Delay Advice (min)	Separation (NM)
1	IBE56J	10:52:56	10:52:56	00	–
2	BAW66C	10:53:15	10:54:15	+01	2.5
3	AUA13H	10:58:18	10:55:18	-03	2.9
4	ACA21Q	10:58:39	10:57:39	-01	4.3
5	AEZ998	11:01:36	10:59:36	-01	4.2
6	RYR76F	11:02:09	11:02:09	00	3.1

Table 17: Traffic Scenario 3 Results. The Sequence Number, Estimated Landing Time (ELDT), Target Landing Time (TLDT), Delay Advice and Separation are provided for each aircraft in the scheduled arrivals. The simulation starting time is 17:00:00.

Traffic Scenario 3					
Sequence N°	Flight	ELDT	TLDT	Delay Advice (min)	Separation (NM)
1	KAL907	17:30:56	17:30:56	00	–
2	TAP65L	17:34:31	17:33:31	-01	4.9
3	DLH99W	17:34:32	17:35:32	+01	4.0
4	EWG7NW	17:41:30	17:37:30	-04	3.8
5	THY1JB	17:46:09	17:41:09	-05	7.7
6	UAE222	17:49:21	17:44:21	-05	6.4

Table 18: Traffic Scenario 4 Results. The Sequence Number, Estimated Landing Time (ELDT), Target Landing Time (TLDT), Delay Advice and Separation are provided for each aircraft in the scheduled arrivals. The simulation starting time is 15:45:00.

Traffic Scenario 4					
Sequence N°	Flight	ELDT	TLDT	Delay Advice (min)	Separation (NM)
1	AFR44G	16:22:19	16:22:19	00	–
2	DLH65T	16:22:25	16:24:25	+02	4.1
3	AUA71K	16:22:47	16:25:47	+03	2.7
4	BAW15R	16:23:15	16:27:15	+04	2.8
5	ITY67Y	16:31:15	16:29:15	-02	4.0
6	VLG62C	16:32:47	16:30:47	-02	2.8
7	RYR99U	16:33:14	16:32:14	-01	2.9
8	WMT77T	16:42:57	16:37:57	-05	10.4

Table 19: Traffic Scenario 5 Results. The Sequence Number, Estimated Landing Time (ELDT), Target Landing Time (TLDT), Delay Advice and Separation are provided for each aircraft in the scheduled arrivals. The simulation starting time is 21:30:00.

Traffic Scenario 5					
Sequence N°	Flight	ELDT	TLDT	Delay Advice (min)	Separation (NM)
1	TAP98G	22:07:56	22:07:56	00	–
2	DLH13W	22:08:05	22:10:05	+02	4.2
3	BAW18U	22:08:15	22:12:15	+04	3.9
4	LOT66H	22:13:18	22:13:18	00	3.0
5	AAL65D	22:13:27	22:15:27	+02	4.5
6	DAL55Y	22:13:39	22:17:39	+04	4.3
7	ACA12X	22:13:39	22:19:39	+06	4.0
8	RYR78I	22:17:09	22:22:09	+05	5.2
9	VLG54N	22:17:51	22:23:51	+06	3.8

In the presented results, it is clear that the “*first come first serve*” principle is respected. Indeed, it is possible to observe that the sequence of flights is given according to the Estimated Landing Time (ELDT) sorted in an increasing order.

Additionally, the delay advice for the first flight in the sequence is always zero in every traffic scenario; this is because it is assumed to be the first flight with no other aircraft ahead of it.

Based on these principles, the simulator appears to work properly, respecting the threshold limits and providing reasonable total delays. The simulator also calculates the spacing in nautical miles between successive landing aircraft. While this data may not be useful for the ATCOs, it is helpful for verifying whether the simulator is working correctly or not. By looking at this data indeed, it is possible to determine if the required minimum separation is maintained, both in terms of defined capacity (e.g. 2.5 NM between aircraft of the same wake turbulence category) and wake turbulence categories.

In the scenarios above it is possible to see that the spacing between successive aircraft never falls below the minimum separation of 2.5 NM. Moreover, in the case of different wake turbulence categories the minimum separation (shown in Tab. 5) is still respected.

Let’s take an example in the Scenario 1 (Tab. 15). The flight “ACA227” is category “Heavy - H”; the following traffic, “AEZ985”, is category “Medium - M”. According to the minimum separation requirements, at least 4 nautical miles are necessary between successive landing aircraft. As shown in the results, the spacing is respected. It should be noted that the AMAN simulator does not optimize the spacing to precisely achieve the 4 NM separation; this is due to rounding and sensitivity considerations. In fact, the exact delay should be expressed with a precision of seconds, but that precision would clearly be difficult to manage for air traffic controllers as they cannot give instructions to adjust the delay by seconds. For this reason, as shown in Alg. 1, rounding is necessary. This rounding is done carefully to make sure the spacing never goes below the minimum, ensuring that the required separation is followed.

It is possible to observe that the threshold limit is respected by looking at the flight “WMT77T” in Scenario 4 (Tab. 18). Indeed, the separation of 10.4 NM shows that the flight could lose more minutes (and so nautical miles) to decrease the separation with the preceding flight, until reaching the 2.5 NM limit (being the previous flight the same wake turbulence category as “WMT77T”). The result confirms that the threshold for losing delay advice is set to 5 minutes, which is different from the threshold for gaining delay advice. In fact, Scenario 5 (Tab. 19) shows that the last flight, “VLG54N”, has a delay advice larger than 5 minutes.

To sum-up, the results show that the AMAN simulator works in an efficient and accurate way, providing reliable outputs. The system respects the defined thresholds and ensures the required separations between aircraft. The delay advice calculations are consistent, and the simulator is stable with different traffic scenarios.

6.2 Human Factors Analysis Results

The methodology described in § 5.4 is applied to this work. Specifically, as a preliminary study, two air traffic controllers from Rome ACC are involved in the test. Questioning only two ATCOs does not provide enough data for statistical stability, hence it is not possible to identify trends in the answers with high certainty. However, this initial interview represents a preliminary step before conducting a full statistical analysis. This first test is intended to evaluate whether the solution is worth further study as well as to identify any suggested modifications to match the ATCOs' needs.

The test is performed separately for each ATCO to prevent mutual influence on their answers and to avoid the development of mental scenarios based on the other subject's answers.

The answers of the questionnaire (see Appendix C) are resumed in Fig. 39. According to their answers the following outcomes have emerged.

1. The subjects are expert air traffic controllers with deep knowledge of the AMAN system.
2. The data accessibility within the proposed interface seems to be overall good.
 - One element is getting more attention than others, a detailed analysis should be done to find out which element is.
 - No attention is given to elements that are easy to ignore.
 - The number of information items the ATCOs are able to perceive is high, this is a positive indicator of the layout of the elements in the interface.
 - A special focus should be given to the question about how many colors the subjects can easily distinguish. A difference was noticed because one ATCO could distinguish many different color shades, while the other could only recognize a few.
3. The situational awareness is overall good but there are indicators suggesting slight modifications.
 - The sequence number and delay advice are correctly interpreted and understood by the ATCOs.

- The target landing time (TLDT) is correctly read.
- Regarding the label's future projection, the information that will change have been correctly identified.
- The future projection related to the timeline seems to cause some confusion. Specifically, one incorrect response and one correct response suggest that further investigation is needed in this area.

The final step of the interview consists of open guided questions, as outlined in Tab. 14. The responses from both controllers are presented in Tab. 20.

The **REMOVE** and **PRESERVE** answers are about what eliminating or keeping in the proposed solution. The following points are highlighted.

1. Both ATCOs have highly appreciated the delay advice in the label, which is a very positive aspect of the solution interface.
2. Both ATCOs do not want the sequence number as the first element before the callsign in the label. One of them prefers having it to the right of the callsign (as reported in “ACHIEVE”), while the other takes a neutral position, saying it can either be included or not.
3. The color gradient is considered a positive feature.

The **AVOID** and **ACHIEVE** answers refer to what element, that is not represented in the proposed solution, should not be included or should be included.

1. Both ATCOs expressed a preference for having the selection of an aircraft on the radar screen visibly reflected in the AMAN interface as well. When an aircraft is selected by clicking on its label or radar track, it highlights. However, this selection is not transmitted to the AMAN interface in the current system. What is desired is for the same aircraft to be highlighted in the AMAN interface as well.
2. One subject wants the sequence number in the label in the right position after the callsign.
3. One subject expresses his/her desire to have reported the Expected Approach Time-EAT²³ in the AMAN interface. This would help the air traffic controller to anticipate the future air traffic scenario, plan, and take appropriate actions.

²³Expected Approach Time - EAT. It is the estimated time at which an aircraft is expected to start its approach to the destination airport; it is particularly important in holding situations.

4. One subject would like dynamic interaction with the user in the case of delay updates and changes. Specifically, he/she would like a feature, such as a brief (of a few seconds) highlight in the label and AMAN interface, to bring the operator attention to the change in delay.
5. One subject does not express any opinions on what to avoid. The other, instead, suggests not including the aircraft type (since the wake turbulence category is sufficient) and route details (as the necessary elements like entry/exit waypoints are already displayed). Additionally, since the ATCO can hide the fourth row of the label when customizing its display, he/she recommends not placing the AMAN information (delay advice and sequence number) in this row to avoid hiding them.

After this structured test, the ATCOs were asked to give critical comments to the current AMAN system (both baseline and solution) and suggest any other improvement that could be useful.

One subject suggests that the delay distribution (not implemented in the simulator) among the sectors crossed by the flight in its route (see delay sharing § 3.2.3) should occur from the inner sectors to the outer sectors, rather than the other way around. This is because small delays that need to be gained or lost in the sectors where the aircraft is cruising at high speed are difficult for the ATCOs to be managed. A possible solution could be to provide delays to the sectors crossed during the cruise and initial descent phases only if the delay exceeds a certain threshold. If the delay is below this threshold, and if it is compatible with airspace capacities, the delay should be assigned to the sectors closer to the destination airport, where the aircraft is already in the approach phase.

Moreover, he/she mentions that the *sequence manager*, responsible for directing and deciding the various AMAN settings, is overloaded. This is because, most of the time, this role is also performed by the area coordinator, who already has a high workload.

Table 20: Human Factors model to understand the controller’s critical thoughts about the presented solution: the answers of the two subjects are presented. The (2) at the end of the sentence means both the ATCOs have provided that answer.

REMOVE (have but don’t want)	PRESERVE (have and want)
<ol style="list-style-type: none"> 1. Sequence number next to callsign (left) - (2) 2. Vertical bars in the label 3. Sequence number in the label 	<ol style="list-style-type: none"> 1. Delay advice number in the label - (2) 2. Sequence number in the label 3. Color gradients
AVOID (don’t have and don’t want)	ACHIEVE (don’t have but want)
<ol style="list-style-type: none"> 1. Aircraft type 2. Route details 3. Delay advice and sequence number 	<ol style="list-style-type: none"> 1. Selection highlight in AMAN timeline - (2) 2. Callsign highlight (for few seconds) when a new delay is provided 3. Status color correspondence between label and timeline 4. EAT (Expected Approach Time) 5. Sequence number next to callsign (right)

HMI ATCOs Questionnaire - Answers	
Subject1	Subject2
1	How many years have you been working as an air traffic controller?
A:	34
2	How many years have you been using the AMAN system?
A:	Since it was installed (2022)
3	One element of the interface focuses your attention more than the others.
A:	4
4	The interface contains one or more elements that are easy to ignore.
A:	3
5	Indicate how many pieces of information you can distinguish without effort.
A:	More than six
6	Indicate how many colors you can distinguish without effort.
A:	More than four colors
7	Indicate the sequence number and the "delay advice" that AMAN assigns to flight "LOT66H".
A:	Sequence number 4, delay advice 00
8	Indicate the time at which AMAN predicts the aircraft "JTY123" will land.
A:	12:49
9	Suppose that flight "AUA13H" changes its sequence number after a short time and requires an additional delay. Indicate which information (one or more) in the label you expect to change.
A:	3: "AUA13H"; -03
10	With the information displayed on the screen, assuming that the delays suggested by AMAN have been followed, indicate the expected scenario after 10 minutes by observing the interface.
A:	All flights from sequence number 1 to sequence number 6 have landed. All flights from sequence number 1 to sequence number 7 have landed.

Figure 39: Questionnaire answers provided by the two questioned subjects involved in the test. Highlighted in green the personal anonymous questions, in light blue the data accessibility questions and in light orange, the situational awareness questions.

Conclusions

Among the various technological solutions developed and implemented by the SESAR community in the context of traffic management, this thesis focused on systems for managing arriving traffic in terminal hubs. In particular, this work studied the Arrival Manager (AMAN) technology through the development of a simulator that replicates the real operational environment. Additionally, due to the low usability of the system observed in the operative air traffic control center, an analysis of the related causes was conducted. The analysis highlighted the impact of Human Factors limitations and the low level of user's acceptance, caused by the inefficient interaction with the interface.

In order to build the simulator and conduct the Human Factors analysis, a first in depth theoretical study about the demand in air transport and the ATM definitions was carried out. Then, the logic algorithm of the conventional AMAN system along with the main Human Factors principles were examined. This allowed to develop the correct simulation environment and a new proposed interface for the following Human Factors studies. Finally, the Human Factors analysis was carried out involving expert air traffic controllers in the context of AMAN.

To build the simulator, several hypotheses were made. The most relevant included the assumption of *single sector operations*, which implies that no delay sharing occurs among the different airspace sectors, and the implementation of an *open-loop simulator*, where the actions of the air traffic controllers are not detected by the simulator. This last hypothesis is due to the constraints imposed by the accessibility to real-time data provided by the FDPS and RDPS and means that the simulator refers to a static scenario not updating during time.

Even though this assumptions may seem highly limiting, they align with the purpose of this thesis, which focuses on the Human Factors related issues. In this context, the simulator works as testing framework to support the analysis.

To simulate the weather and include the wind effect in the computations, a model is developed. While the model works correctly, the resolution of the data sources is on a large scale (covering the European airspace).

The simulator is stable for the different scenarios and delivers reasonable results. The outputs were presented through an interface designed to replicate the current HMI used in the air traffic control centers. This interface, called "Baseline Interface" in this work, replicated all the information provided by the real AMAN HMI, except for the distance to go and the reference fix. The new HMI, called "Solution Interface" in this work, proposed to integrate the AMAN information directly into the aircraft labels to facilitate the controllers in managing the arriving traffic.

Additionally, a color gradient representing the severity of the delay advices was implemented in the solution interface.

The proposed solution was evaluated using Human Factors methodologies, focusing specifically on workload, data accessibility and situational awareness. The study was presented to two expert air traffic controllers, having a deep knowledge of the AMAN system. They were asked to answer to guided questions about the new solution. **The study revealed an overall positive feedback for the new solution in its design, where situational awareness, workload and data accessibility were improved.**

In particular, the representation of the delay advice in the radar HMI labels seemed to be very useful, as it enhanced data accessibility and reduced the ATCOs' workload by eliminating the need to frequently shift the focus from the radar HMI to the AMAN HMI. The color gradient as well represented a positive element in the analysis, as it allowed to visual understand the magnitude of the delay, hence improving situational awareness. The study also highlighted a critical aspect of the proposed solution related to the position of the sequence number in the label. Indeed, for priority reasons, the preference to have the callsign displayed first rather than the sequence number, is underlined. Additionally, the inclusion of the sequence number in the label seemed to be superfluous.

To conclude, some recommendations are done for future developments.

1. It is suggested to use wind charts referred to the Italian airspace in order to achieve higher spatial resolution and more accurate wind information.
2. It is recommended to include the distance to go and the reference fix in the interface since they represent essential information for the ATCOs.
3. Since the study suggests the need of a connected environment between the AMAN display and the radar interface, where any selection or modification made in one HMI is reflected on the other interface, it is recommended to implement the solution interface taking into account possible upgrades to connect the two interfaces.
4. To conclude, as the Human Factors analysis conducted in this study is preliminary, it is suggested to present the solution to a larger group of individuals with deep knowledge of the AMAN system and high experience in the ATC environment. Finally, conducting a test with new air traffic controllers, who are not familiar with the AMAN system, could provide interesting results, being the subjects not biased by their experience.

References

- [1] Eurostat. *Air passenger transport by type of schedule, transport coverage and country*. Accessed on October 2024. EU, 2024. URL: <https://ec.europa.eu/eurostat/databrowser/view>.
- [2] ASSAEROPORTI. *Dati di Traffico*. Accessed on October 2024. ASSAEROPORTI, 2024. URL: <https://assaeroporti.com/statistiche/>.
- [3] Eurocontrol. *Daily Punctuality - Airports*. Accessed on October 2024. Eurocontrol, 2023. URL: <https://www.eurocontrol.int/Economics/DailyPunctuality-Airports.html>.
- [4] ENAV. *ARRIVAL MANAGER*. Accessed on November 2024. ENAV, 2023. URL: <https://www.enav.it/media/news/arrival-manager-da-oggi-operativo-anche-presso-milano-acc>.
- [5] Gennaro Esposito. *Regolamentazione Aeronautica*. Fifth Edition. Antonio Esposito Edizioni, 2012. ISBN: 978-88-900857-4-1.
- [6] ICAO. *Air Traffic Management, Procedures for Air Navigation Services*. Fifteenth Edition, DOC4444 ATM/501. ICAO, 2007.
- [7] ICAO. *ANNEX 11, Air Traffic Services*. Fifteenth Edition. ICAO, 2018.
- [8] Fabrizio Pescara. *Algoritmo di ottimizzazione della Sequenza di partenze e arrivi in modalità single runway operations*. Elaborato Finale di Laurea. Università di Bologna, 2016.
- [9] ENAV. *Aeronautical Information Publication AIP*. Accessed on December 2024. ENAV, 2024. URL: <https://www.enav.it/services/list/aip>.
- [10] Eurocontrol. *What is a Slot*. Accessed on November 2024. 2016. URL: <https://www.eurocontrol.int/article/what-is-a-slot>.
- [11] ICAO. *ANNEX 2, Air Traffic Services*. Fifteenth Edition. ICAO, 2018.
- [12] Helios Economics and Policy Services. *The impact of fragmentation in European ATM/CNS*. Final Report. Eurocontrol, Performance Review Commission, 2006.
- [13] Prof. Ing. Hartmut Fricke. *Impact of Fragmentation on ATM System Performance*. Technische Universität Dresden, Institute of Logistics and Aviation, 2019.
- [14] European Commission. *SES Performance and Charging*. Accessed on November 2024. EU, 2023. URL: https://transport.ec.europa.eu/transport-modes/air/single-european-sky/ses-performance-and-charging_en.

- [15] European Commission. *PRB Annual Monitoring Report 2023*. Accessed on November 2024. EU, 2023. URL: https://eu-single-sky.transport.ec.europa.eu/news/prb-annual-monitoring-report-2023-2024-09-26-0_en.
- [16] European Commission. *The SESAR Project*. Accessed on November 2024. EU, 2023. URL: https://transport.ec.europa.eu/transport-modes/air/single-european-sky/sesar-project_en.
- [17] SESAR Joint Undertaking. *Delivering the Digital European Sky*. Brochure. SESAR Joint Undertaking, 2024.
- [18] European Commission. *Single European Sky*. Accessed on November 2024. EU, 2023. URL: https://transport.ec.europa.eu/transport-modes/air/single-european-sky_en.
- [19] SESAR Joint Undertaking. *Projects and Results: Innovation Pipeline*. Accessed on December 2024. SESAR, 2024. URL: <https://www.sesarju.eu/innovation-pipeline>.
- [20] NASA. *Technology Readiness Levels*. Accessed on December 2024. NASA, 2023. URL: <https://www.nasa.gov/directorates/somd/space-communications-navigation-program/technology-readiness-levels/>.
- [21] SESAR Joint Undertaking. *PJ19.04: Performance Framework*. Accessed on December 2024. SESAR Joint Undertaking, 2019.
- [22] SESAR Joint Undertaking. *SESAR Solutions Catalogue 2021*. Fourth Edition. SESAR Joint Undertaking, 2021.
- [23] SESAR. *Continuous descent operations (CDO) using point merge*. Release 5 SESAR Solution 11. SESAR JU, 2016.
- [24] DGAC ICAO AIRBUS. *Introduction to RNAV*. ICAO.
- [25] SESAR. *Optimised use of runway configuration for multiple runway airports*. SESAR 2020 TS IRS - PJ.02- 08. SESAR JU, 2020.
- [26] SESAR. *Reduced separation based on local runway occupancy time characterisation (ROCAT)*. SESAR 2020 TS IRS - PJ.02- 08. SESAR JU, 2020.
- [27] SESAR. *DMAN Baseline for integrated AMAN DMAN*. Release 1 SESAR Solution 106. SESAR JU, 2011.
- [28] SESAR. *Digital SESAR Solutions Catalogue*. Accessed on January 2025. SESAR. URL: <https://www.sesarju.eu/catalogue>.
- [29] Eurocontrol. *AMAN. Implementation Guidelines and Lessons Learned*. Eurocontrol, 2010.

- [30] V. Kharchenko et al. *Analysis of the flight object concept*. Ningbo University of Technology, 2014.
- [31] Taguchi et al. *Distributed Radar Data Processing System*. United States, Patent Application Publication, 2006.
- [32] Nuic et al. *Advanced Aircraft Performance Modeling for ATM: Enhancements to the BADA Model*. 24th Digital Avionics System Conference, Washington D.C. EUROCONTROL, 2005.
- [33] Korn et al. *4D Trajectory Management in the Extended TMA: Coupling AMAN and 4D FMS for Optimized Approach Trajectories*. 25th International Congress of the Aeronautical Sciences. German Aerospace Center, DLR, 2006.
- [34] Bimal Subedi. *Arrival Manager (AMAN) and its Implementation Study in Vilnius International Airport*. Bachelor's Degree Final Work. Technikos Universitetas Vilniaus Gedimino, 2015.
- [35] EUROCONTROL. *Specification for Trajectory Prediction*. Edition 2.0, EUROCONTROL-SPEC-0143. EUROCONTROL, 2017.
- [36] SESAR. *Extended Arrival Management (E-AMAN) horizon*. Release 4 SESAR Solution 05. SESAR JU, 2015.
- [37] Boston Air Group. *About Human Factors in Aviation*. Accessed on January 2025. 2024. URL: <https://www.bostonairgroup.com>.
- [38] Peter G.A.M. JORNA. *ATM Human Factors and Human Resources Considerations*. Nationaal Lucht-en Ruimtevaartlaboratorium (NLR).
- [39] Human Performance Research Group. *NASA TASK LOAD INDEX (TLX)*. V1.0, Moffett Field. California. NASA Ames Research Center.
- [40] M. R. Endsley and Garland D. J. *Theoretical Underpinnings of Situation Awareness: a Critical Review*. Lawrence Erlbaum Associates, 2000.
- [41] CAA. *Situation Awareness (SA)*. CAA - Civil Aviation Authority of New Zealand.
- [42] Eurocontrol. *Base of Aircraft Data*. Accessed on December 2024. URL: <https://www.eurocontrol.int/model/bada>.
- [43] WAFC London. *Europe wind charts*. Accessed on December 2024. AVINOR. URL: <https://www.aerbrava.com/en/meteo/europe-wind-chart/>.
- [44] ENAC. *METAR and TAF*. Safety Promotion Leaflet. ENAC, 2021.
- [45] Roel Nicolai. *The Enigma of the Origin of Portolan Charts*. Appendix B: Calculation of the Length of a Rhumb Line, pp. 467–470. Brill, 2016.

[46] G. Messina V. Nastro. *Fondamenti di Navigazione Aerea*. HOEPLI, 2015.

A Appendix A: The Rhumb Line Model

The **rhumb line** is a line on the surface of a sphere that crosses all the meridians at the same constant angle. Unlike a great circle, that is the shortest path between two points in the sphere, the rhumb line presents a constant true course TC and is the most widely used route for short distances because of its comfort (constant course). A visual representation of a generic rhumb line is given in Fig. 40.

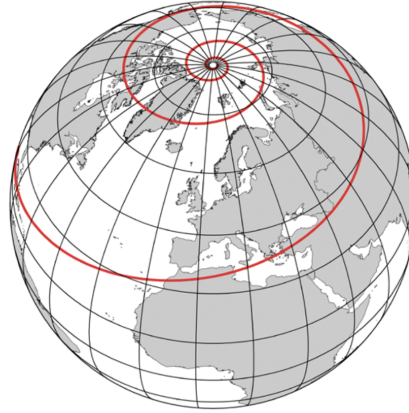


Figure 40: Representation of a generic rhumb line in the global sphere; it is possible to see how the angle between the meridians and the route (true course TC) is constant [45].

The mathematics beyond the rhumb line holds under the main assumption of short distances. Indeed, considering distances below 350 NM and latitudes under 60° , it is possible to neglect the earth curvature; this allows to work with flat triangles where classical euclidean formulations are applied [46].

Before moving to the mathematical explanations used to solve the problem, some basic air navigation concepts are given. In particular, the main definitions of latitude and longitude are provided and represented in Fig. 41.

Latitude. The latitude of a point is the angle ϕ measured from the equator plane to the parallel passing by the point. Its codomain is $[-90^\circ; 90^\circ]$ and it is defined positive going from the equator to the North pole and negative to the South pole.

Longitude. The longitude of a point is the angle λ at the earth's center, measured from the Greenwich fundamental meridian to the meridian passing by the point. Its codomain is $[-180^\circ; 180^\circ]$ and it is defined positive going from the Greenwich meridian toward East and negative toward West.

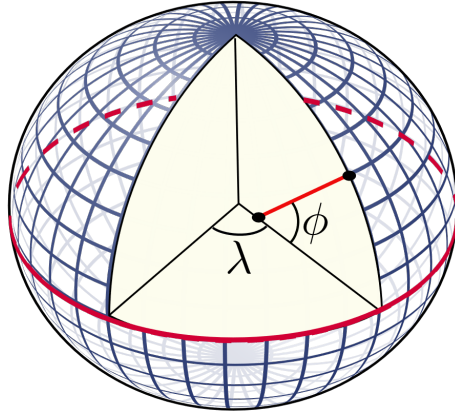


Figure 41: Representation of the Latitude and Longitude in the earth's sphere.

It is important to highlight that the nautical mile is defined as $\frac{1}{60}$ of degree (1') in the maximum circles, which are the equator and all the meridians. For this reason, 1' of latitude corresponds to 1 NM along the meridians and 1' of longitude corresponds to 1 NM only at the equator. To calculate the corresponding distance at a given parallel it is necessary to multiply the corresponding length at the equator by the cosine of the latitude at which the parallel refers:

$$D_{\phi} = D_{equator} \cdot \cos(\phi) \quad (12)$$

Considering an aircraft moving from the point A to the point B (see Fig. 42), it is possible to extract the rhumb line triangle, represented in Fig. 43. This triangle allows to solve the mathematics behind the rhumb line method.

It presents one leg equals to $\Delta\lambda \cdot \cos(\phi_m)$ obtained using Eq. 12. Since ϕ is not constant, a good approximation that avoids integration is obtained using the medium latitude between A and B. According to the previous discussion, the vertical leg of the triangle, corresponds directly to $\Delta\phi_{AB}$.

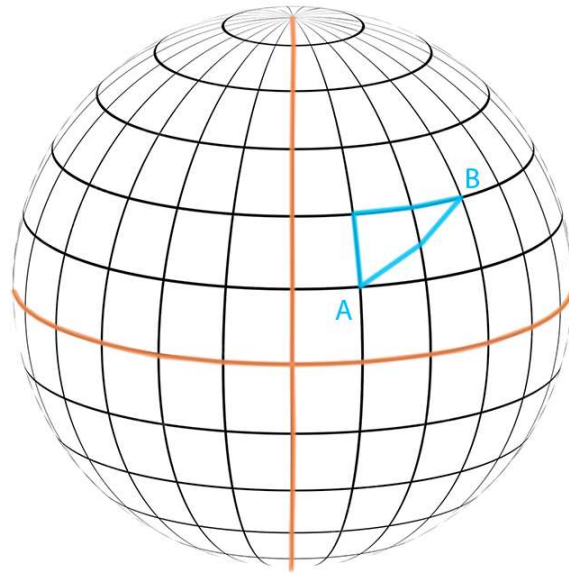


Figure 42: The rhumb line triangle in the earth sphere model.

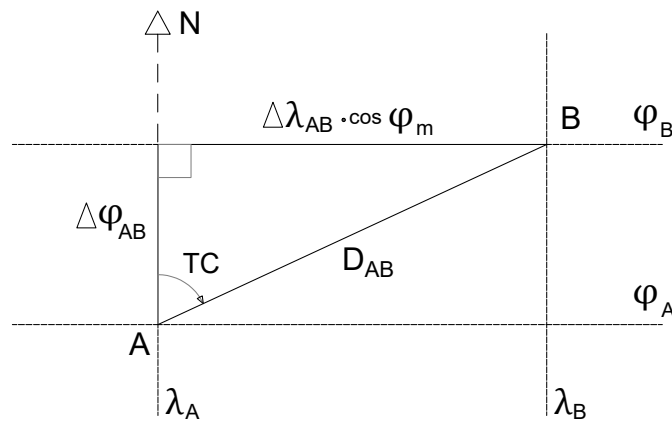


Figure 43: The rhumb line triangle.

1st Rhumb Line Problem

The first rhumb line problem is encountered when the true course and distance are unknown, but the geographical coordinates of the departure and destination points are provided.

The solution is obtained by applying trigonometric laws to the rhumb line triangle.

$$TC_{AB}^* = atan\left(\frac{\Delta\lambda_{AB} \cdot \cos(\phi_m)}{\Delta\phi_{AB}}\right) \quad (13)$$

$$D_{AB} = \frac{\Delta\phi'_{AB}}{\cos(TC_{AB})} \quad (14)$$

where $\Delta\phi_{AB} = \phi_B - \phi_A$ (positive if flying North) and $\Delta\lambda_{AB} = \lambda_B - \lambda_A$ (positive if flying East). Note that Eq. 13 requires an additional correction, as the codomain of the *atan* function, in absolute terms, is $[0, 90]$, whereas true courses are always defined as positive angles measured clockwise from geographical North:

- flying NE: $TC_{AB} = TC_{AB}^*$
- flying SE: $TC_{AB} = 180^\circ - |TC_{AB}^*|$
- flying SW: $TC_{AB} = 180^\circ + |TC_{AB}^*|$
- flying NW: $TC_{AB} = 360^\circ - |TC_{AB}^*|$

2nd Rhumb Line Problem

The second rhumb line problem allows to calculate the destination latitude and longitude when the departure airport geographical coordinates are given along with the distance and the required true course to get to the destination. Still using the trigonometric laws applied to the rhumb line triangle in Fig. 43, the problem is easily solved:

$$\Delta\phi'_{AB} = D_{AB} \cdot \cos(TC_{AB}) \quad (15)$$

$$\phi_B = \phi_A + \Delta\phi_{AB} \quad (16)$$

$$\phi_m = \frac{\phi_A + \phi_B}{2} \quad (17)$$

$$\Delta\lambda'_{AB} = \frac{D_{AB} \cdot \sin(TC_{AB})}{\cos(\phi_m)} \quad (18)$$

$$\lambda_B = \lambda_A + \Delta\lambda_{AB} \quad (19)$$

B Appendix B: The Wind Problem

To account for the wind effect, the velocity used in time calculations is the ground speed (GS). It is derived from the true airspeed (TAS) by assuming a two-dimensional scenario, where the flight path angle γ ²⁴ is considered to be zero.

This simplification reduces the problem to a vector addition, which can be visualized as a triangle, as illustrated in Fig. 44 [46].

$$\overrightarrow{TC/GS} = \overrightarrow{TH/TAS} + \overrightarrow{WD/WV} \quad (20)$$

Where $\overrightarrow{TC/GS}$ represents the ground speed vector in direction of true course, $\overrightarrow{TH/TAS}$ the true air speed vector in direction of true heading and $\overrightarrow{WD/WV}$ the wind velocity vector in the opposite direction of WD (representing the direction from which the wind blows).

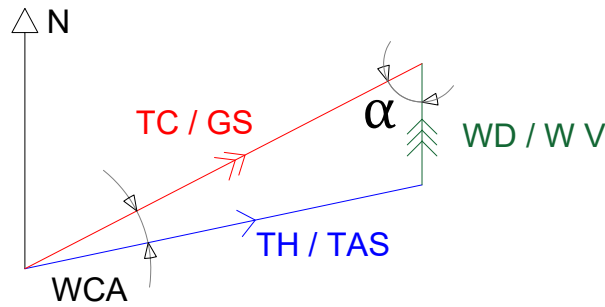


Figure 44: The wind triangle with the vectors $\overrightarrow{TC/GS}$, $\overrightarrow{TH/TAS}$ and $\overrightarrow{WD/WV}$.

This can be solved mathematically using the trigonometric laws (see Fig. 44). Indeed, the α angle can be easily derived from geometrical calculations.

$$\alpha = TC - (WD \pm 180^\circ) \quad (21)$$

²⁴Flight Path Angle - γ . It is the angle between the local horizon and the velocity vector.

Applying the sinus theorem the Wind Correction Angle (WCA)²⁵, can be derived:

$$\frac{TAS}{\sin(\alpha)} = \frac{WV}{\sin(WCA)} \quad (22)$$

$$WCA = \text{asin} \left(\frac{WV}{TAS} \cdot \sin(\alpha) \right) \quad (23)$$

Applying again the sinus theorem:

$$\frac{TAS}{\sin(\alpha)} = \frac{GS}{\sin(180^\circ - (\alpha + |WCA|))} \quad (24)$$

Being $\sin(180^\circ - (\alpha + |WCA|)) = \sin(\alpha + |WCA|)$ for the goniometric laws, it is possible to get the ground speed.

$$GS = \frac{TAS}{\sin(\alpha)} \cdot \sin(\alpha + |WCA|) \quad (25)$$

Finally, applying geometrical sum of angles the true heading is calculated.

$$TH = TC + (\pm WCA) \quad (26)$$

²⁵Wind Correction Angle - WCA. It represents the angular correction the pilot must consider to take into account the wind effect and fly along the route (TC) without drifting. It is defined positive when taken clockwise with respect to $\overrightarrow{TC}/\overrightarrow{GS}$ and negative in the counterclockwise sense.

C Appendix C: HMI ATCOs Questionnaire

For each question in the section “Data Accessibility” and “Situational Awareness”, a random scenario figure with the same features as the solution interface (see Fig. 36) is displayed.

1. Personal anonymous questions.

(a) How many years have you been working as an air traffic controller?

(b) How many years have you been using the AMAN system?

- Less than one year
- About one/two years
- Since it was installed (2022)

2. Data Accessibility Questions.

(a) One element of the interface focuses your attention more than the others.

Strongly Disagree ◯ ◯ ◯ ◯ ◯ Strongly Agree

(b) The interface contains one or more elements that are easy to ignore.

Strongly Disagree ◯ ◯ ◯ ◯ ◯ Strongly Agree

(c) Indicate how many pieces of information you can distinguish without effort.

- Less than two
- Between two and four
- Between four and six
- More than six

(d) Indicate how many colors you can distinguish without effort.

- two colors
- three colors
- four colors
- More than four

3. Situational Awareness Questions.

(a) Indicate the sequence number and the “delay advice” that AMAN assigns to flight “LOT66H”.

- (b) Indicate the time at which AMAN predicts the aircraft “ITY123” will land.
- (c) Suppose that flight “AUA13H” changes its sequence number after a short time and requires an additional delay. Indicate which information (one or more) in the label you expect to change.
- 3
 - “AUA13H”
 - 03
 - 220
 - 190
 - RIT
 - 16
 - 65
 - M
 - 110 (green)
 - “coo”
 - 110 (cyan)
 - “xfi”
 - NE1
- (d) With the information displayed on the screen, assuming that the delays suggested by AMAN have been followed, indicate the expected scenario after 10 minutes by observing the interface.
- Only flight “AFR44G” has landed.
 - Only flights “AFR44G” and “DLH65T” have landed.
 - All flights from sequence number 1 to sequence number 3 have landed.
 - All flights from sequence number 1 to sequence number 4 have landed.
 - All flights from sequence number 1 to sequence number 5 have landed.
 - All flights from sequence number 1 to sequence number 6 have landed.
 - All flights from sequence number 1 to sequence number 7 have landed.
 - All flights have landed.

D Appendix D: Simulation Scenarios

Table 21: Traffic Scenario 1. Scheduled arriving flights and the corresponding flight plan details.

Traffic Scenario 1									
ID	Flight	Aircraft	Departure	Exit WPT	Route	STAR	Entry WPT	FL	Wake Turbulence
1	ITY123	A320	LICJ	LURON	LURON ... LAT	LAT3A	LAT	320	M
2	RYR456	B738	LIBD	TOPNO	TOPNO ... LAT	LAT3A	LAT	300	M
3	WMT789	A320	LICC	PEKOD	UXUTA ... LAT	LAT3A	LAT	340	M
4	AUA327	B738	LOWW	VELUG	VELUG ... MOPUV	MOPUV3A	MOPUV	330	M
5	BAW147	E190	EGKK	PELEG	PELEG ... RITEB	RITEB3A	RITEB	350	M
6	AEZ985	AT72	LIPY	ANC	ANC ... RITEB	RITEB3A	RITEB	210	M
7	UAE222	A388	OMDB	LUXIL	LUXIL ... LAT	LAT3A	LAT	380	S
8	IBE556	A320	LEMD	POZZO	POZZO ... VALMA	VALMA3A	VALMA	300	M
9	ACA227	B772	CYYZ	LAGEN	LAGEN ... ELKAP	ELKAP3A	ELKAP	350	H

Table 22: Traffic Scenario 2. Scheduled arriving flights and the corresponding flight plan details.

Traffic Scenario 2									
ID	Flight	Aircraft	Departure	Exit WPT	Route	STAR	Entry WPT	FL	Wake Turbulence
1	EWG7NW	A320	EDDF	LUPOS	LUPOS ... RITEB	RITEB3A	RITEB	310	M
2	DLH99W	A320	EDDF	GAVRA	GAVRA ... RITEB	RITEB3A	RITEB	310	M
3	THY1JB	B738	LTFM	KATTI	KATTI ... MOPUV	MOPUV3A	MOPUV	330	M
4	QTR60B	B772	OTBD	KAPPO	KAPPO ... LAT	LAT3A	LAT	380	H
5	UAE222	A388	OMDB	LUXIL	LUXIL ... LAT	LAT3A	LAT	380	J
6	TAP65L	A320	LPPT	ROMPO	ROMPO ... VALMA	VALMA3A	VALMA	340	M
7	KAL907	B772	RKSI	ASPIR	ASPIR ... MOPUV	MOPUV3A	MOPUV	210	H

Table 23: Traffic Scenario 3. Scheduled arriving flights and the corresponding flight plan details.

Traffic Scenario 3									
ID	Flight	Aircraft	Departure	Exit WPT	Route	STAR	Entry WPT	FL	Wake Turbulence
1	RYR76F	B738	LIBD	TOPNO	TOPNO ... LAT	LAT3A	LAT	300	M
2	AUA13H	B738	LOWW	VELUG	VELUG ... MOPUV	MOPUV3A	MOPUV	330	M
3	BAW66C	E190	EGKK	PELEG	PELEG ... RITEB	RITEB3A	RITEB	350	M
4	AEZ998	AT72	LIPY	ANC	ANC ... RITEB	RITEB3A	RITEB	210	M
5	IBE56J	A320	LEMD	POZZO	POZZO ... VALMA	VALMA3A	VALMA	300	M
6	ACA21Q	B772	CYYZ	LAGEN	LAGEN ... ELKAP	ELKAP3A	ELKAP	350	H

Table 24: Traffic Scenario 4. Scheduled arriving flights and the corresponding flight plan details.

Traffic Scenario 4									
ID	Flight	Aircraft	Departure	Exit WPT	Route	STAR	Entry WPT	FL	Wake Turbulence
1	RYR99U	B738	LICJ	LURON	LURON ... LAT	LAT3A	LAT	320	M
2	VLG62C	A320	LICJ	LURON	LURON ... LAT	LAT3A	LAT	340	M
3	ITY67Y	A320	LIBD	TOPNO	TOPNO ... LAT	LAT3A	LAT	300	M
4	WMT77T	A320	LICC	PEKOD	UXUTA ... LAT	LAT3A	LAT	340	M
5	DLH65T	A320	EDDF	PELEG	PELEG ... RITEB	RITEB3A	RITEB	330	M
6	BAW15R	E190	EGKK	PELEG	PELEG ... RITEB	RITEB3A	RITEB	350	M
7	AFR44G	A320	LFPG	PELEG	PELEG ... RITEB	RITEB3A	RITEB	310	M
8	AUA71K	A320	LOWW	PELEG	PELEG ... RITEB	RITEB3A	RITEB	370	M

Table 25: Traffic Scenario 5. Scheduled arriving flights and the corresponding flight plan details.

Traffic Scenario 5									
ID	Flight	Aircraft	Departure	Exit WPT	Route	STAR	Entry WPT	FL	Wake Turbulence
1	VLG54N	A320	LICJ	LURON	LURON ... LAT	LAT3A	LAT	320	M
2	RYR78I	B738	LIBD	TOPNO	TOPNO ... LAT	LAT3A	LAT	300	M
3	ACA12X	B772	CYYZ	LAGEN	LAGEN ... ELKAP	ELKAP3A	ELKAP	350	H
4	LOT66H	B738	LOWW	VELUG	VELUG ... MOPUV	MOPUV3A	MOPUV	330	M
5	BAW18U	E190	EGKK	PELEG	PELEG ... RITEB	RITEB3A	RITEB	350	M
6	DLH13W	E190	EDDM	PELEG	PELEG ... RITEB	RITEB3A	RITEB	330	M
7	UAE222	A388	OMDB	LUXIL	LUXIL ... LAT	LAT3A	LAT	360	J
8	TAP98G	A320	LPPT	POZZO	POZZO ... VALMA	VALMA3A	VALMA	300	M
9	DAL55Y	B772	KPHL	LAGEN	LAGEN ... ELKAP	ELKAP3A	ELKAP	350	H
10	AAL65D	B772	KJFK	LAGEN	LAGEN ... ELKAP	ELKAP3A	ELKAP	330	H